Sudan University of Science and Technology
College of Graduate Studies

Study of Pulmonary Artery Pressure and Resistance in Sudanese Using Echocardiography

دراسة ضغط ومقاومة الشريان الرئوي لدى السودانيين باستخدام الموجات فوق الصوتية للقلب

A thesis submitted for fulfillment of the requirements of PhD degree in Diagnostic Medical Ultrasound

By

ImadAldien Fadul Algazouly Dahab

Supervisor

Dr. Mohamed Mohamed Omer Mohamed Yousef

Associate Professor

Co- Supervisor

Professor. Mohammed El-Fadil Mohamed Gar-Anabi

2022

الآية


بسم الله الرحمن الرحيم
﴿أَلَا بِذِكْرِ اللَّهِ تَطْمَئِنَّ الْقُلُوبُ﴾
صدق الله العظيم ،،،
الرعد ٢٨

Dedication

I dedicate this research to:

Allah, who is the greatest and the most merciful, for giving me the power and capacity to accomplish this work.

Soul of my father

Mother,

Family,

Friends,

&

Everyone who teach me a word

Acknowledgement

First and above all, thanks and praises to Allah, the almighty for providing me this opportunity and granting me the capability to proceed successfully, and the prayers and peace be upon the merciful prophet Mohamed.

I want to express my sincere thanks and deep graduate to my faithful supervisor A.prof. Mohamed Omer for guidance throughout this thesis and sharing his knowledge through the entire study.

I would also like to pass my special thanks to my Co Supervisor Prof. Mohammed El-Fadil, my friends and colleagues whom help me in my thesis.

I'm sincerely thanking the participants without whom the study would not have been feasible. The Sudan University of Science and Technology.

Abstract

Echocardiography is an important non-invasive cardiac procedure which has revolutionized the practice of cardiology globally. Indirect assessment of mean pulmonary arterial pressure (MPAP) may assist management of critically ill patients with pulmonary hypertension and right heart dysfunction; however, this has not been validated in Sudan, the purpose of this study was to Study the Pulmonary Artery Pressure and Resistance in Sudanese Using Echocardiography. This was a cross-sectional observational study done using transthoracic color flow continuous wave Doppler echocardiography in Military hospital, Omdurman, Sudan. A total of three hundred consecutive patients 157 males and 143 females, their ages ranged from 20 to 69 years were studied. Age, weight, Right ventricle (RV) Dimensions (Cm), TV MAX ms, and Maximum velocity of tricuspid regurgitation (TR) were taken for all patients. The results of this study showed that the mean ± standard deviation of the patient age, weight (independent variables), Pulmonary artery systolic pressure (PASP), Right ventricle (RV) and tricuspid regurgitation (TR) Maximum velocity was: 37.2±11.1 years, 61.4±10.0 kg, 37.4±10.8 mmHg, 2.3±0.1 cm and 2.8±0.4 ms (dependent variables) respectively. The results also showed that there is strong and significance correlation between the dependent and independent variables at p <0.001 which gives a direct linear relationship where the

dependent variables can be predicted successfully using patient age and weight; where for age the PASP increased by 0.68 mmHg/year starting at 12.2mmHg, TVmax increased by 0.024 ms/year starting at 1.9ms and RV increases by 0.006 cm/year starting at 2.1cm. also the patient weight can be used to predicted RV and PASP, where the RV increased by 0.005 cm/kg starting at 2.02 cm and PASP increased by 0.52 mmHg/kg starting at 5.4 mmHg. PASP mean for Sudanese's is 33.08 mmHg . In conclusion the parameters of the pulmonary artery pressure and resistance can be predicted for the patient using the age and body weight as normative data for better judgment.

المستخلص

الموجات فوق الصوتية للقلب هو إجراء غير جراحي للقلب أحدث ثورة في ممارسة أمراض القلب على مستوى العالم. قد يساعد التقييم غير المباشر لمتوسط ضغط الشرايين الرئوية في علاج المرضى المصابين بأمراض خطيرة كالمصابين بارتفاع ضغط الدم الرئوي واختلال القلب الأيمن ؛ ومع ذلك ، لم يتم التحقق من صحة ذلك في السودان ، و كان الهدف من البحث هو دراسة ضغط الشريان الرئوي والمقاومة في السودانيين باستخدام الموجات فوق الصوتية للقلب. كانت هذه الدراسة مقطعية مستعرضة اجريت باستخدام تدفق الالوان المستمرة عبر الصدربتقنية الدوبلر للموجات فوق الصوتيه للقلب في المستشفى العسكري ، أم درمان ، السودان. شملت الدراسه ثلاثمائة مريض ١٥٧ من الذكور و ١٤٣ من الإناث ، تراوحت أعمارهم بين ٢٠ إلى ٦٩ عامًا، تم قياس العمر و الوزن، وأبعاد البطين الأيمن (سم) ، و ارتجاع الصمام ثلاثي الشرفات. أظهرت نتائج هذه الدراسة أن متوسط عمر المريض ووزنه (المتغيرات المستقلة) وضغط الشريان الرئوي الانقباضي وابعاد البطين الأيمن و سرعته القصوى (المتغيرات التابعة) كانت: ٣٧,٢ ± ١١,١ سنة ، ٦١,٤ ± ١٠,٠ كجم ، ٣٧,٤ ± ١٠,٨ مم زئبق ، ٢,٣ ± ٠,١ سم و ٢,٨ ± ٠,٤ مللي ثانية على التوالي. أظهرت النتائج أيضًا أن هناك ارتباطًا قويًا ودلالة بين المتغيرات التابعة والمستقلة عند درجة معنوية اقل من ٠,٠٠١> مع وجود علاقة خطية مباشرة حيث يمكن التنبؤ بالمتغيرات التابعة بكفاءة وذلك باستخدام عمر المريض ، نجد ان ضغط الشريان الرئوي الانقباضي تزيد بمقدار ٠,٦٨ مم زئبق في السنة بدءًا من ١٢,٢ مم زئبق ، و كذلك السرعة القصوى للبطين الايمن تزيد بمقدار ٠,٠٢٤ مللي ثانية في السنة بدءًا من ١,٩ مللي ثانية وايضا تزيد ابعاد البطين الأيمن بمقدار ٠,٠٠٦ سم في السنة بدءًا من ٢,١ سم. و ايضا كذلك يمكن استخدام وزن المريض للتنبؤ بأبعاد البطين الأيمن و تقدير ضغط الشريان الرئوي الانقباضي ، حيث تزيد ابعاد البطين الايمن بمقدار ٠,٠٠٥ سم لكل كجم من وزن الجسم بدءًا من ٢,٠٢ سم ويزداد ضغط الشريان الرئوي الانقباضي بمقدار ٠,٥٢ مم زئبق لكل كجم من وزن الجسم بدءًا من ٥,٤ مم زئبق وان متوسط

ضغط الشريان الرئوي الانقباضي لدى السودانيين هو٣٣,٠٨ مم زئبق. في الختام ، يمكن التنبؤ بمفردات ضغط الشريان الرئوي ومقاومته للمريض كبيانات معيارية وذلك باستخدام العمر ووزن الجسم.و من ثم اتخاذ القرار المناسب

Table of Contents

Chapter Five
Discussion, Conclusion and Recommendations

List of Tables

List of Figures

List of Abbreviations

Abbreviation	Meaning
ECG	Electrocardiograph
ECHO	Echocardiography
EF	Ejection faction
HCM	Hypertrophic cardiomyopathy
LA	Left atrium
CW	Continuous wave
E-wave	Early wave of mitral flow
IAS	Interatrial septum
IVS	Interventricular septum
LV	Left Ventricle
LVEDD	Left ventricular end–diastolic diameter
LVESD	Left ventricular end–systolic diameter
LVH	Left ventricular hypertrophy
M-mode	Motion mode
PHT	Pulmonary hypertension
PW	Pulsed wave
PAP	Pulmonary artery pressure
RA	Right atrium
RV	Right ventricle
A4C	Apical four chamber
AT	Acceleration time
BSA	Body surface area
BSE	British Society of Echocardiography
CI	Cardiac index
CO	Cardiac output
CW	Continuous wave
DT	Deceleration time
EI	Eccentricity index
FAC	Fractional area change
HR	Heart rate
IVC	Inferior vena cava

IVCT	Isovolumetric contraction time
IVRT	Isovolumetric relaxation time
LA	Left atrium
LV	Left ventricle
PA	Pulmonary artery
PAP	Pulmonary artery pressure
PASP	Pulmonary artery systolic pressure
PDP	Pulmonary arterial end diastolic pressure
PH	Pulmonary hypertension
PHT	Pressure half-time
PR	Pulmonary regurgitation
PRVBD	Pulmonary regurgitant velocity at the beginning of diastole
PRVED	Pulmonary regurgitant velocity at the end of diastole
PS	Pulmonary stenosis
PSAX	Parasternal short axis
PV	Pulmonary valve
PVR	Pulmonary vascular resistance
PW	Pulsed wave
RA	Right atrium
RAA	Right atrial area
RAP	Right atrial pressure
RHC	Right heart catheterisation
RIMP	Right ventricular index of myocardial performance
RV	Right ventricle
RVAd/s	Right ventricular area in diastole/systole
RVD	Right ventricular diameter
RVOT	Right ventricular outflow tract
RVSP	Right ventricular systolic pressure
SV	Stroke volume
SVi	Stroke volume index
TAPSE	Tricuspid annular plane systolic excursion
TR	Tricuspid regurgitation
TRV	Tricuspid regurgitation velocity
TV	Tricuspid valve
Vmax	Maximum velocity

VTI Velocity time integral

Chapter one

1.1. Introduction:

Transthoracic echocardiogram (TTE) is a common noninvasive screening tool used to assess patients with shortness of breath(Frost et al. 2018).. Pulmonary hypertension (PH), often noted on TTE as elevated pulmonary artery systolic pressure (PASP), is caused by a heterogeneous group of disorders and is well recognized to be associated with higher morbidity and mortality, regardless of cause(McLaughlin et al. 2009). It is particularly important to identify patients who may have World Health Organization (WHO) group 1 pulmonary arterial hypertension (PAH) or WHO Group 4 chronic thromboembolic PH, since it has significant implications for their prognosis and management strategies. Unfortunately, in spite of published guidelines, there has been no meaningful decrease in the time from symptom onset to diagnosis of PAH in the past 20 years. On the other hand, there is a rising tendency to the misuse of PAH-specific therapies in patients with left heart disease (LHD) or lung disease associated PH(Kim et al, 2018). Although there are limitations to the echocardiographic estimations of PH severity, the estimated PASP of 60 mm Hg (any peak tricuspid regurgitation velocity >3.4 m/s) is consistent with a high probability of PH, even in the absence of other associated echocardiographic findings(Arcasoy , et al. 2003,Galiè , et al. 2015). In addition to estimating PASP, TTE can assess right ventricular size and function. Right ventricular enlargement is categorized as normal, mild, moderate, or severe based on right ventricular basal diameter(Rudski, et al.. 2010). This measure is easy to perform, widely available, and has strong associations with the outcome in PH(Forfia et al, 2006). Elevated pulmonary artery pressure (PAP) increases the static and the pulsatile afterload of the right ventricle, leading to right ventricular enlargement and dysfunction(Thenappan et al,2016). Pathological wave reflection because of

elevated pulmonary vascular impedance can cause systolic deceleration or “notching” of the right ventricular outflow tract Doppler flow velocity envelope in patients with PH. The notching can be midsystolic or late systolic in nature. Both mid and late systolic notching have been associated with elevated pulmonary vascular resistance, poor right ventricular function, and worse outcomes(Arkles, et al.. 2011, Takahama, et al. 2017). Left atrial enlargement is a strong indicator of PHLHD. In fact, left atrial enlargement has been considered the hemoglobin A1C of left-sided filling pressures. Left atrial volume index >43 mL/m2 by cardiac magnetic resonance imaging differentiates PH-LHD from precapillary PH with a 97% sensitivity and 100% specificity(Crawley et al,2013). An echocardiographic model based on lateral mitral E/E’ ratio, left atrial anteroposterior diameter, pulmonary artery acceleration time, and midsystolic notching of the right ventricular outflow tract pulse Doppler has been proposed to differentiate precapillary PH from PH-LHD(Opotowsky et al, 2012).

Pulmonary hypertension (PH) is defined as a hemodynamic state in which the pressure in the pulmonary arterial tree is elevated2.(Stepienet al. (2009), Kellihan et al. 2012). Pulmonary hypertension is not a specific disease, but a consequence of a wide range of primary cardiopulmonary and systemic etiologies(McLaughlin , 2009). Although PH was first described during an autopsy in 1891 as “pulmonary vascular sclerosis”, it was not until mid-1900 when pulmonary artery pressures could be directly measured via heart catheterization that factors regulating pulmonary artery pressure (PAP) were understood(Stepien,2008). Due to the debilitating clinical symptoms and the negative prognostic impact PH has in both people (Rich& Rabinovitch, 2008).and animals(Borgarelli et al ,2015), there is a focus on prompt diagnosis and treatment of this condition. Historically, a reliable and easily obtained clinical diagnosis of PH has been challenging. The accepted gold standard is direct measurement of the PAP using right heart catheterization(B

recker et al,1994).. This is rarely done in animals, however, due to invasiveness, cost, potential risk, and the need for heavy sedation or general anesthesia which can affect cardiac output (CO) and measured pressures. Doppler echocardiography (DE) has made it possible to evaluate PAP non-invasively(Thenappan et al,2007), Lewis et al ,2013). The assessment of variables potentially influencing the accuracy of DE-based PAP estimation is the focus of this thesis. The pulmonary vascular resistance (PVR) is a good surrogate for pulmonary vascular disease at a certain level in patient with congenital heart disease. The surgical planning, risk of the procedure, and clinical decision are aligned with the presence or absence of significant pulmonary vascular disease (Lopes et al, 2014).Although several clinical and noninvasive procedures give valuable data of hemodynamic condition of the patient with congenital heart defect (CHD), such as using Doppler echocardiography, which is a commonly implemented method for non-invasive measurement of pulmonary arterial pressure; however, Doppler echocardiography on the whole has a weakness in quantitative measurement because of limited acoustic window especially for evaluation of pulmonary circulation and the operator dependency for data acquisition (Mansencal, et al 2005). In the current era, phase-contrast magnetic resonance imaging (MRI) is counted as an added non-invasive method for assessment of hemodynamics of pulmonary or systemic circulation (Lotz et al 2002) . These techniques offer the prospect for precise estimation of pulmonary circulation parameters, and their measurements were more accurate and reproducible than Doppler echocardiography (Lee et al,1997).. Despite that nonetheless invasive right and left heart cardiac catheterization remains to be the gold-standard procedure of calculation PVR in the CHD field (Rosenzweig et al, 2019).. The PVR calculation is based on the hydraulic version of Ohm’s law (9).

1.2. Problem of the study:

Echocardiography is an important noninvasive cardiac procedure which has revolutionized the practice of cardiology globally. Indirect assessment of mean pulmonary arterial pressure (MPAP) may assist management of critically ill patients with pulmonary hypertension and right heart dysfunction; however, this has not been validated in Sudan.

1.3. Objective of the study:

1.3.1. General objective:

The main objective of this study was to Study the Pulmonary Artery Pressure and Resistance in Sudanese Using Echocardiography.

1.3.2. Specific objectives:

- To find normal pulmonary artery pressure values and co-relate with echocardiogram finding.
- To identify the correlation between raise pulmonary artery and possibility of illness.
- To evaluate the relation between the normal pulmonary pressure, Doppler blood flow, main pulmonary pressure, pulmonary artery pressure. And the heart
- To substantiate the use of echocardiography in diagnosis of pulmonary artery diseases.
- To compare the normal pulmonary artery pressure in Sudanese people with stander values.

1.4 Research outline:

The research included five chapters. Chapter one deal with the general introduction of the research, problem statement and the objectives of the study. Chapter two deals with literatures review cover the theoretical background and previous studies. Chapter three deal with the methodology of the study, including materials, method

and equipment. Chapter four will cover the results. And chapter five covers discussion, conclusion, recommendations and references.

Chapter Two

Literature Review and Background Studies

Theoretical background and literature review

2.1 Anatomy of the heart

The heart, slightly larger than a clenched fist, is a double, self-adjusting, suction and pressure pump, the parts of which work in unison to propel blood to all parts of the body. Right side of the heart (right heart) receives poorly oxygenated (venous) blood from the body through the SVC and IVC and pumps it through the pulmonary trunk to the lungs for oxygenation. [37]

The left side of the heart (left heart) receives well-oxygenated (arterial) blood from the lungs through the pulmonary veins and pumps it into the aorta for distribution to the body. The heart has four chambers: right and left atria and right and left ventricles. The atria are receiving chambers that pump blood into the ventricles (the discharging chambers). The synchronous pumping actions of the heart's two atrioventricular (AV) pumps (right and left chambers) constitute the cardiac cycle . The cycle begins with a period of ventricular elongation and filling (diastole) and ends with a period of ventricular shortening and emptying (systole) (Moore, and Dalley, 2006).

The wall of each heart chamber consists of three layers

-Endocardium, a thin internal layer (endothelium and sub endothelial connective tissue) or lining membrane of the heart that also covers its valves.

-Myocardium, a thick, helical middle layer composed of cardiac muscle.

-Epicardium, a thin external layer (mesothelium) formed by the visceral layer of serous pericardium.

The walls of the heart consist mostly of thick myocardium, especially in the ventricles.

When the ventricles contract, they produce a wringing motion because of the double helical orientation of the cardiac muscle fibers (Moore, and Dalley, 2006).

2.1.1The apex of the heart

Is formed by the inferolateral part of the left ventricle.

Lies posterior to the left 5th intercostal space in adults, usually approximately 9 cm (a hand's breadth) from the median plane.

Remains motion less throughout the cardiac cycle.

Is where the sounds of mitral valve closure are maximal (apex beat), the apex underlies the site where the heartbeat may be auscultated on the thoracic wall(Moore, and Dalley, 2006).

2.1.2The base of the heart

Is the heart's posterior aspect (opposite the apex), is formed mainly by the left atrium, with a lesser contribution by the right atrium.

Faces posteriorly toward the bodies of vertebrae T6-T9 and is separated from them by the pericardium, oblique pericardial sinus, esophagus, and aorta, extends superiorly to the bifurcation of the pulmonary trunk and inferiorly to the coronary groove, receives the pulmonary veins on the right and left sides of its left atrial portion and the superior and inferior vena cava at the superior and inferior ends of its right atrial portion(Moore, and Dalley, 2006).

2.1 .3 The surfaces of the heart

The four surfaces of the heart are the:

Anterior (sternocostal) surface, formed mainly by the right ventricle,diaphragmatic (inferior) surface, formed mainly by the left ventricle and partly by the right ventricle; it is related mainly to the central tendon of the diaphragm,right pulmonary surface, formed mainly by the right atrium,left pulmonary surface, formed mainly by the left ventricle; it forms the cardiac impression of the left lung

and the SVC enters its right side. Posterior to the aorta and pulmonary trunk and anterior to the SVC, this border forms the inferior boundary of the transverse pericardial sinus(Moore, and Dalley, 2006).

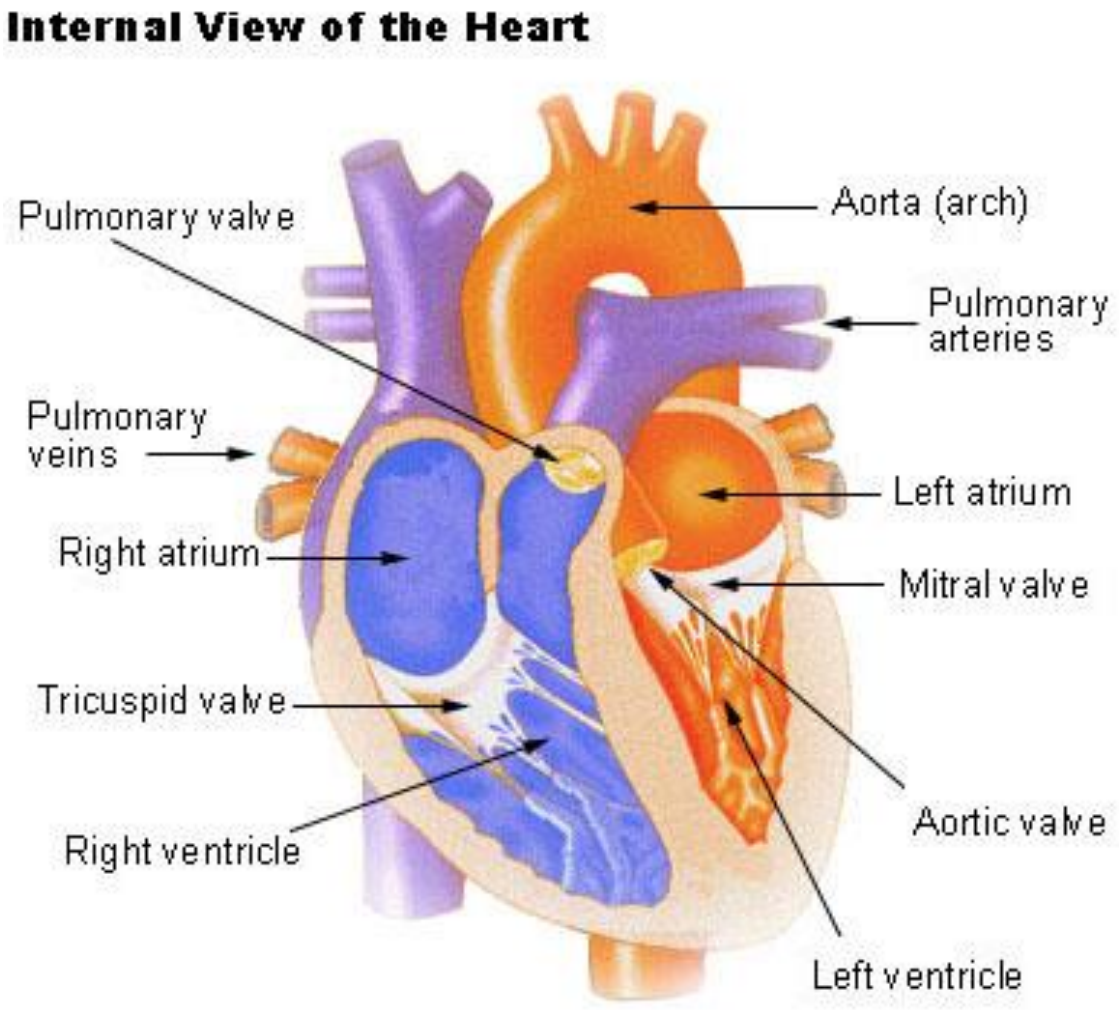

Figure 2.1 Gross anatomy of the heart (Buba, et al., 2008).

2.1.4 Right Atrium

The right atrium forms the right border of the heart and receives venous blood from the SVC, IVC, and coronary sinus. The ear-like right auricle is a conical muscular pouch that projects from this chamber like an add-on room, increasing the capacity of the atrium as it overlaps the ascending aorta (Buba, et al., 2008).

2.1.5 Right Ventricle

The right ventricle forms the largest part of the anterior surface of the heart, a small part of the diaphragmatic surface, and almost the entire inferior border of the heart. Superiorly it tapers into an arterial cone, the conus arteriosus (infundibulum), which leads into the pulmonary trunk. The interior of the right ventricle has irregular muscular elevations (trabeculae carneae). A thick muscular ridge, the supraventricular crest, separates the ridged muscular wall of the inflow part of the chamber from the smooth wall of the conus arteriosus, or outflow part. The inflow part of the ventricle receives blood from the right atrium through the right AV (tricuspid) orifice located posterior to the body of the sternum at the level of the 4th and 5th intercostal spaces.

The tricuspid valve guards the right AV orifice. The bases of the valve cusps are attached to the fibrous ring around the orifice (Snell, 2000).

2.1.6 Left Atrium

The left atrium forms most of the base of the heart. The valve less pairs of right and left pulmonary veins enters the smooth-walled atrium. In the embryo, there is only one common pulmonary vein, just as there is a single pulmonary trunk. The wall of this vein and four of its tributaries were incorporated into the wall of the left atrium, in the same way that the sinus venous was incorporated into the right atrium(Snell, 2000).

2.1.7 Left Ventricle

The left ventricle forms the apex of the heart, nearly all its left (pulmonary) surface and border, and most of the diaphragmatic surface because arterial pressure is much higher in the systemic than in the pulmonary circulation.

The interior of the left ventricle has Walls that are two to three times as thick as that of the right ventricle (Snell, 2000).

The mitral valve has two cusps, anterior and posterior. The mitral valve is located posterior to the sternum at the level of the 4th costal cartilage. Each of its cusps receives tendinous cords from more than one papillary muscle (Snell, 2000).

2.1.8 Vasculature of the Heart

The blood vessels of the heart comprise the coronary arteries and cardiac veins, which carry blood to and from most of the myocardium. The blood vessels of the heart are affected by both sympathetic and parasympathetic innervations(Moore, and Dalley, 2006).

2.1.8.1 Arterial Supply of the Heart

The coronary arteries, the first branches of the aorta, supply the myocardium and epicardium. The right and left coronary arteries arise from the corresponding aortic sinuses at the proximal part of the ascending aorta. The coronary arteries supply both the atria and the ventricles; however, the atrial branches are usually small and not readily apparent in the cadaveric heart. The ventricular distribution of each coronary artery is not sharply demarcated. [1]The right coronary artery (RCA) arises from the right aortic sinus of the ascending aorta and passes to the right side of the pulmonary trunk, running in the coronary groove. Near its origin, the RCA usually gives off an ascending sinuatrial nodal branch The RCA then descends in the coronary groove and gives off the right marginal branch, which supplies the right border of the heart as it runs toward the apex of the heart the RCA supplies

The right atrium, most of right ventricle, part of the left ventricle (the diaphragmatic surface), part (usually the posterior third) of the IV septum. The SA node (in approximately 60% of people), the AV node (in approximately 80% of people) (Moore, and Dalley, 2006).

The left coronary artery (LCA) arises from the left aortic sinus of the ascending aorta , passes between the left auricle and the left side of the pulmonary trunk, and runs in the coronary groove the LCA divides into two branches, the anterior IV

branch (left anterior descending (LAD) branch) and the circumflex branch . The anterior IV branch passes along the IV groove to the apex of the heart(Fig 2.2**)** (Moore, and Dalley, 2006).

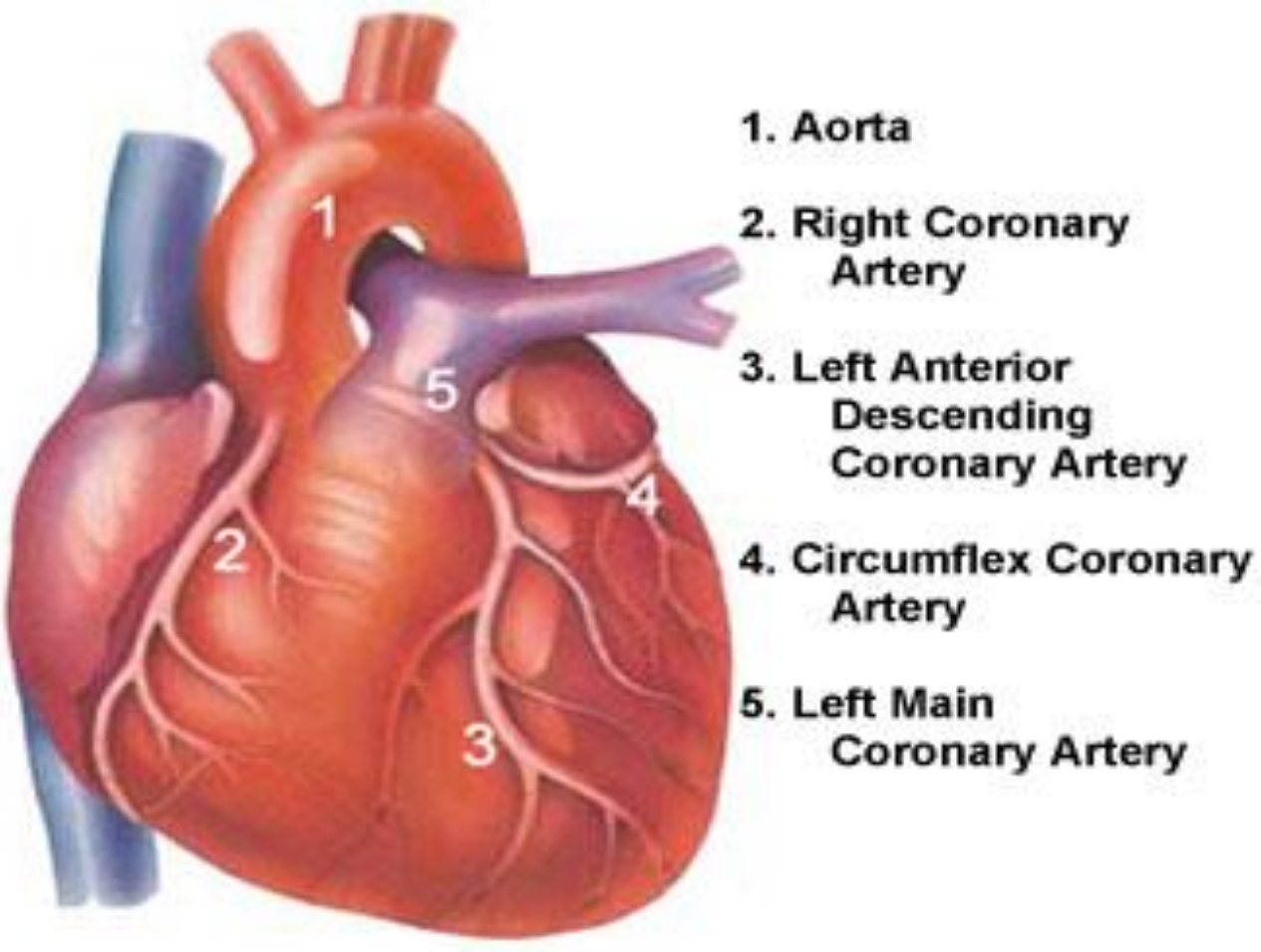

Figure 2.2 arteries of the heart (Buba, et al., 2008).

2.2.8.2 Venous Drainage of the Heart

The heart is drained mainly by veins that empty into the coronary sinus and partly by small veins that empty into the right atrium. The coronary sinus, the main vein of the heart, is a wide venous channel that runs from left to right in the posterior part of the coronary groove. The coronary sinus receives the great cardiac vein at its left end and the middle cardiac vein and small cardiac veins at its right end. The

left posterior ventricular vein and left marginal vein also open into the coronary sinus.

The great cardiac vein is the main tributary of the coronary sinus. Its first part (anterior interventricular vein) begins near the apex of the heart and ascends with the anterior IV branch of the LCA .The great cardiac vein drains the areas of the heart supplied by the LCA. The middle cardiac vein (posterior IV vein) accompanies the posterior interventricular branch (usually arising from the RCA), and a small cardiac vein accompanies the right marginal branch of the RCA. [37]

Some cardiac veins do not drain via the coronary sinus. Several small anterior cardiac veins begin over the anterior surface of the right ventricle; cross over the coronary groove, and usually end directly in the right atrium sometimes they enter the small cardiac vein. The smallest cardiac veins are minute vessels that begin in the capillary beds of the myocardium and open directly into the chambers of the heart, chiefly the atria. Although called veins, they are valve less communications with the capillary beds of the myocardium and may carry blood from the heart chambers to the myocardium(Fig 2.3**)** (Moore, and Dalley, 2006).

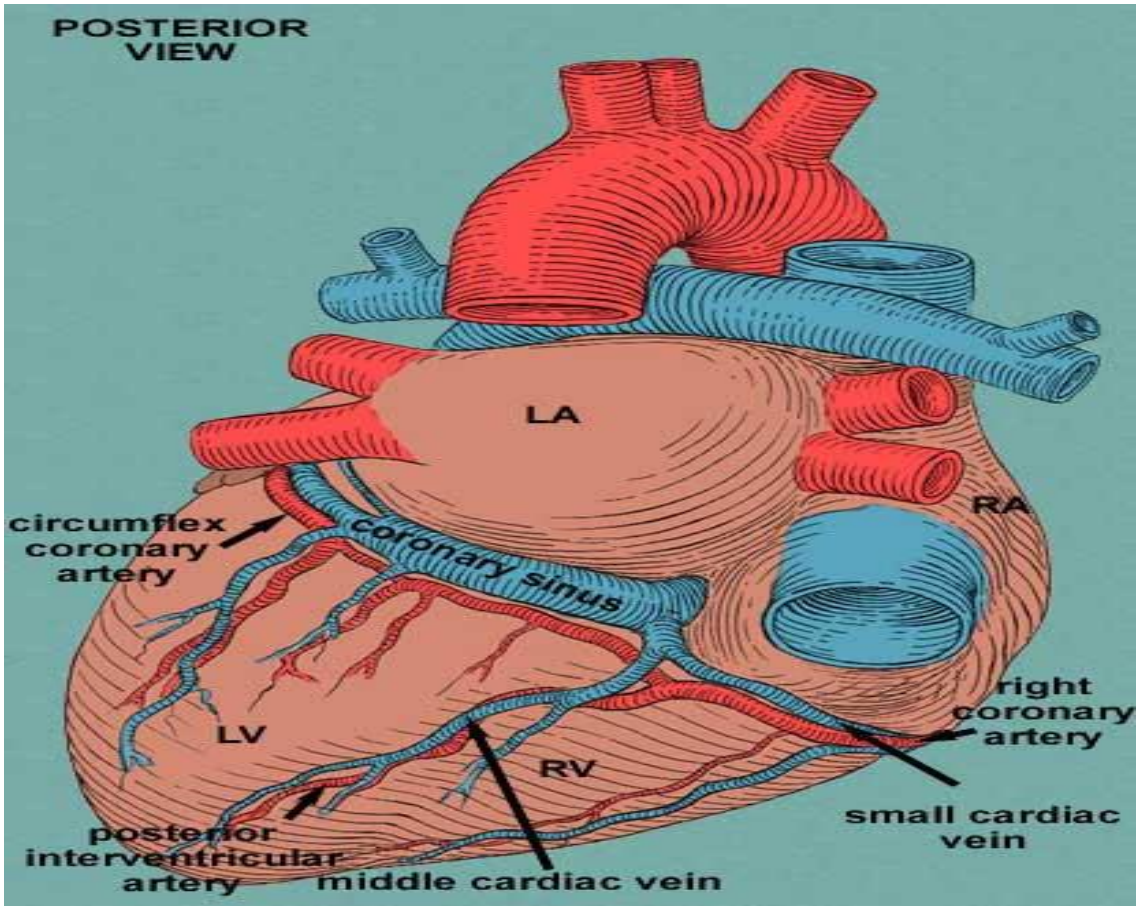

Figure 2.3 venues drainage of the heart (Buba, et al., 2008).

2.1.9 Lymphatic Drainage of the Heart

Lymphatic vessels in the myocardium and subendocardial connective tissue pass to the subepicardial lymphatic plexus. Vessels from this plexus pass to the coronary groove and follow the coronary arteries. A single lymphatic vessel, formed by the union of various vessels from the heart, ascends between the pulmonary trunk and left atrium and ends in the inferior tracheobronchial lymph nodes, usually on the right side (Snell, 2000).

2.1.10 Innervations of the Heart

The heart is supplied by autonomic nerve fibers from the cardiac plexus which is often quite artificially divided into superficial and deep portions.

The sympathetic supply is from presynaptic fibers, with cell bodies in the intermediolateral cell columns of the superior five or six thoracic segments of the spinal cord, and postsynaptic sympathetic fibers, with cell bodies in the cervical and superior thoracic paravertebral ganglia of the sympathetic trunks. The postsynaptic fibers traverse cardiopulmonary splanchnic nerves and the cardiac plexus to end in the SA and AV nodes and in relation to the terminations of parasympathetic fibers on the coronary arteries. Sympathetic stimulation causes increased heart rate; impulse conduction; force of contraction; and, at the same time, increased blood flow through the coronary vessels to support the increased activity (Moore, and Dalley, 2006).

The parasympathetic supply is from presynaptic fibers of the vagus nerves. Postsynaptic parasympathetic cell bodies (intrinsic ganglia) are located in the atrial wall and interatrial septum near the SA and AV nodes and along the coronary arteries. Parasympathetic stimulation slows the heart rate, reduces the force of the contraction, and constricts the coronary arteries, saving energy between periods of increased demand. Postsynaptic parasympathetic fibers release acetylcholine, which binds with muscarinic receptors to slow the rates of depolarization of the pacemaker cells and atrioventricular conduction and decrease atrial contractility (Moore, and Dalley, 2006).

2.2 Physiology of the heart The heart is the muscular organ of the circulatory system that constantly pumps blood throughout the body. Approximately the size of a clenched fist, the heart is composed of cardiac muscle tissue that is very strong and able to contract and relax rhythmically throughout a person's lifetime. (William 2003) The human heart is actually two pumps in one. The right side receives oxygen-poor blood from the various regions of the body and delivers it to the lungs. In the lungs, oxygen is absorbed in the blood. The left side of the heart

receives the oxygen-rich blood from the lungs and delivers it to the rest of the body (Ganong, , 2003)

The heart has four separate compartments or chambers. The upper chamber on each side of the heart, which is called an atrium, receives and collects the blood coming to the heart. The atrium then delivers blood to the powerful lower chamber, called a ventricle, which pumps blood away from the heart through powerful, rhythmic contractions (Ganong, , 2003)

2.2.1Mechanical events of the cardiac cycle

2.2.1.1 Events in Late Diastole

Late in diastole, the mitral and tricuspid valves between the atria and ventricles are open and the aortic and pulmonary valves are closed. Blood flows into the heart throughout diastole, filling the atria and ventricles. The rate of filling declines as the ventricles become distended, and especially when the heart rate is low the cusps of the atrioventricular (AV) valves drift toward the closed position the pressure in the ventricles remains low (Ganong, , 2003)

2.2.1.2AtrialSystole

Contraction of the atria propels some additional blood into the ventricles, but about 70% of the ventricular filling occurs passively during diastole. Contraction of the atrial muscle that surrounds the orifices of the superior and inferior vena cava and pulmonary veins narrows their orifices, and the inertia of the blood moving toward the heart tends to keep blood in it; however, there is some regurgitation of blood into the veins during atrial systole (Ganong, , 2003)

2.2.1.3VentricularSystole

At the start of ventricular systole, the mitral and tricuspid (AV) valves close. Ventricular muscle initially shortens relatively little, but intraventricular pressure

rises sharply as the myocardium presses on the blood in the ventricle (Ganong, , 2003)

This period of isovolumetric (isovolumic, isometric) ventricular contraction lasts about 0.05 s, until the pressures in the left and right ventricles exceed the pressures in the aorta (80 mm Hg) and pulmonary artery (10 mm Hg) and the aortic and pulmonary valves open. During isovolumetric contraction, the AV valves bulge into the atria, causing a small but sharp rise in atrial pressure (Ganong, , 2003)

When the aortic and pulmonary valves open, the phase of ventricular ejection begins. Ejection is rapid at first, slowing down as systole progresses. The intraventricular pressure rises to a maximum and then declines somewhat before ventricular systole ends. Peak left ventricular pressure is about 120 mm Hg, and peak right ventricular pressure is 25 mm Hg or less. Late in systole, the aortic pressure actually exceeds the ventricular, but for a short period momentum keeps the blood moving forward. The AV valves are pulled down by the contractions of the ventricular muscle, and atrial pressure drops. The amount of blood ejected by each ventricle per stroke at rest is 70-90 mL. The end-diastolic ventricular volume is about 130 mL. Thus, about 50 mL of blood remains in each ventricle at the end of systole (end-systolic ventricular volume), and the ejection fraction, the percent of the end-diastolic ventricular volume that is ejected with each stroke, is about 65%. The ejection fraction is a valuable indexofventricularfunction (Ganong, , 2003)

2.2.1.1Early Diastole

Once the ventricular muscle is fully contracted, the already falling ventricular pressures drop more rapidly. This is the period of protodiastole. It lasts about 0.04 s. It ends when the momentum of the ejected blood is overcome and the aortic and pulmonary valves close, setting up transient vibrations in the blood and blood vessel walls. After the valves are closed, pressure continues to drop rapidly during

the period of isovolumetric ventricular relaxation. Isovolumetric relaxation ends when the ventricular pressure falls below the atrial pressure and the AV valves open, permitting the ventricles to fill. Filling is rapid at first, then slows as the next cardiac contraction approaches. Atrial pressure continues to rise after the end of ventricular systole until the AV valves open, then drops and slowly rises again until the next atrial systole (Guyton, 2006).

2.2.2 Electrical Conduction System

The heart is composed primarily of muscle tissue. A network of nerve fibers coordinates the contraction and relaxation of the cardiac muscle tissue to obtain an efficient, wave-like pumping action of the heart (Fig 2.4) (Guyton, 2006).

1. Sinoatrial node (SA node)
2. Atrioventricular node (AV node)
3. Common AV Bundle
4. Right & Left Bundle Branches

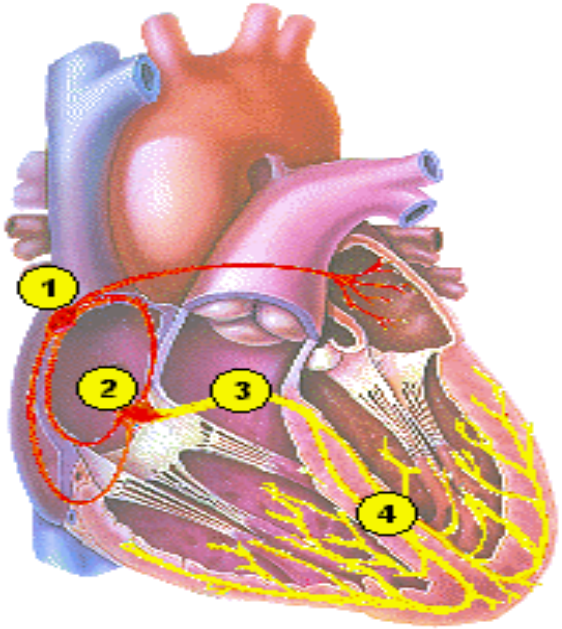

Figure 2.4 Electrical Conduction System of heart (Buba, et al., 2008).

The Sinoatrial Node (often called the SA node or sinus node) serves as the natural pacemaker for the heart. Nestled in the upper area of the right atrium, it sends the electrical impulse that triggers each heartbeat. The impulse spreads through the atria, prompting the cardiac muscle tissue to contract in a coordinated wave-like manner.

The impulse that originates from the sinoatrial node strikes the Atrioventricular node (or AV node) which is situated in the lower portion of the right atrium. The atrioventricular node in turn sends an impulse through the nerve network to the ventricles, initiating the same wave-like contraction of the ventricles (Guyton, 2006).

The electrical network serving the ventricles leaves the atrioventricular node through the Right and Left Bundle Branches. These nerve fibers send impulses that cause the cardiac muscle tissue to contract (Guyton, 2006).

2-3 Pathology of the heart

2-3 -1 Right Heart Failure

The symptomatic and prognostic relevance of the right ventricle in a myriad of conditions, including pulmonary arterial hypertension (PAH), left heartfailure, and after implantation of left ventricular assist devices (LVADs), has renewed interest in the right ventricle as more than a mere conduit for transmitting blood to the lungs. Accordingly, there has been growing interest in proper and ac-curate assessment of right ventricular (RV) function. Because right heart failure is typically aconsequence of increased afterload, a careful study of functional interactions between the right ventricle and pulmonary vascular system is warranted. Traditional hemodynamics by right heart catheterization (RHC) is routinely used to draw in-ferences on RV function, preload, and afterload. However, more robust methods for characterizing function, load, ventricular-

vascular coupling, and diastole are available and can more accurately interpret hemodynamics in patients with RV failure. This article reviews traditional and gold-standard hemodynamic assessments of the right ventricle in health and disease. (Verdecchia P 1990).

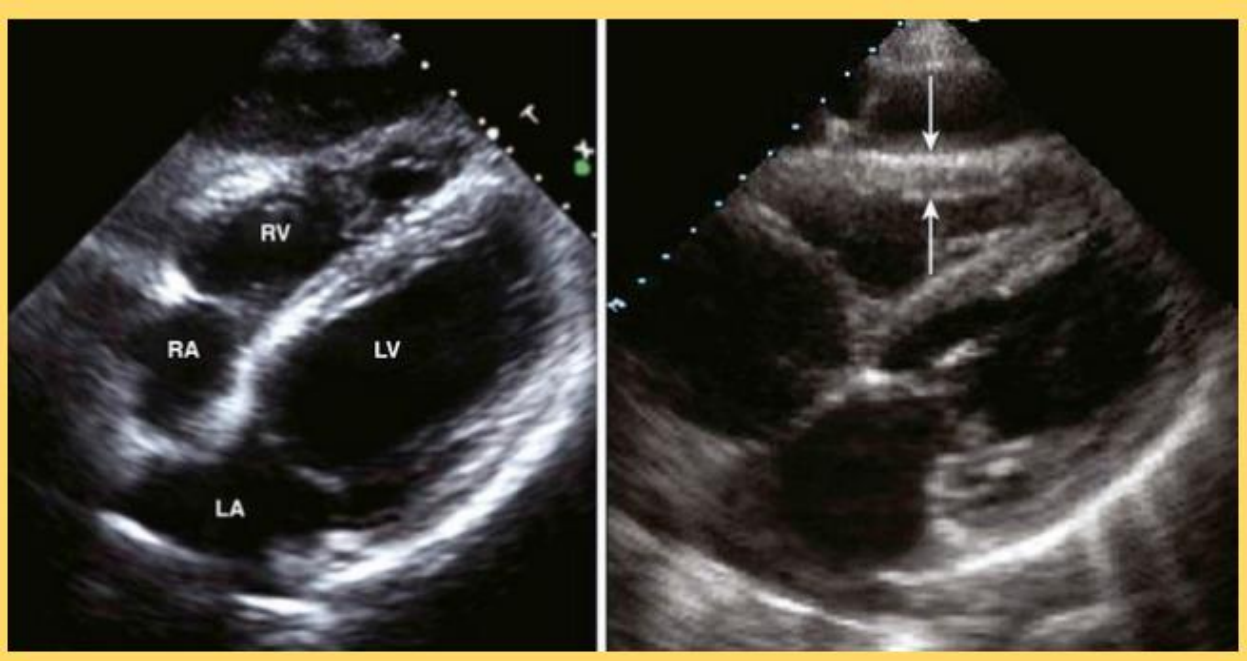

Figure (2.5): 2D echocardiogram from the subcostal view of a normal heart (left panel) and the heart in a patient with RV hypertrophy (right panel) showing measurement of RV free wall thickness (arrows),(Pleister, et al 2015)

2-3-2 Hypertensive heart disease

The cause of hypertensive heart disease is chronically elevated blood pressure (BP); however, the causes of elevated BP are diverse. Essential hypertension accounts for 90% of cases of hypertension in adults. Secondary causes of hypertension account for the remaining 10% of cases of chronically elevated BP.

According to the Framingham Study, hypertension accounts for about one quarter of heart failure cases.[In the elderly population, as many as 68% of heart failure

cases are attributed to hypertension .Community-based studies have demonstrated that hypertension may contribute to the development of heart failure in as many as 50-60% of patients. In patients with hypertension, the risk of heart failure is increased by 2-fold in men and by 3-fold in women.

Uncontrolled and prolonged elevation of BP can lead to a variety of changes in the myocardial structure, coronary vasculature, and conduction system of the heart. These changes in turn can lead to the development of left ventricular hypertrophy (LVH), coronary artery disease (CAD), various conduction system diseases, and systolic and diastolic dysfunction of the myocardium, complications that manifest clinically as angina or myocardial infarction, cardiac arrhythmias (especially atrial fibrillation), and congestive heart failure (CHF).

Thus, hypertensive heart disease is a term applied generally to heart diseases, such as LVH, coronary artery disease, cardiac arrhythmias, and CHF, that are caused by the direct or indirect effects of elevated BP. Although these diseases generally develop in response to chronically elevated BP, marked and acute elevation of BP can lead to accentuation of an underlying predisposition to any of the symptoms traditionally associated with chronic hypertension.

2-3 -3 Valvular disease

The diagnosis and management of commonly occurring valvular heart diseases for the primary care provider. Basic understanding of pathologic murmurs is important for appropriate referral. Echocardiography is the gold standard for diagnosis and severity grading. Patients with progressive valvular heart disease should be followed annually by cardiology and imaging should be performed based on the severity of valvular dysfunction. Surgery or intervention is recommended only when symptoms dictate or when changes in left ventricular function occur. Surgery or intervention should be performed after discussion by a heart team, including cardiologists and cardiac surgeons. (Kannel W, Cobb J.1992).

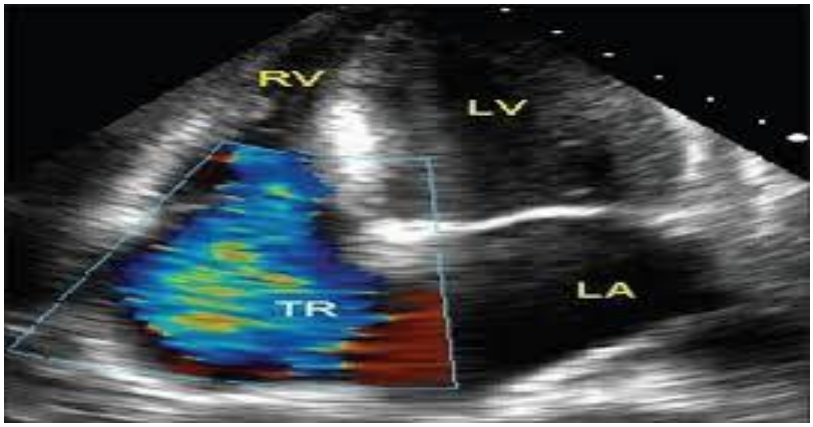

Figure (2.6): Tricuspid regurgitation (Kannel W, Cobb J.1992).

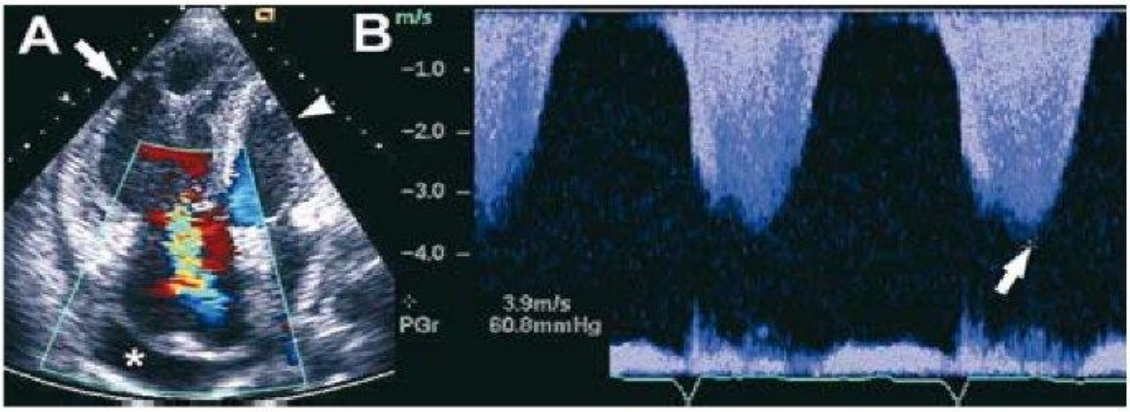

Figure (2.7): Mitral regurgitation, (Verdecchia P 1990).

2-3 -4 Left heart disease

Pulmonary hypertension (PH) is frequent in left heart disease (LHD), as a consequence of the underlying condition. Significant advances have occurred over the past 5 years since the 5th World Symposium on Pulmonary Hypertension in 2013, leading to a better understanding of PH-LHD, challenges and gaps in evidence. PH in heart failure with preserved ejection fraction represents the most complex situation, as it may be misdiagnosed with group 1 PH. Based on the latest

evidence, we propose a new haemodynamic definition for PH due to LHD and a three-step pragmatic approach to differential diagnosis. This includes the identification of a specific "left heart" phenotype and a non-invasive probability of PH-LHD. Invasive confirmation of PH-LHD is based on the accurate measurement of pulmonary arterial wedge pressure and, in patients with high probability, provocative testing to clarify the diagnosis. Finally, recent clinical trials did not demonstrate a benefit in treating PH due to LHD with pulmonary arterial hypertension-approved therapies.

Figure (2.8): Concentric LVH (Verdecchia P 1990).

2-3 -5 Left atrial abnormalities

Frequently underappreciated, structural and functional changes of the left atrium are very common in patients with hypertension. The increased afterload imposed on the LA by the elevated LV end-diastolic pressure secondary to increased BP leads to impairment of the left atrium and left atrial (LA) appendage function, plus increased LA size and thickness.

Increased LA size accompanying hypertension in the absence of valvular heart disease or systolic dysfunction usually implies chronicity of hypertension and may correlate with the severity of LV diastolic dysfunction.

In addition to LA structural changes, these patients are predisposed to atrial fibrillation. Atrial fibrillation, with loss of atrial contribution in the presence of diastolic dysfunction, may precipitate overt heart failure, (Avdić S, et al 2007).

Figure (2.9): Dilated Right, left atrium.

2-3 -6 Congenital heart disease

Pulmonary arterial hypertension (PAH) is commonly associated with congenital heart disease (CHD) and relates to type of the underlying cardiac defects and repair history. Large systemic to pulmonary shunts may develop PAH if untreated or repaired late. PAH, when present, markedly increases morbidity and mortality in patients with CHD. Significant progress has been made for patients with Eisenmenger syndrome in pathophysiology, prognostication and disease-targeting therapy (DTT), which needs to be applied to routine patient care. Patients with PAH-CHD and systemic to pulmonary shunting may benefit from late defect closure if pulmonary vascular resistance (PVR) is still normal or near normal. Patients with PAH and coincidental defects, or previous repair of CHD should be managed as those with idiopathic PAH. Patients with a Fontan circulation, despite not strictly fulfilling criteria for PAH, may have elevated PVR; recent evidence

suggests that they may also benefit from DTT, but more data are required before general recommendations can be made. CHD-PAH is a lifelong, progressive disease; patients should receive tertiary care and benefit from a proactive DTT approach. Novel biomarkers and genetic advances may identify patients with CHD who should be referred for late defect closure and/or patients at high risk of developing PAH despite early closure in childhood. Ongoing vigilance for PAH and further controlled studies is clearly warranted in CHD. (Van Dissel,et al,2017)

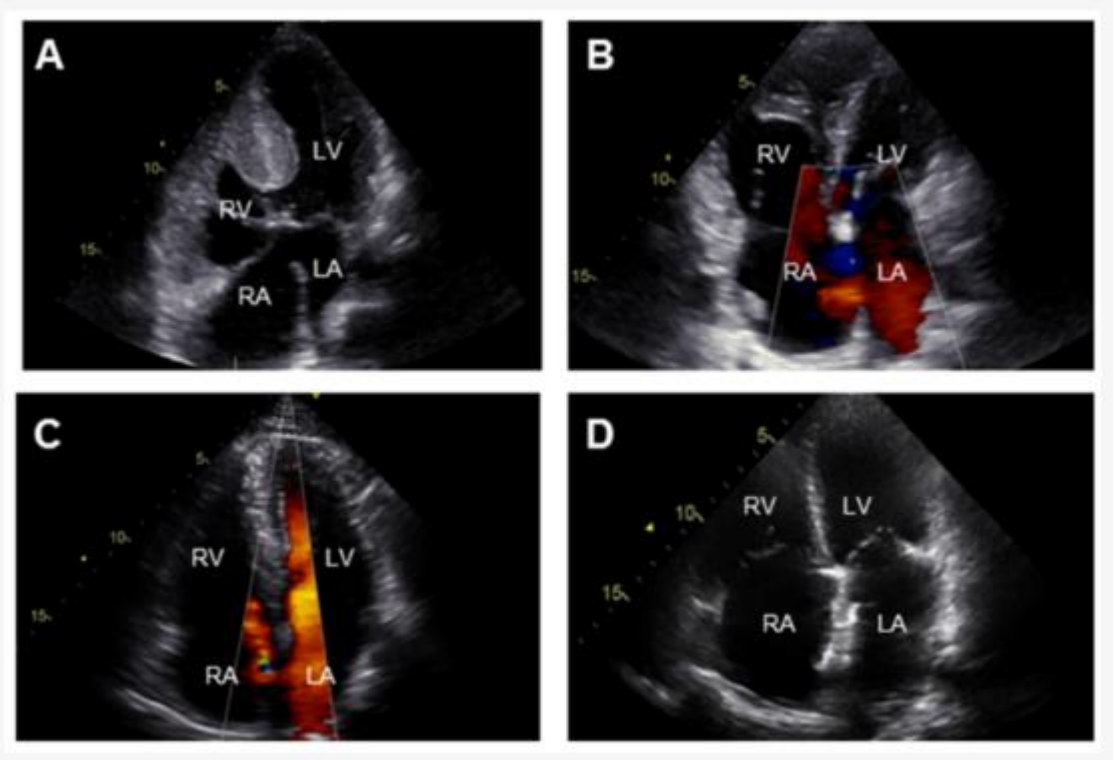

Figure (2.10):. Transthoracic echocardiographic (apical four chamber view) images of the 4 clinical subgroups in pulmonary arterial hypertension associated with congenital heart disease (PAH-CHD): (A) Eisenmenger syndrome: atrioventricular septal defect; (B) PAH associated with prevalent systemic-to-pulmonary shunt lesion: atrial septal defect with left-to-right shunt; (C) PAH associated with small or coincidental cardiac defect: secundum atrial septal defect; (D) PAH after defect closure: closed atrial septal defect. LA = left atrium; LV = left ventricle; RA = right atrium; RV = right ventricle.(Van Dissel,et al,2017)

2-3 -7 .Myocardial ischemia

Patients with angina have a high prevalence of hypertension. Hypertension is an established risk factor for the development of coronary artery disease, almost doubling the risk. The development of ischemia in patients with hypertension is multifactorial.

Importantly, in patients with hypertension, angina can occur in the absence of epicardial coronary artery disease. The reason for this is 2-fold. Increased afterload secondary to hypertension leads to an increase in LV wall tension and transmural pressure, compromising coronary blood flow during diastole. In addition, the microvasculature beyond the epicardial coronary arteries has been shown to be dysfunctional in patients with hypertension, and it may be unable to compensate for increased metabolic and oxygen demand, (Avdić S, et al 2007).

The development and progression of arteriosclerosis, the hallmark of coronary artery disease, is exacerbated in arteries subjected to chronically elevated BP. Shear stress associated with hypertension and the resulting endothelial dysfunction cause impairment in the synthesis and release of the potent vasodilator nitric oxide. A decreased nitric oxide level promotes the development and acceleration of arteriosclerosis and plaque formation. Morphologic features of the plaque are identical to those observed in patients without hypertension.

2-4-Echocardiography:

Echocardiography is a simple ultrasound of the heart performed by ultrasound specialist its done with the patient lying down. The specialist uses a computer with a transducer attachment and a clear jelly like substance is wiped on the skin and helps the transducers accuracy .this is the same technology used to look at fetuses during pregnancy .the transducers is then pushed against the patients chest.it emits

sound waves that (echo) back when they hit an object like aheart valve allowing a moving image to be seen on screen

2-4-1 Sites of transducer placement:

Air being a poor conductor of **ultrasound**, the transducer should be placed at points without lung interference .Such sites are(left parasternal space (standard point) apex of the heart , suprasternal notch (to study aorta & major branches) , xiphisternum – useful in patients emphysematous lung , right parasternal space in dextroposition&dextrocardia, and oesophagus,using a trans—oesophageal transducer

2-4-1-1 Right Heart Imaging Protocol

The protocol includes the measurement of a range of parameters assessed from windows (parasternal, apical and subcostal view), which is first described using Doppler examination and secondly using M-mode examination. The aim of the measures selected is to determine the pressure within, and the capacity and function of, the RV.

2-4-1-2 Parasternal views

In normal subjects the anterior RV wall is thin; its mass is less than one sixth and its diameter less than one third of the LV.

In the parasternal long-axis view, the moderator band is usually seen close to the IVS traversing the RV and care should be taken not to include the moderator band in the measurements of the IVS. In significant PH, the LV cavity may be reduced in size in both systole and diastole, with deviation (bowing) of the septum towards the LV (fig. (2-7). a and b).

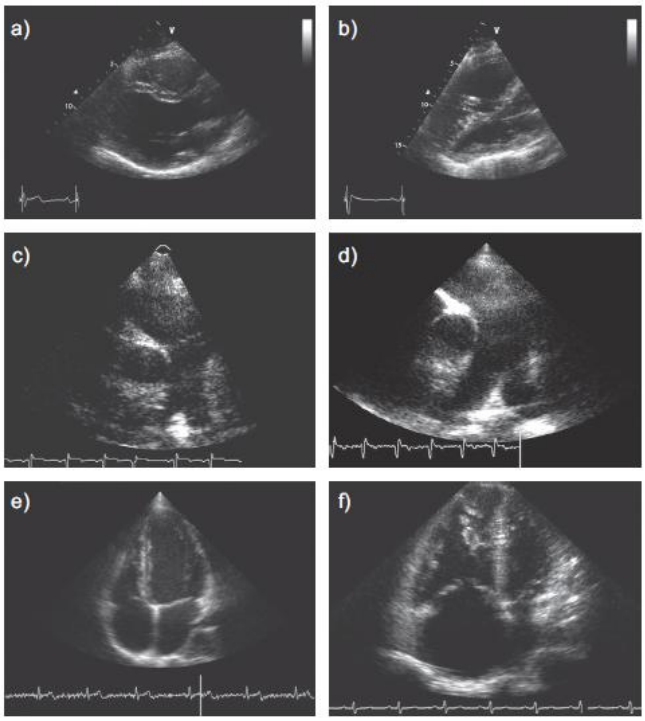

Figure (2-11). a) Normal parasternal long-axis view. Note that the right ventricle is less than one third of the size of the left ventricle. b) Parasternal long-axis view in pulmonary hypertension (PH). Severely dilated right ventricle with hypertrophy of the moderator band and the right ventricular free wall. The left ventricular cavity is small due to chronic right ventricular pressure overload. c) Normal parasternal long-axis view of the right ventricular outflow tract (RVOT) showing the main pulmonary trunk, branches of the pulmonary artery and the pulmonary valve. d) Parasternal long-axis view of the RVOT in PH showing the dilated pulmonary artery and branches. e) Normal apical four-chamber view. f) Apical four-chamber view in PH showing marked right ventricular dilation and hypertrophy.

The long-axis view of the RV inflow tract may also allow for optimal alignment for estimation of TRV when the tricuspid regurgitant jet is eccentric. Abnormalities of the leaflets and subvalvular apparatus should also be assessed to

exclude primary valvular pathology. In addition, this view may be used to provide a qualitative estimate of RV systolic function.

The long- and short-axis views of the right ventricular outflow tract (RVOT) are useful for the assessment of the main pulmonary artery, which is dilated in relation to the adjacent aorta in PH, and pulmonary regurgitation (fig. (2-7). c and d).

However, we are not aware of any data to suggest that dilation of the pulmonary artery is a sensitive measurement for detection of PH using echocardiography.

As well as demonstrating the atria and RV, the short-axis view of the aorta and left atrium shows the aortic, tricuspid and pulmonary valves simultaneously, making this a useful view for the assessment of structural valvular abnormalities. It can also help to identify an atrial septal defect using a zoom view of the interatrial septum with colour Doppler imaging. RV dilation and hypertrophy, as well as dilation of the pulmonary artery, can also be seen in this view. Finally, the degree of distortion of the LV and IVS arising due to increased pressure in the RV during diastole and systole (LV eccentricity index) can be quantified using a short-axis view at the level of left ventricular papillary muscles. While in a normal situation the LV appears circular in shape, in systole and diastole dilation of the RV and increased RV pressure in severe PH shifts the IVS to the left, giving the LV a characteristic D-shape. Consequently, a RV that is dilated purely due to volume overload will deviate the septum, mainly in diastole, due to raised end diastolic pressure and, conversely, a pressure-loaded RV will deviate the septum in systole. When pressure overload is severe the septum may even be deviated into the LV cavity itself.

Apical four-chamber views

A number of parameters influenced by the presence of PH can be assessed in this view, including RV dilation and hypertrophy, with systolic dysfunction and reduced myocardial tissue velocities being quantifiable by tissue Doppler imaging.

In PH, the apex is frequently hypertrophied and akinetic, and careful examination of the apex should be performed to exclude thrombus or an apical mass .(Grapsa et al,2011).. Diastolic opening of the tricuspid leaflets, which can also be assessed in this view,

becomes less vigorous as PH progresses. The tricuspid valve leaflet adjacent to the free wall may be either the anterior (most commonly) or posterior leaflet, depending on the exact rotation and angulation of the image plane. Tricuspid leaflets are uniformly echogenic, with normal coaptation in systole. When significant tricuspid regurgitation develops in PH, careful identification of any structural abnormalities is needed to ensure primary tricuspid incompetence is differentiated from secondary incompetence due to the annular dilation.

The interatrial and interventricular septums can be clearly delineated (fig. (2-7). e and f). Drop-out artefact is commonly seen in the region of fossa ovalis and this should not be mistaken for an atrial septal defect. The use of tissue Doppler imaging to the septal and lateral LV walls may help to identify significant LV diastolic dysfunction.

Subcostal view

The subcostal view allows the degree of RV dysfunction and the thickness of the RV walls to be estimated. This assessment is particularly useful in patients where parasternal or apical window views are difficult to image, such as those with COPD.

It provides the best view for the measurement of RV inferior wall thickness and determines the presence of an atrial septal defect. The diameter of the inferior vena cava measured at rest and during inspiration in this view can be used to provide an estimate of right atrial pressure (Pra).

Doppler examination

As part of a full echocardiographic assessment, Doppler examination should be performed in the following sequence:(colour Doppler in all apical projections, colour Doppler in parasternal projections (long axis/short axis), pulsed-wave Doppler for transmitral velocities , pulsed-wave Doppler for LV outflow tract, pulsed-wave Doppler for the tricuspid inflow, pulsed-wave Doppler for the RVOT Continuous-wave Doppler across the LV outflow aortic valve, Continuous-wave Doppler across the tricuspid valve (for tricuspid regurgitation); Continuous-wave Doppler across the pulmonary valve (for pulmonary regurgitation), Tissue Doppler imaging (TDI) of the RV free wall.

ressure Measurements in PH

PRA can be estimated by measurement of the diameter of the inferior vena cava at end-expiration and during sharp inspiration using M-mode in the subcostal view (fig. (2-8).

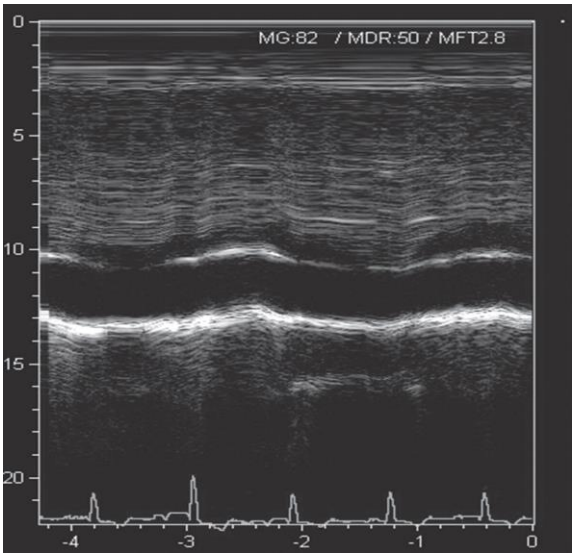

Figure. (2-12). Right atrial pressure: M-mode during sniff manoeuvre.

High PRA is associated with dilation of the vena cava (normal range 1.5–2.5 cm) and/or failure of the segment adjacent to the right atrium to collapse by at least 50% with inspiration .

Inferior vena cava diameter 20 mm with respiratory variation of diameter ,50% has been shown to be significantly associated with mortality in patients with PAH (Brierre et al. 2010)..

TRV reflects the difference in pressure between the RV and the right atrium and can be measured from continuous wave Doppler of the tricuspid regurgitant jet from the apical fourchamber view, or from the parasternal RV inflow view if the regurgitant jet is eccentric (fig. (2-9).).

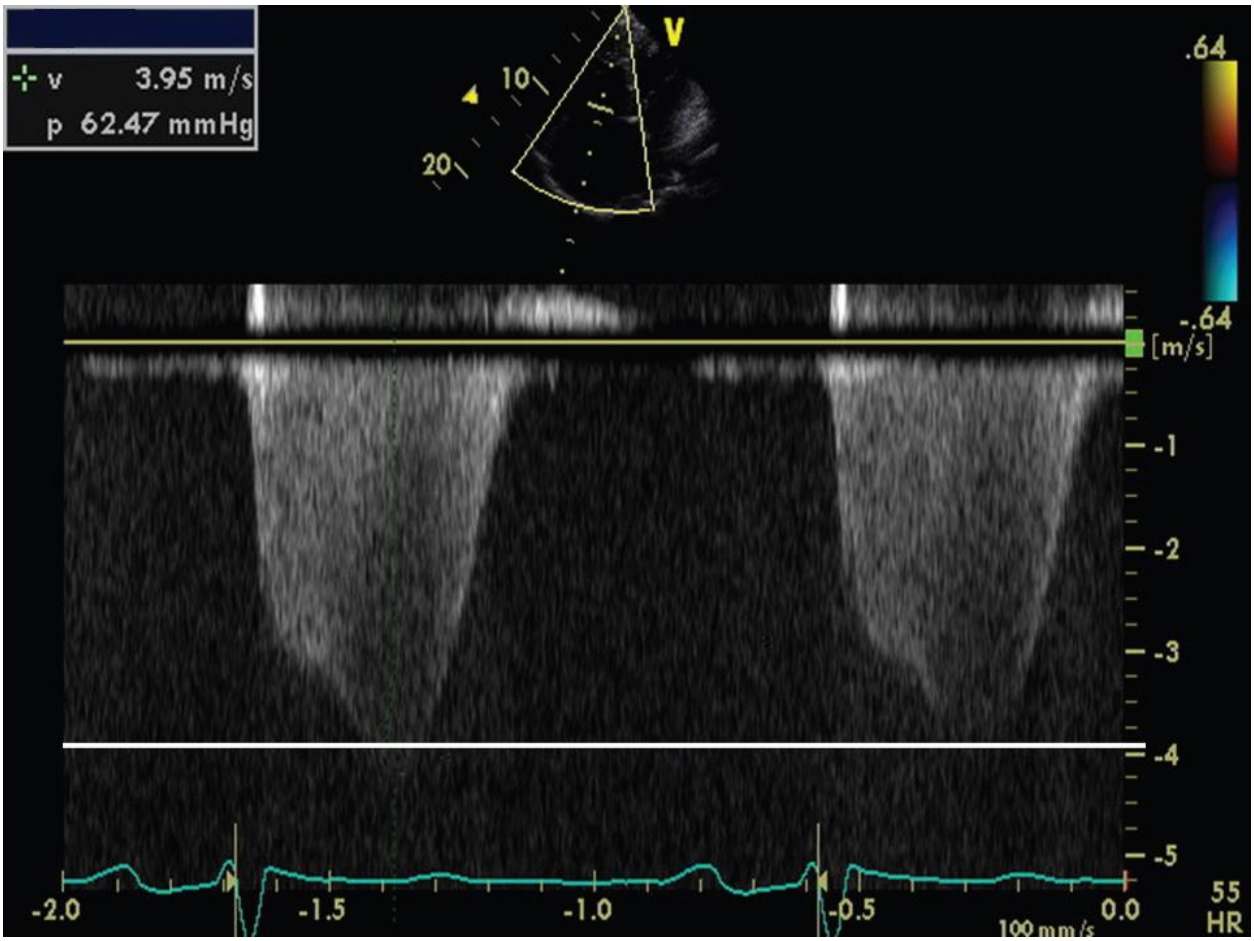

Figure. (2-13). the peak tricuspid regurgitant velocity.

When pulmonary stenosis is absent, the RV systolic pressure (RVSP) is assumed to be equivalent to the systolic Ppa and can be calculated from the TRV using the Bernoulli equation, using estimated Pra from

inferior vena cava diameter .(Grapsa et al,2011).

systolic Ppa5RVSP54(TRVend)^2 +Pra

where TRVend is peak TRV at end diastole.

Mean Ppa and pulmonary end-diastolic pressure are not routinely used in the diagnosis or follow-up of PH, but may be useful when TRV cannot be used or is unreliable. In 2D-echocardiography, the pulmonary valve is best imaged fromthe parasternal short-axis at the level of the aortic valve (fig. 1c and 1d). Pulmonary valvular motion can be determined with M-mode echocardiography and may show mid-diastolic closure. Mean Ppa and pulmonary enddiastolic pressure can be derived from the TRV at the beginning (PRVbd) and end (PRVed) of diastole, respectively (fig. (2-10).). pulmonary end-diastolic pressure54(PRVed)2+Pra mPpa54(PRVbd)2

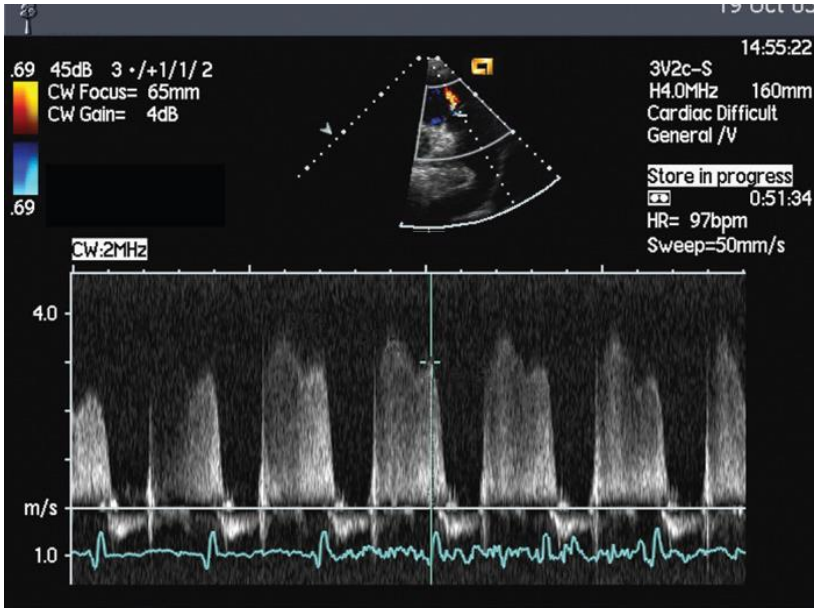

Figure. (2-14). Pulmonary regurgitant velocity at the start of diastole (PRVbd) and end-diastole (PRVed).

By positioning the sample volume at the centre of the pulmonary artery (ideally at the annulus) in the short-axis view, acceleration time can be measured in the parasternal short-axis view (fig. (2-11).

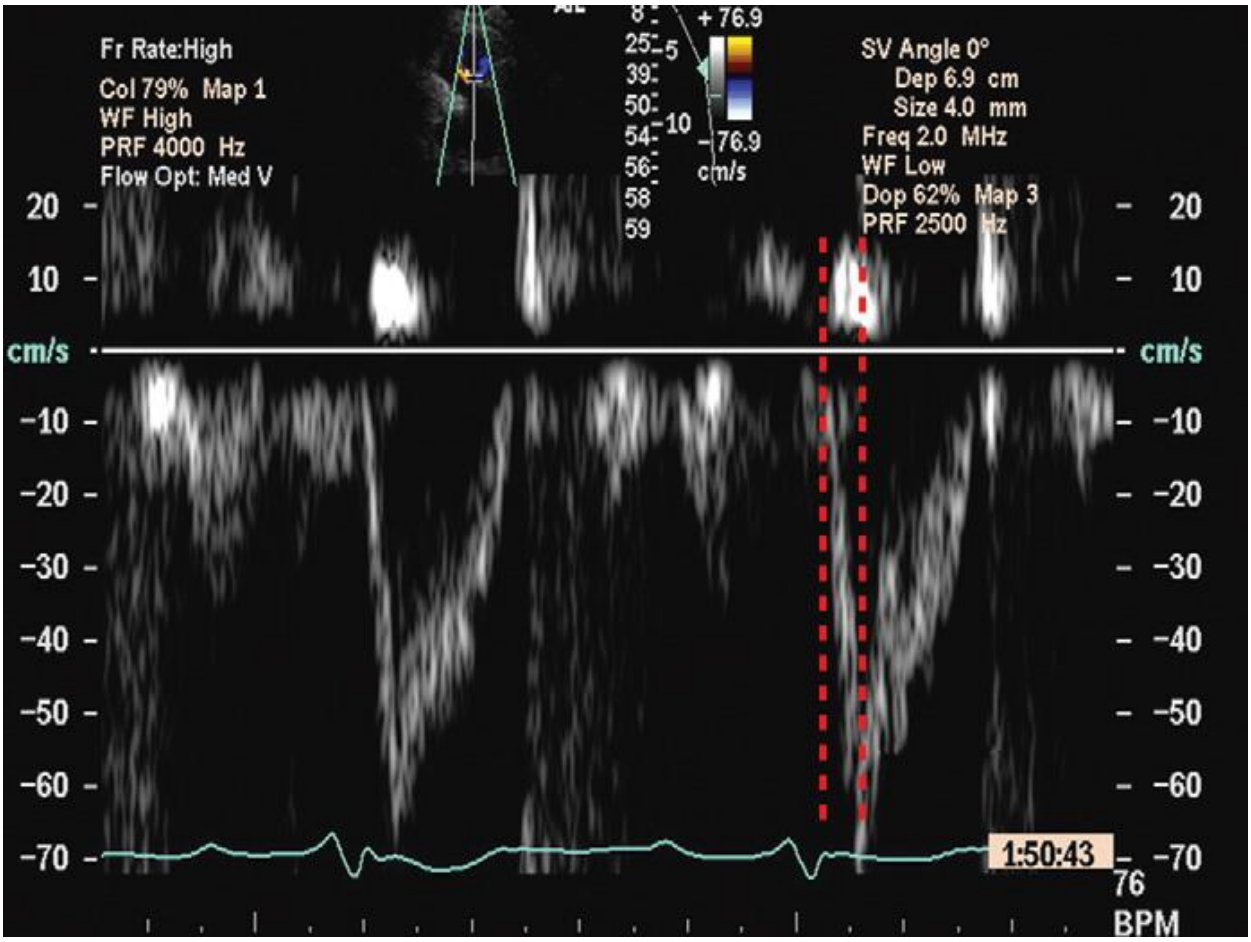

Figure. (2-15). .Acceleration time (AT) measured across the pulmonary outflow tract in the parasternal short-axis view.

Cardiac Chamber Cavity Measurements in PH

Right atrial volume index is calculated from the apical four chamber view or from the subcostal view, and is measured at maximum atrial volume at end-systole. The single plane area– length method is used and right atrium volume is measured using the area and the long-axis length of the atrium (fig. (2-15). a and b) .

right atrium volume index5(0.85 A2/L)/BSA where A is the atrium area in any view (cm2), L is the long-axis atrium length (cm) and BSA is body surface area.

RV fractional area change (%)5 (end-diastolic area - end-systolic area)/end-diastolic area LV eccentricity index is the ratio of the minor axis of the LV parallel to the septum (D2) divided by the minor axis perpendicular to the septum (D1) and is measured in the parasternal short-axis view at the level of the LV papillary muscles (fig. (2-15). c and d) in both end diastole and end systole.

Measures of function in PH

Myocardial performance index of the RV, also known as the Tei index, is made up of a combination of systolic and diastolic measurements. It has a number of advantages as a functional measure, including: 1) being relatively unaffected

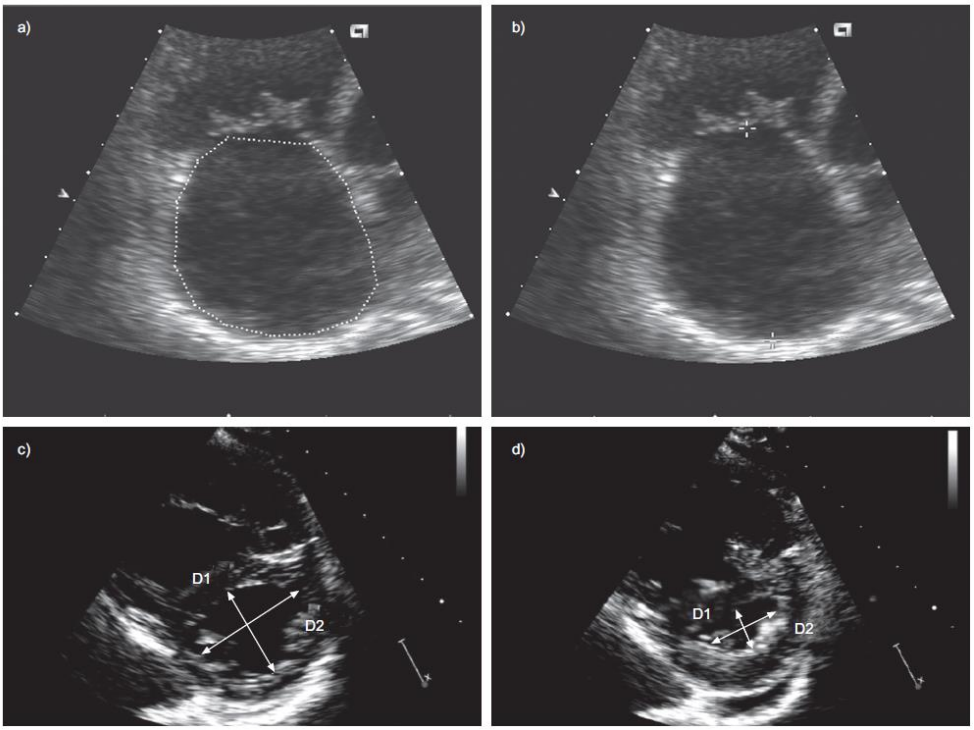

Figure (2-16. a) Measurement of the right atrial a) area and b) long axis for calculation of right atrial volume. c) Measurement of the left ventricular eccentricity index in end-diastole and d) end-systole. DI: minor axis perpendicular to the septum; D2: minor axis of the left ventricle parallel to the septum.

by heart rate, loading conditions or the presence and severity of tricuspid regurgitation; 2) having good reproducibility; 3) being quick to calculate; 4) not relying on the use of geometric models; and 5) being able to be applied even in the presence of a difficult acoustic window.

The Tei index can be measured either from colour Doppler imaging (apical four-chamber view for the tricuspid inflow pattern and the parasternal short-axis RVOT view for the determination of ejection time) or tissue Doppler imaging (fig. 2-13). The Tei index should be indexed for heart rate, as described previously for RVOT acceleration time. In patients with idiopathic PAH the index correlates with symptoms and values .0.88 predict poor survival (Tei et al ,1996).

Systolic (S') wave velocity is a measure of myocardial contraction and may be determined from the average of three TDI signals from different cardiac cycles . Like TAPSE, S' wave velocity is load dependent and may be pseudonormal under conditions of increased volume loading . Unlike most indices of function, S' wave velocity requires correction when heart rate is.100 bpm or falls to ,70 bpm. Therefore, S' wave velocity should be indexed for heart rate, as described previously for RVOT acceleration time.

Normal values and those in PH obtained by echocardiography.Isovolumic relaxation time (IVRT) of the RV is defined as the time from pulmonary valve closure to tricuspid valve opening and can be measured either by pulsed-wave Doppler from tricuspid inflow or with tissue Doppler imaging of the RV free wall. Prolongation of IVRT indicates poor myocardial relaxation, which is highly suggestive of PH, although it does not provide prognostic value (fig. 2-15).

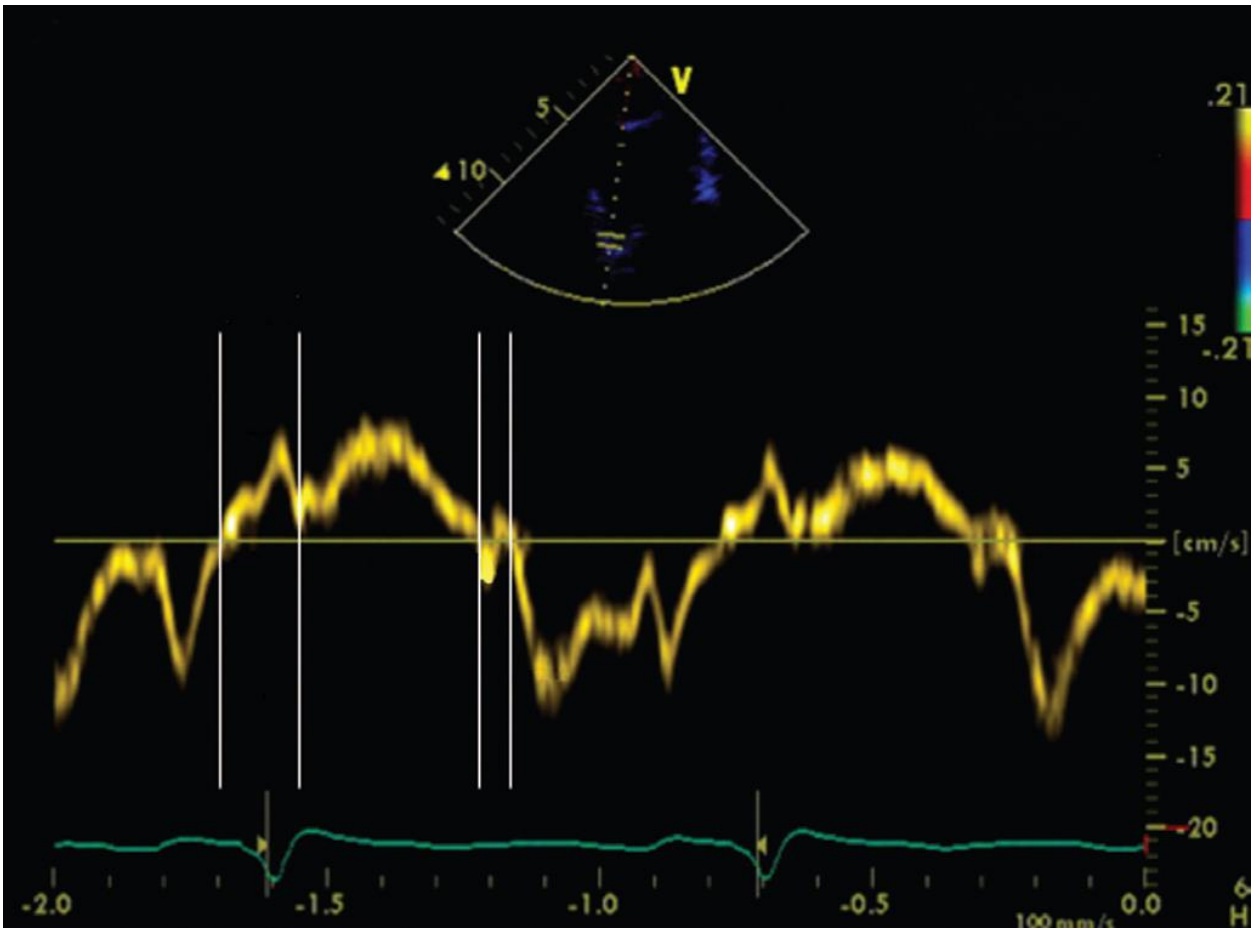

Figure (2-17). Measurement of myocardial performance index (MPI) using tissue Doppler imaging. S': systolic wave; IVCT: isovolumic contraction time; IVRT: isovolumic relaxation time.

IVRT should be indexed for heart rate as described previously for RVOT acceleration time.

TAPSE is the reflection of the movement of base to apex shortening of the RV in systole and can be derived from the four-chamber view (fig. 2-16).

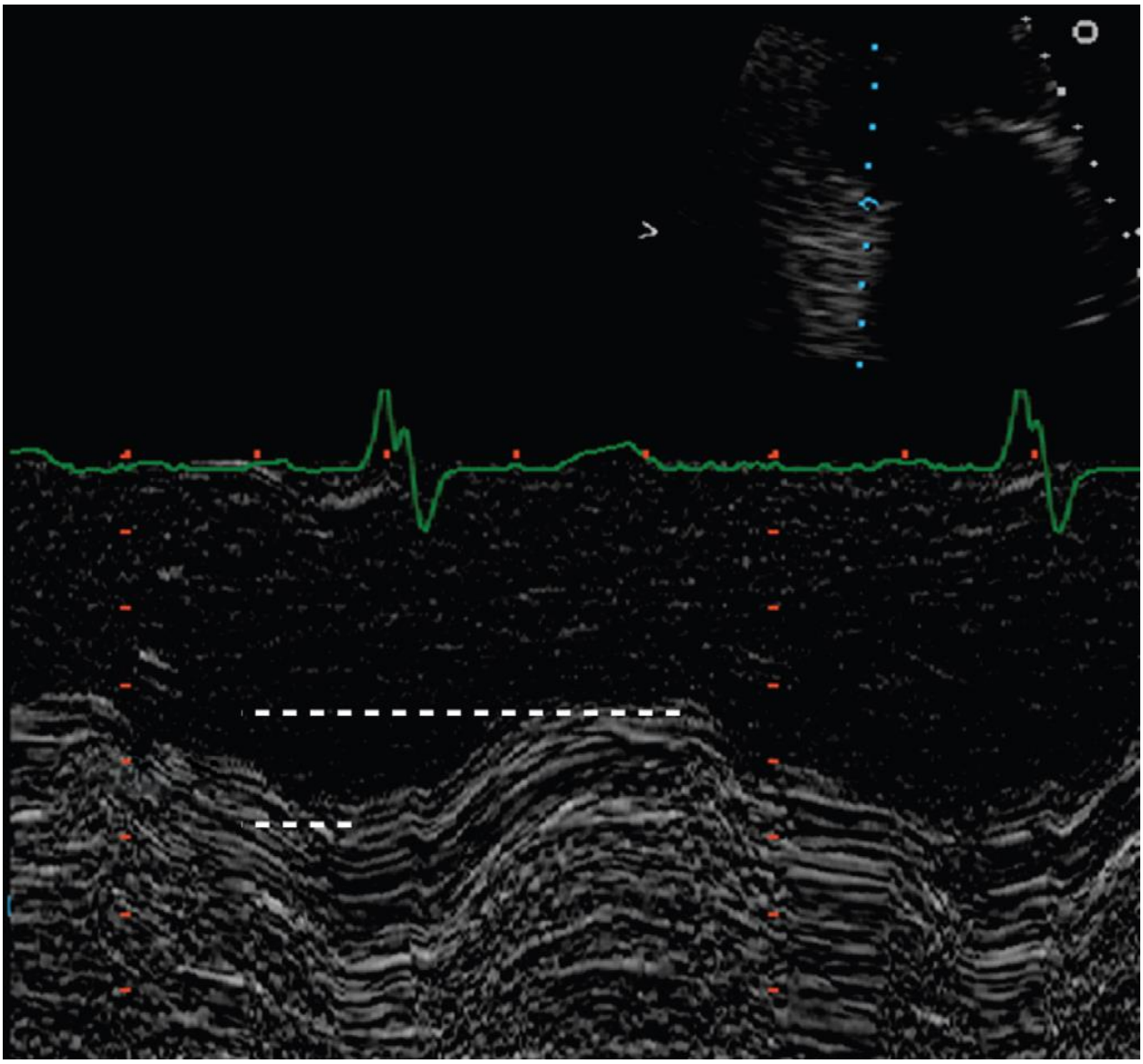

Figure (2-18. Measurement of tricuspid annular plane systolic excursion (TAPSE); ET: ejections time.

When measuring TAPSE, it is important to ensure that the entire RV is included in the view, in particular that there is no dropout in the endocardial outline along the IVS and RV free wall. Maximal TAPSE is defined by the total excursion of the tricuspid annulus from its highest position after atrial ascent to the peak descent during ventricular systole .(Kaul et al ,1984). A TAPSE of ,15 mm is associated with a significantly higher risk of mortality compared with a TAPSE

2-5 Previous Studies

In reviewing of literature there are some published studies regarding Pulmonary Artery Pressure and Resistance Using Echocardiographys by many researchers .The following is a summary of the most relevant studies:

Lin, et al in (2009). Studied The correlation between right descending pulmonary artery diameter and echocardiographyestimated systolic pulmonary artery pressure In a total of 229 subjects enrolled, SPAP was estimated by transthoracic Doppler echocardiography. PH was defined as SPAP greater than 30 mmHg. RDPAD was measured on a chest X-ray (postero-anterior view) taken within one month of the echocardiography.We applied two-sample Student's t-test to test the difference of RDPAD between groups with and without PH. Linear regression analysis was performed to assess the relationship between SPAP and RDPAD. Receiver operating characteristic (ROC) curve was done to seek a potential cut-off point of RDPAD that discriminated between PH and non-PH.they found Two-sample Student's t-test revealed RDPAD were higher in the PH group than the non-PH group ($p = 0.024$). Linear regression analysis showed SPAP = 20.9 + 0.53*RDPAD ($p = 0.047$), which implied a positive association between RDPAD and SPAP. However, ROC curve analysis did not find any satisfactory cut-off point of RDPAD for predicting PH. Even with RDPAD value of mean + 2SD of the non-PH group, its sensitivity and specificity, positive predictive value, negative predictive value, overall accuracy, positive likelihood ratio, and negative likelihood value were 6.7%, 97.9%, 66.8%, 62.3%, 62.5%, 3.1, and 0.95, respectively.

Bossone in (2013). Echocardiography in pulmonary arterial hypertension: from diagnosis to prognosis. Pulmonary arterial hypertension is most often diagnosed in its advanced stages because of the nonspecific nature of early symptoms and signs.

Although clinical assessment is essential when evaluating patients with suspected pulmonary arterial hypertension, echocardiography is a key screening tool in the diagnostic algorithm. It provides an estimate of pulmonary artery pressure, either at rest or during exercise, and is useful in ruling out secondary causes of pulmonary hypertension. In addition, echocardiography is valuable in assessing prognosis and treatment options, monitoring the efficacy of specific therapeutic interventions,and detecting the preclinical stages of disease.

Howard et al in (2012). Studied Echocardiographic assessment of pulmonary hypertension: standard operating procedure. ABSTRACT: Patients with suspected pulmonary hypertension (PH) should be evaluated using a multimodality approach to ensure that they receive a correct diagnosis. The series of investigations required includes clinical evaluation, noninvasive imaging techniques and right heart catheterisation (considered to be the ‘‘gold standard’’ for the diagnosis of PH). Current guidelines recommend that a detailed echocardiographic assessment is performed in all patients with suspected PH. In this review we summarise a protocol adopted by the National Pulmonary Hypertension Centres of UK and Ireland and approved by the British Society of Echocardiography for the evaluation of these patients. The views and measurements described are recommended for diagnosis, assisting in prognosis and providing a noninvasive means of following disease progression or response to therapy.

Sbano et al (2003) . reviewed The role of Doppler echocardiography in the evaluation of pulmonary hypertension , they revealed that A precise evaluation of pulmonary pressure is of fundamental importance in the diagnosis and management of patients with pulmonary hypertension (PH). Doppler echocardiography is a low cost, non-invasive method that is widely used for anatomical and functional assessment of the right cardiac chambers and estimation of pulmonary pressure and the hemodynamic data obtained correlates well with

that obtained through cardiac catheterization. Although the most appropriate and common technique for determining pulmonary pressure is measurement of the gradient between right ventricle and right atrium through tricuspid regurgitation, it can also be determined by analysis of pulmonary regurgitation or systolic pulmonary flow. When transthoracic echocardiography does not provide adequate viewing, transesophageal echocardiography is an excellent option, allowing for high quality imaging of cardiac structures and detection of some PAH-related disorders. In the literature, the role of echocardiography in the diagnosis of PAH, as well as in therapeutic and prognostic evaluation has been well established. In pulmonary thromboembolism patients, right ventricular dysfunction, an important indicator for thrombolytic therapy, can be detected using echocardiography. In addition, echocardiography is currently being widely used for monitoring therapeutic response in patients with primary PH, in the assessment of chronic obstructive pulmonary disease and in the follow up of lung transplant patients.

Augustine et al (2018). Studied Echocardiographic assessment of pulmonary hypertension: a guideline protocol from the British Society of Echocardiography,Pulmonary hypertension is defined as a mean arterial pressure of ≥25 mmHg as confirmed on right heart catheterisation. Traditionally, the pulmonary arterial systolic pressure has been estimated on echo by utilising the simplified Bernoulli equation from the peak tricuspid regurgitant velocity and adding this to an estimate of right atrial pressure. Previous studies have demonstrated a correlation between this estimate of pulmonary arterial systolic pressure and that obtained from invasive measurement across a cohort of patients. However, for an individual patient significant overestimation and underestimation can occur and the levels of agreement between the two is poor. Recent guidance has suggested that echocardiographic assessment of pulmonary hypertension should be limited to determining the probability of pulmonary hypertension being

present rather than estimating the pulmonary artery pressure. In those patients in whom the presence of pulmonary hypertension requires confirmation, this should be done with right heart catheterisation when indicated. This guideline protocol from the British Society of Echocardiography aims to outline a practical approach to assessing the probability of pulmonary hypertension using echocardiography and should be used in conjunction with the previously published minimum dataset for a standard transthoracic echocardiogram.

Kanwar et al . (2021). Studied Elevated Pulmonary Pressure Noted on Echocardiogram: A Simplified Approach to Next Steps. An elevated right ventricular/pulmonary artery systolic pressure suggestive of pulmonary hypertension (PH) is a common finding noted on echocardiography and is considered a marker for poor clinical outcomes, regardless of the cause. Even mild elevation of pulmonary pressure can be considered a modifiable risk factor, informing the trajectory of patients'clinical outcome. Although guidelines have been published detailing diagnostic and management algorithms, this echocardiographic finding is often underappreciated or not acted upon. Hence, patients with PH are often diagnosed in clinical practice when hemodynamic abnormalities are already moderate or severe. This results in delayed initiation of potentially effective therapies, referral to PH centers, and greater patient morbidity and mortality. This mini-review presents a succinct, simplified case-based approach to the "next steps" in the work-up of PH, once elevated pulmonary pressures have been noted on an echocardiogram. Our goal is for clinicians to develop a good overview of diagnostic approach to PH and recognition of high-risk features that may require early referral.

Thienemann et al (2014). Studied Rationale and design of the Pan African Pulmonary hypertension Cohort (PAPUCO) study: implementing a contemporary registry on pulmonary hypertension in Africa. Pulmonary hypertension (PH) is a

devastating, progressive disease with increasingly debilitating symptoms and usually shortened overall life expectancy due to a narrowing of the pulmonary vasculature and consecutive right heart failure. Little is known about PH in Africa, but limited reports suggest that PH is more prevalent in Africa compared with developed countries due to the high prevalence of risk factors in the region.

A multinational multicenter registry-type cohort study was established and tailored to resource-constraint settings to describe disease presentation, disease severity and aetiologies of PH,comorbidities, diagnostic and therapeutic management, and the natural course of PH in Africa. PH will be diagnosed by specialist cardiologists using echocardiography (right ventricular systolic pressure >35 mm Hg, absence of pulmonary stenosis and acute right heart failure), usually accompanied by shortness of breath, fatigue, peripheral oedema and other cardiovascular symptoms, ECG and chest X-ray changes in keeping with PH as per guidelines (European Society of Cardiology and European Respiratory Society (ESC/ERS) guidelines). Additional investigations such as a CT scan, a ventilation/ perfusion scan or right heart catheterisation will be performed at the discretion of the treating physician. Functional tests include a 6 min walk test and the Karnofsky Performance Score. The WHO classification system for PH will be applied to describe the different aetiologies of PH. Several substudies have been implemented within the registry to investigate specific types of PH and their outcome at up to 24 months. Data will be analysed by an independent institution following a data analyse plan.

Farrag, et al (2012). Studied Prevalence and severity of pulmonary hypertension in asymptomatic rural residents with schistosomal infection in the Nile Delta. Their aim was to assess the prevalence of PHTN together with assessment of right ventricular (RV) function in asymptomatic rural residents previously infected with

schistosomiasis. Three hundred and seventy asymptomatic people from an endemic area in the Nile Delta were screened for antibodies against schistosomiasis. All were scheduled for transthoracic echocardiographic study to assess pulmonary artery systolic (PASP) and diastolic (PADP) pressures as well as RV function. PASP >40 mmHg was considered elevated. Seropositive (SP) and seronegative (SN) groups had comparable age and body mass index. PASP >40 mmHg was met in 18 subjects (Range 42–72 mmHg) (8.6%) of SP group and in no subject in SN group (P = 0.000). Compared with SN group, the SP group had higher mean values of PASP (30 ± 10 vs. 24 ± 7 mmHg, P < 0.000) and PADP (12 ± 4 vs. 9 ± 3 mmHg, P < 0.000). The SP group had lower values of RV ejection fraction.

Bouhemad et al (2008). Studied Echocardiographic Doppler estimation of pulmonary artery pressure in critically ill patients with severe hypoxemia. Their study was aimed at determining whether the transesophageal approach could offer an alternative. includedFifty-one consecutive sedated and ventilated patients with severe hypoxemia (arterial oxygen tension/fraction of inspired oxygen < 300) were prospectively studied. Mean PAP measured from the pulmonary artery catheter was compared with several indices characterizing pulmonary artery blood flow assessed using transesophageal echocardiography: preejection time, acceleration time, ejection duration, preejection time on ejection duration ratio, and acceleration time on ejection duration ratio. In a subgroup of 20 patients, systolic PAP measured from the pulmonary artery catheter immediately before withdrawal was compared with Doppler study of regurgitation tricuspid flow performed immediately after pulmonary artery catheter withdrawal using either the transthoracic or the transesophageal approach. They found that Weak and clinically irrelevant correlations were found between mean PAP and indices of pulmonary artery flow. A statistically significant and clinically relevant correlation was found

between systolic PAP and regurgitation tricuspid flow. In 3 patients (14%), pulmonary artery pressure could not be assessed echocardiographically.

Sheikhzadeh et al (2014). Studied The main pulmonary artery in adults: a controlled multicenter study with assessment of echocardiographic reference values, and the frequency of dilatation and aneurysm in Marfan syndrome. Echocardiographic upper normal limits of both main pulmonary artery (MPA) diameters (MPA-d) and ratio of MPA to aortic root diameter (MPA-r) are not defined in healthy adults. Accordingly, frequency of MPA dilatation based on echocardiography remains to be assessed in adults with Marfan syndrome (MFS). They enrolled 123 normal adults (72 men, 52 women aged 42 ± 14 years) and 98 patients with MFS (42 men, 56 women aged 39 ± 14 years) in a retrospective cross-sectional observational controlled study in four tertiary care centers. We defined outcome measures including upper normal limits of MPA-d and MPA-r as 95 quantile of normal persons, MPA dilatation as diameters > upper normal limits, MPA aneurysm as diameters >4 cm, and indication for surgery as MPA diameters >6 cm. their Results revealed that MPA diameters revealed normal distribution without correlation to age, sex, body weight, body height, body mass index and body surface area. The upper normal limit was 2.6 cm (95% confidence interval (CI) =2.44-2.76 cm) for MPA-d, and 1.05 (95% CI = .86–1.24) for MPA-r. MPA dilatation presented in 6 normal persons (4.9%) and in 68 MFS patients (69.4%; P < .001), MPA aneurysm presented only in MFS (15 patients; 15.3%; P < .001), and no patient required surgery. Mean MPA-r were increased in MFS (P < .001), but ratios >1.05 were equally frequent in 7 normal persons (5%) and in 8 MFS patients (10.5%; P = .161). MPA-r related to aortic root diameters (P = .042), reduced left ventricular ejection fraction (P = .006), and increased pulmonary artery systolic pressures (P = .040). No clinical manifestations of MFS and no FBN1 mutation characteristics related to MPA diameters. Conclusions: We established 2.6 cm for

MPA-d and 1.05 for MPA-r as upper normal limits. MFS exhibits a high prevalence of MPA dilatation and aneurysm. However, patients may require MPA surgery only in scarce circumstances, most likely because formation of marked MPA aneurysm may require LV dysfunction and increased PASP.

Chapter three

Material and Methods

A total of three hundred consecutive participants arriving at the echocardiography department of the Military hospital in Omdurman were recruited in this study. The sample consisted of 157 males and 143 females. Their ages ranged from 20 to 69(mean: 37.24, SD: 11.065) years. The study duration was form 2015 – 2021.PAP measurements were taken for all patients. Maximum velocity of tricuspid regurgitation (TR) obtained by continuous-wave Doppler with adding right atrial (RA) pressure was used for measuring sPAP by TTE (sPAP(TRVmax)).

3-1**Materials :**

Equipment used:Ultrasound machine MY LAB 50 SN 03486 (transducer):convex (5MHz) MyLab™50 offers high-performance standards without compromise for General Imaging and cardiac ultrasound scanning. The modular architecture and unique scalability of MyLab™50 make it adaptable to a variety of clinical applications both in general imaging and cardiovascular configurations for adults and children, including cardiac, main and peripheral vascular, abdominal, small parts, breast, ob/gyn, urology and musculoskeletal.

Fig. (3-1)

Figure (3-1): Ultrasound machine MY LAB 50 SN 03486 (transducer)**:** convex (5MHz)

3-2 Subjects & selection method:

In a total of 300 subjects enrolled, SPAP was estimated by transthoracic Doppler echocardiography.. The flow chart depicted in Fig. (3-2) is used to assess the probability of PH. If the tricuspid regurgitation velocity (TRV) is >3.4 m/s then the echocardiographic probability of PH is high. If the TRV is ≤3.4 m/s, then other echocardiographic parameters suggesting PH must be used to assign the probability of PH. These parameters are split into three categories (A: the ventricles; B: the pulmonary artery; C: the inferior vena cava (IVC) and right atrium (RT)). Parameters from at least two different categories are needed to determine the probability of PH.

Echocardiography also provides information about the etiology and prognosis in patients with PH. Patients with established PH or high probability for PH should have a full assessment to exclude left-sided heart disease or intracardiac shunts as the cause of PH. Right ventricular dilatation and dysfunction are considered poor prognostic markers in patients with PH.

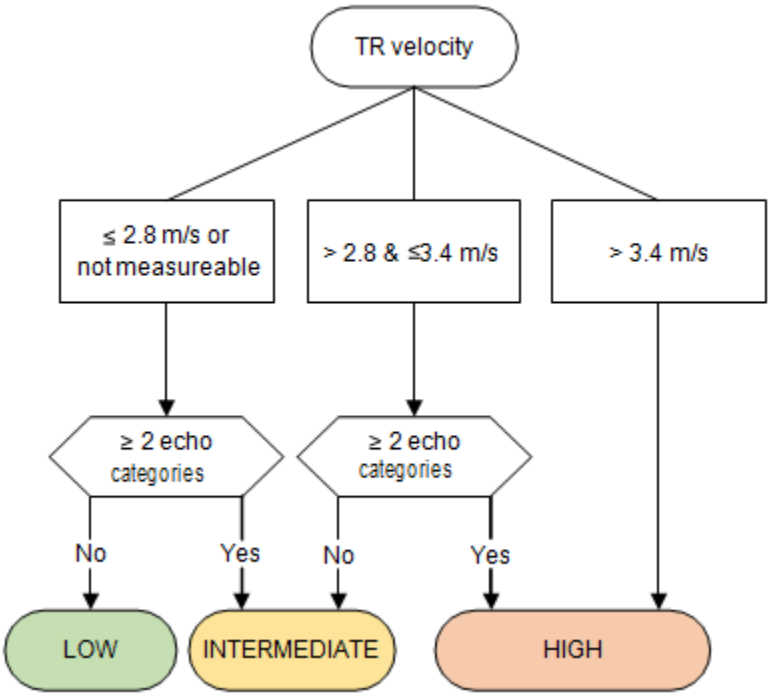

Figure (3-2): Flow chart to assess the probability of pulmonary hypertension using parameters identified from within ≥2 categories (the ventricles, pulmonary artery, or the inferior vena cava and right atrium) in conjunction with tricuspid regurgitation velocity. Adapted from ESC/ERS Guidelines for the diagnosis and treatment of pulmonary hypertension (Galiè et al,2016).

Inclusion criteria:

1. Male and female with age between 20-69 years old
2. A population and their weight between 20-100 Kg.

Exclusion criteria:

1. Pregnant women;
2. Patients with abnormal heart disorders
3. Patients less than 20 years old.
4. Patients with a previous history of angina, severe vascular disease, or another life-threatening disease.

Procedure methodology:

As part of a full echocardiographic assessment, Doppler examination should be performed in the following sequence: 1) color Doppler in all apical projections; 2) color Doppler in parasternal projections (long axis/short axis); 3) pulsed-wave Doppler for transmitral velocities; 4) pulsed-wave Doppler for left ventricles (LV) outflow tract; 5) pulsed-wave Doppler for the tricuspid inflow; 6) pulsed-wave Doppler for the RVOT; 7) continuous-wave Doppler across the LV outflow aortic valve; 8) continuous-wave (CW) Doppler across the tricuspid valve (for tricuspid regurgitation); 9) continuous-wave Doppler (WC)across the pulmonary valve (for pulmonary regurgitation); and 10) tissue Doppler imaging (TDI) of the RV free wall.

A pulmonary regurgitation (PR) signal is obtained in the parasternal short-axis view using color Doppler. CW Doppler at a sweep speed of 100 mm/s is used to measure the peak PR velocity. Peak pressure difference (measured by the Bernoulli equation) is then added to the RAP. This method has been validated against gold standard catheter measurements. Mean PAP can be approximated from the peak PR Doppler signal using the following formula: mPAP = 4(PRpeak velocity)^2 + RAP(Abbas et al,2003).

Mean pulmonary pressure is calculated by the formula: **mPAP = 90 − (0.62*AT_{RVOT})**. For example, if the AT_{RVOT} is 80 ms, the mPAP = 90 −(0.62*80), that is 40.4 mmHg (normal < 25 mmHg). On the other hand, if the AT_{RVOT} is 137 ms, then the calculated mPAP is 90 − (0.62*137) = 5.06 mmHg. **Figures (3-3,4,5)**: represent sonographic appearance for pulmonary artery by Echocardiogram.

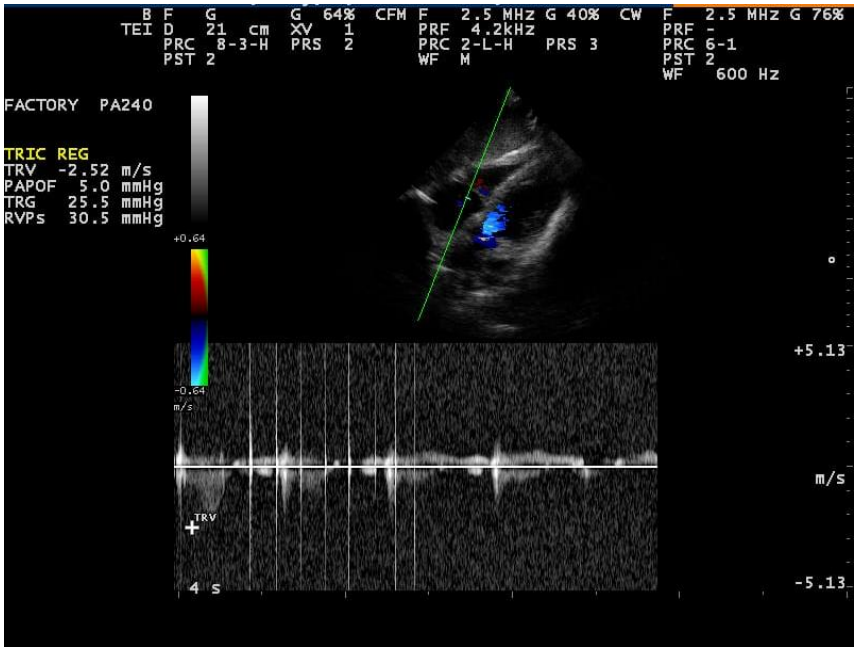

Figure (3-3): 70 yrs. M with mild tricuspid regurgitant jet TV max (2.52 m/s) PAP 5 mmHg the PASP 30.5 mmHg (Bernoulli equation) 4 $(TV\ max)^2$ + PAP,

Figure (3-4): 42 yrs. M with moderate Tricuspid regurgitant jet TV max (3. 23 m/s) PAP elvated by 10 mmHg with PASP 51.7 mmHg (Bernoulli equation) 4 (TV max)2 + PAP.

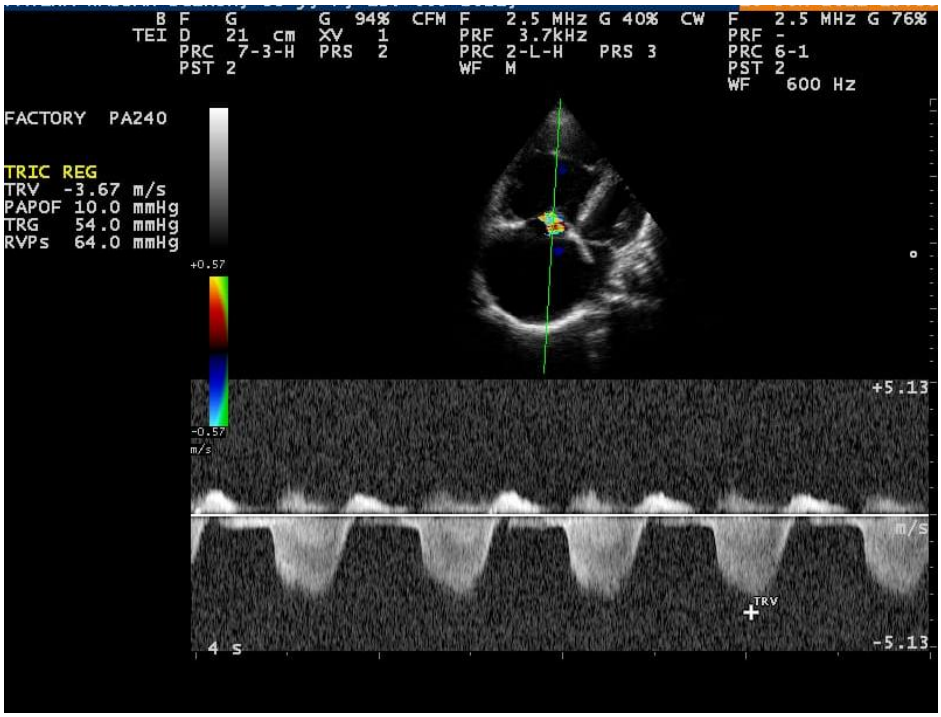

Figure (3-5): 38 yrs. F with sever Tricuspid regurgitant jet TV max (3. 67 m/s) PAP elvated by 10 mmHg with PASP 64 mmHg (Bernoulli equation) 4 (TV max)2 + PAP.

3-3 Data analysis.

The SPSS 21 statistical software was used for data analysis. Statistical significance of variables was estimated using chi –square for categorical variables and student t – test for continuous variables. Pearson correlation coefficient analysis was used to determine relationship between echocardiographic findings and weight and age. Results with a p value <0.05 were regarded as being statistically significant.

3.4. Ethical considerations:

No part of this study relies on data which normaly was collected from routine scaning. All patients were informed, that the result of examination was form part of research project. No patient identification or individual patient detail was bublished, and all specific information relating to patient's identities was protected in the same way.

Chapter Four

Results

A total of three hundred consecutive patients arriving at the echocardiography department of the Military hospital in Omdurman were recruited in this study. The sample consisted of 157 males and 143 females. Their ages ranged from 20 to 69(mean: 37.24, SD: 11.065) years. The two groups were comparable in age and sex distribution. The baseline characteristics of all subjects are as shown in the table below.

Table (4-1): Baseline characteristics of the subjects

Descriptive Statistics					
	N	Minimum	Maximum	Mean	Std. Deviation
Age(Yrs)	300	20.0	69.0	37.243	11.0646
Weight(Kg)	300	40	90	61.35	10.031
RV dimensions(Cm)	300	2.0	2.8	2.296	.1134
TVMAXms	300	2	4	2.80	.368
PASPmmHg	300	26.0	80.0	37.440	10.8199
Valid N (listwise)	300				

Table (4-2): Frequency distribution of participants Gender:

Gender	Frequency	Percent
Male	157	52.3
Female	143	47.7
Total	300	100.0

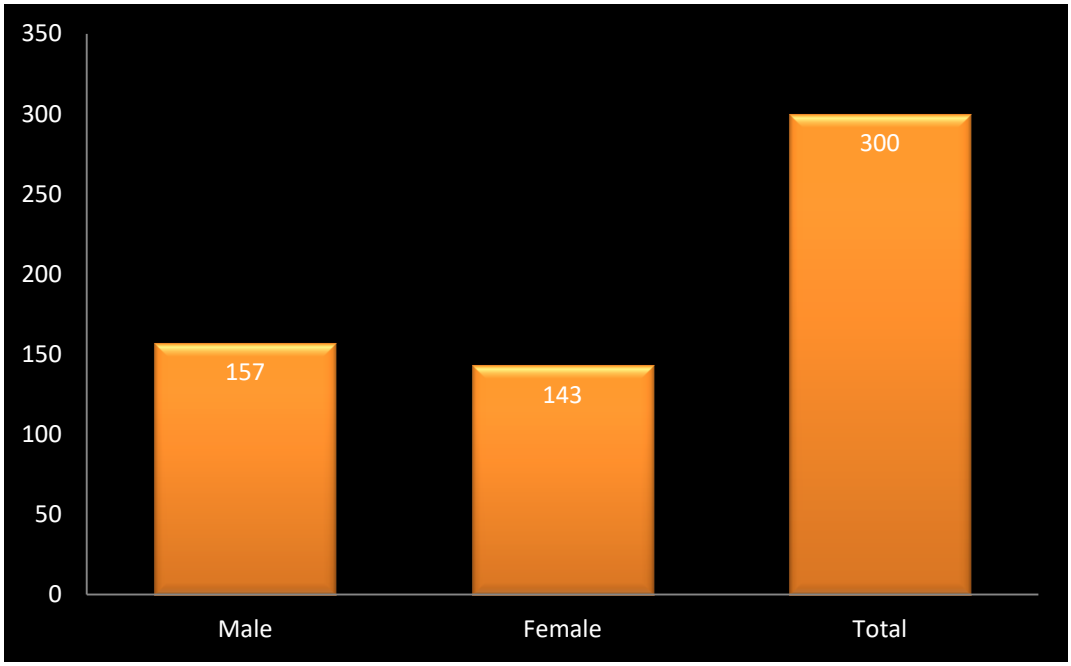

Figure (4-1): Frequency distribution of participants Gender

Table (4-3): Frequency distribution of Age group

Age(Yrs)	Frequency
20-30	11
30-40	101
40-50	107
50-60	55
>60	26
Total	300

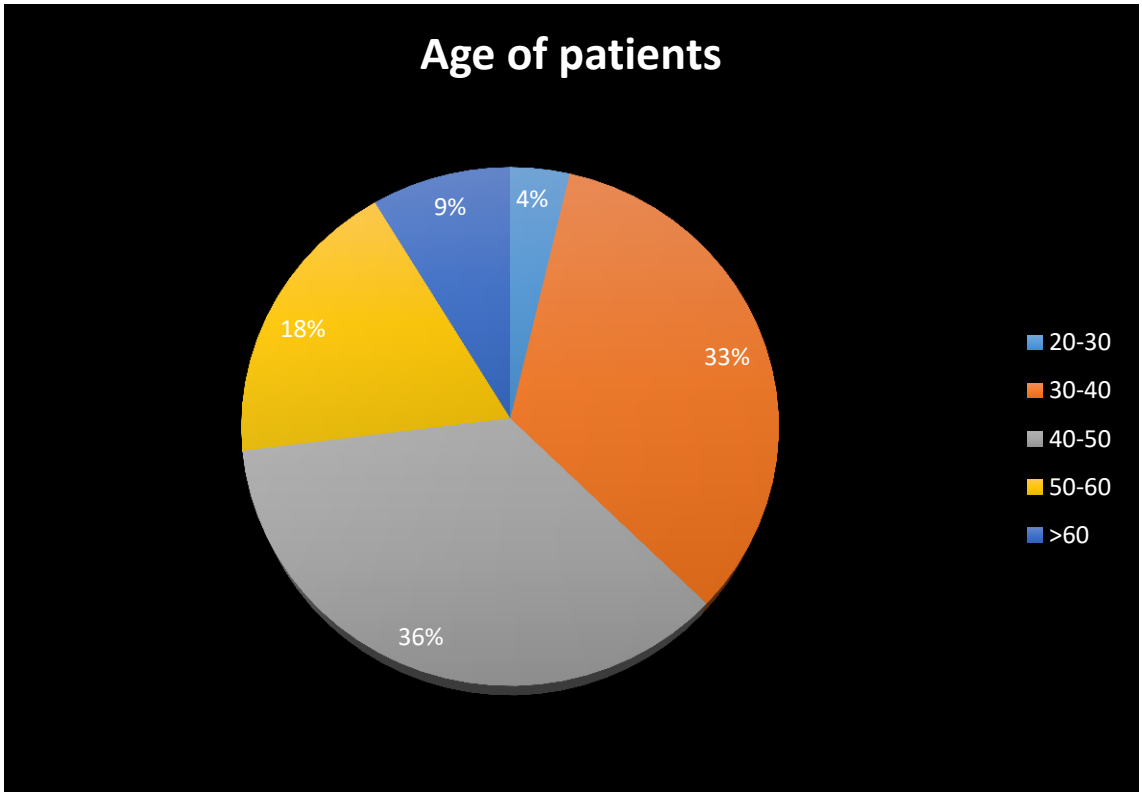

Figure (4-2): Frequency distribution of Age group

Table (4-4): The distribution frequency of weight of the patients

Weight(Kgs)	Frequency
20-40	111
40-60	127
60-80	57
80-100	5
Total	300

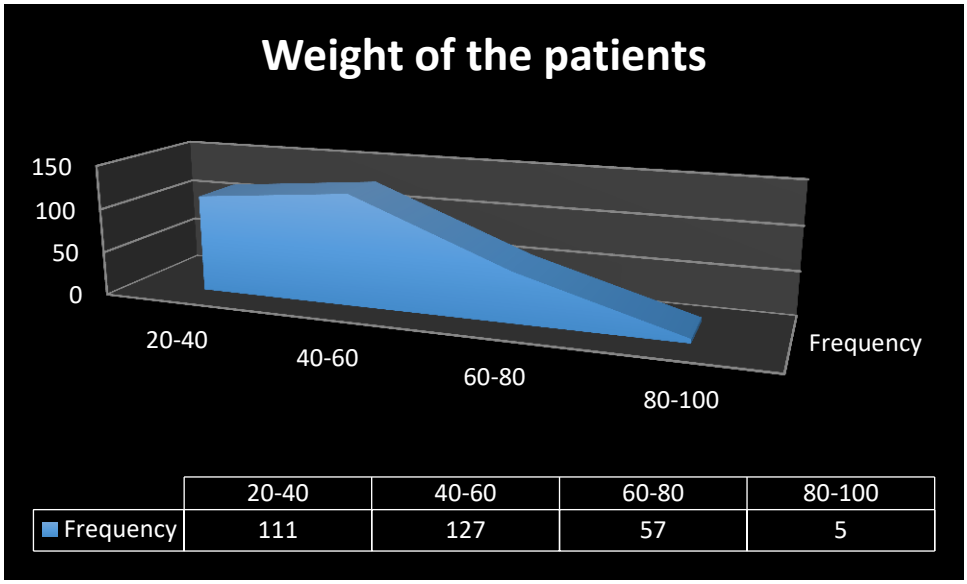

Figure (4-3): The distribution frequency of weight of the patients

Table (4-5): The correlation between the Patient Age(Yrs), Weight(Kg),RV dimensions(Cm),TVMAXms and PASPmmHg

		Age(Yrs)	Weight(Kg)	RV dimensions(Cm)	TVMAX(ms)	PASP(mmHg)
Age(Yrs)	Pearson Correlation	1	.664**	.536**	.719**	.694**
	Sig. (2-tailed)		.000	.000	.000	.000
	N	300	300	300	300	300
Weight(Kg)	Pearson Correlation	.664**	1	.405**	.522**	.484**
	Sig. (2-tailed)	.000		.000	.000	.000
	N	300	300	300	300	300
RV Dimensions(Cm)	Pearson Correlation	.536**	.405**	1	.677**	.675**
	Sig. (2-tailed)	.000	.000		.000	.000
	N	300	300	300	300	300
TVMAXms	Pearson Correlation	.719**	.522**	.677**	1	.992**
	Sig. (2-tailed)	.000	.000	.000		.000
	N	300	300	300	300	300
PASPmmHg	Pearson Correlation	.694**	.484**	.675**	.992**	1
	Sig. (2-tailed)	.000	.000	.000	.000	
	N	300	300	300	300	300
**. Correlation is significant at the 0.01 level (2-tailed).						

Table (4-6): Frequency distribution of RV dimensions(Cm)					
		Frequency	Percent	Valid Percent	Cumulative Percent
Valid	2.1	1	.3	.3	.3
	2.1	19	6.3	6.3	6.7
	2.2	79	26.2	26.3	33.0
	2.3	133	44.0	44.3	77.3
	2.4	42	13.9	14.0	91.3
	2.5	17	5.6	5.7	97.0
	2.6	6	2.0	2.0	99.0
	2.7	2	.7	.7	99.7
	2.8	1	.3	.3	100.0
	Total	300	99.3	100.0	
Missing	System	2	.7		
Total		302	100.0		

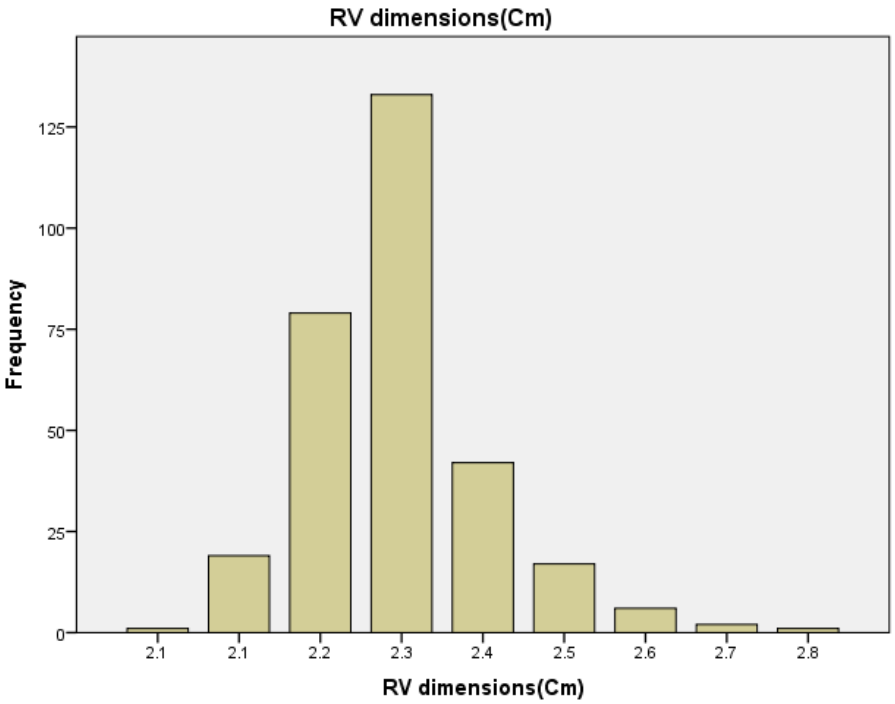

Figure (4-4): Frequency distribution of RV Dimensions

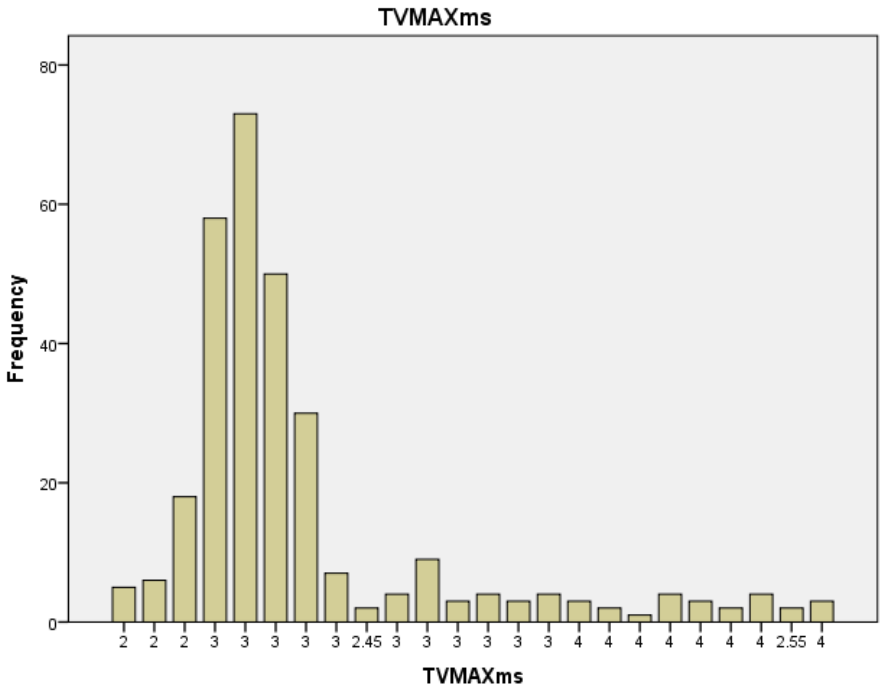

Figure (4-5): Frequency distribution of TV max

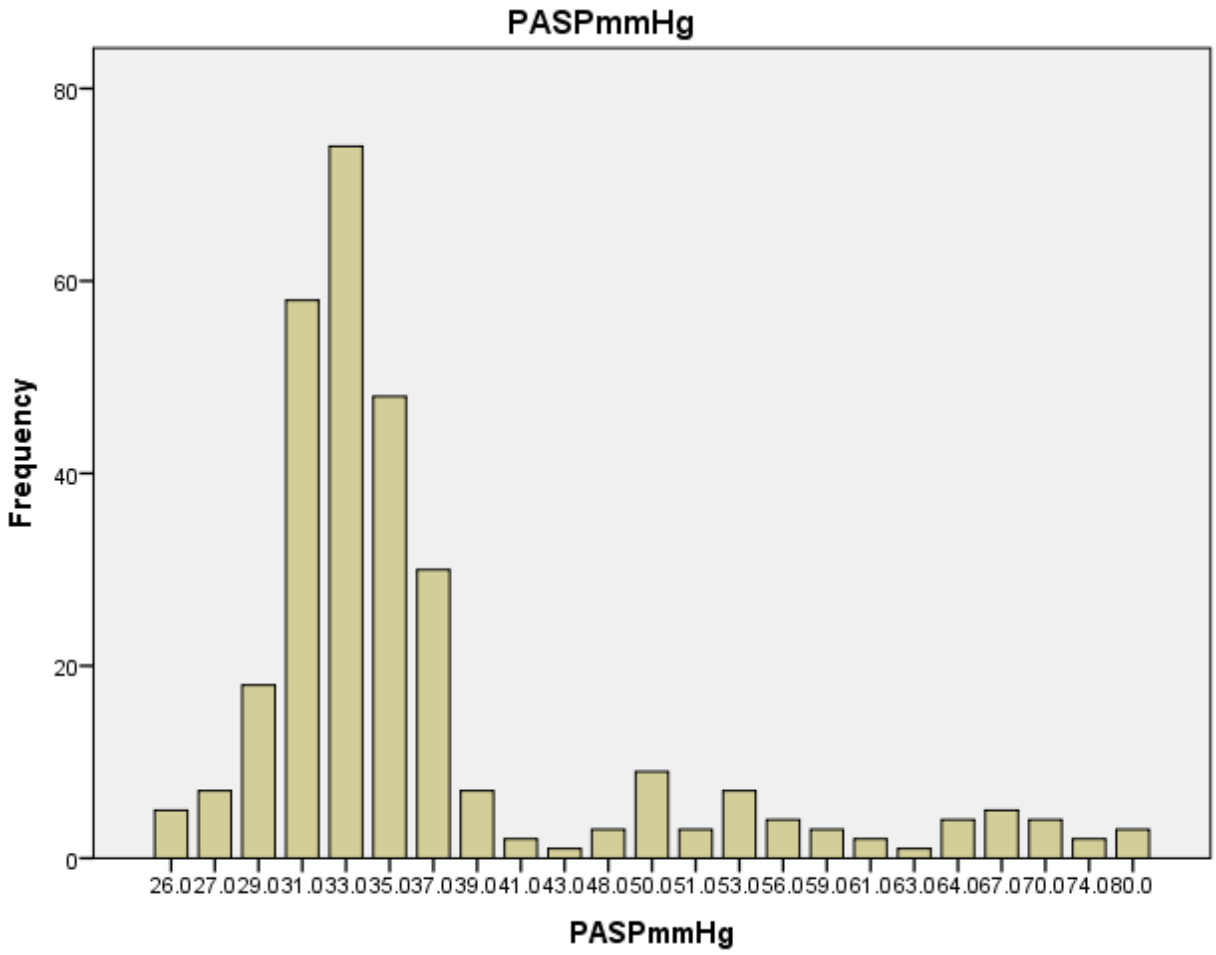

Figure (4-6): Frequency distribution of PASP

Table (4-7): Frequency distribution of TR-max

TR-max	Frequency	Percent
Mild TR	250	83.3
Moderate TR	29	9.7
Severe TR	21	7.0
Total	300	100.0

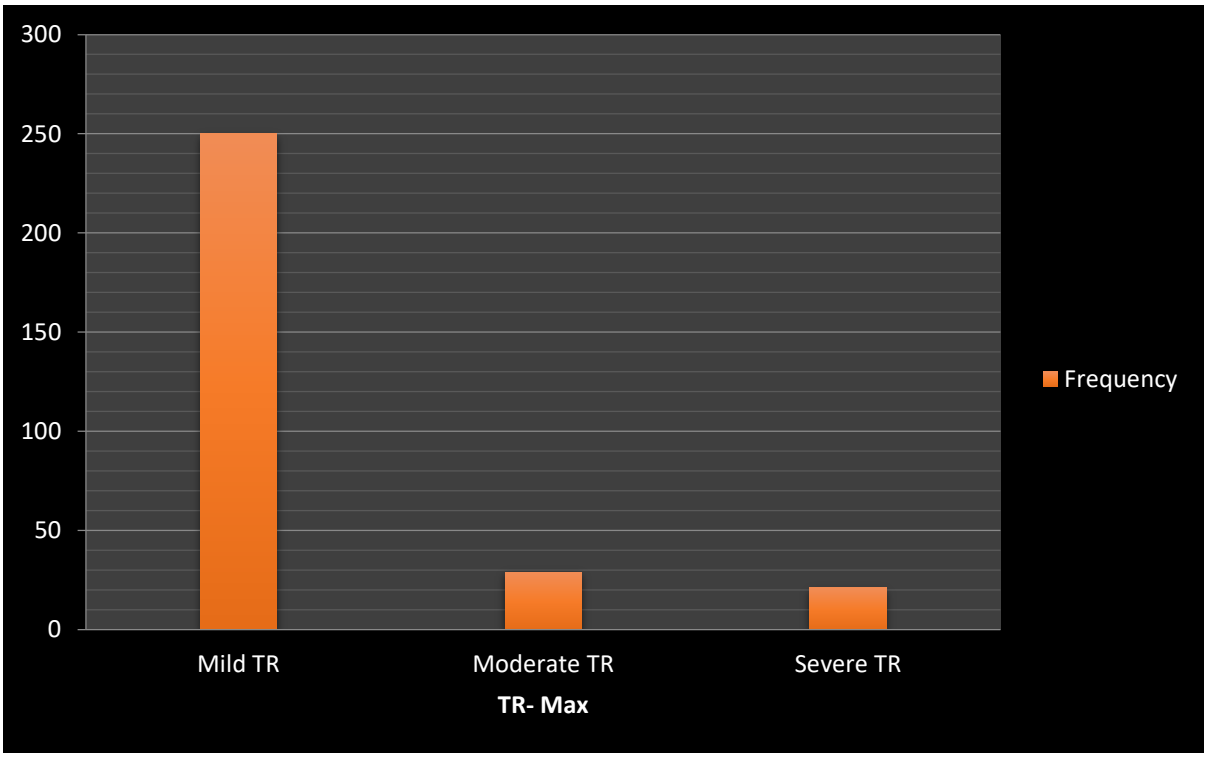

Figure (4-7): Frequency distribution of TR-max

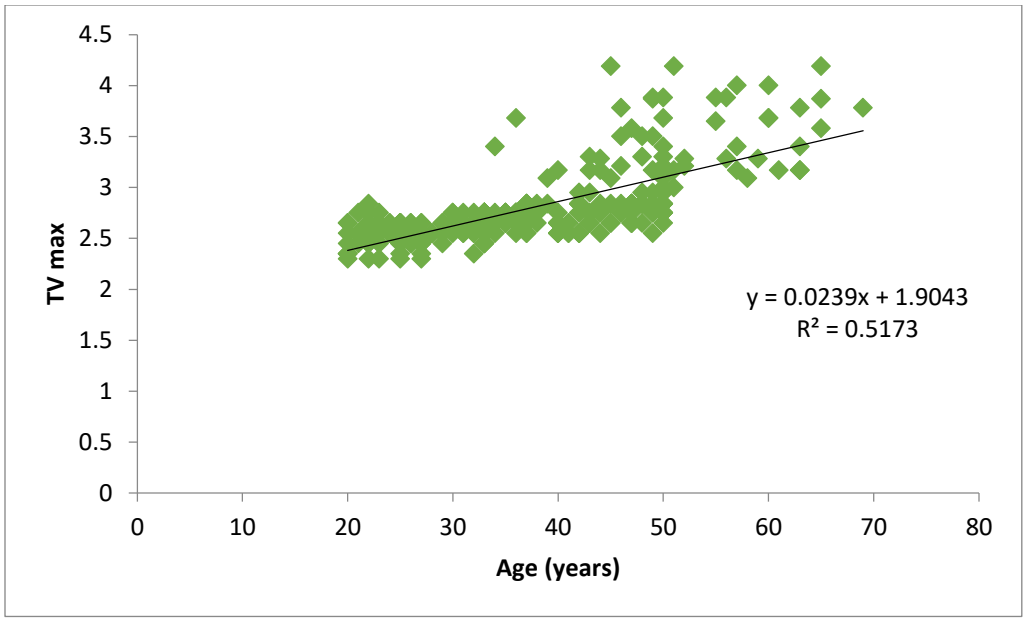

Figure (4-8): Linear regression analysis the correlation between Age (years) and TV max

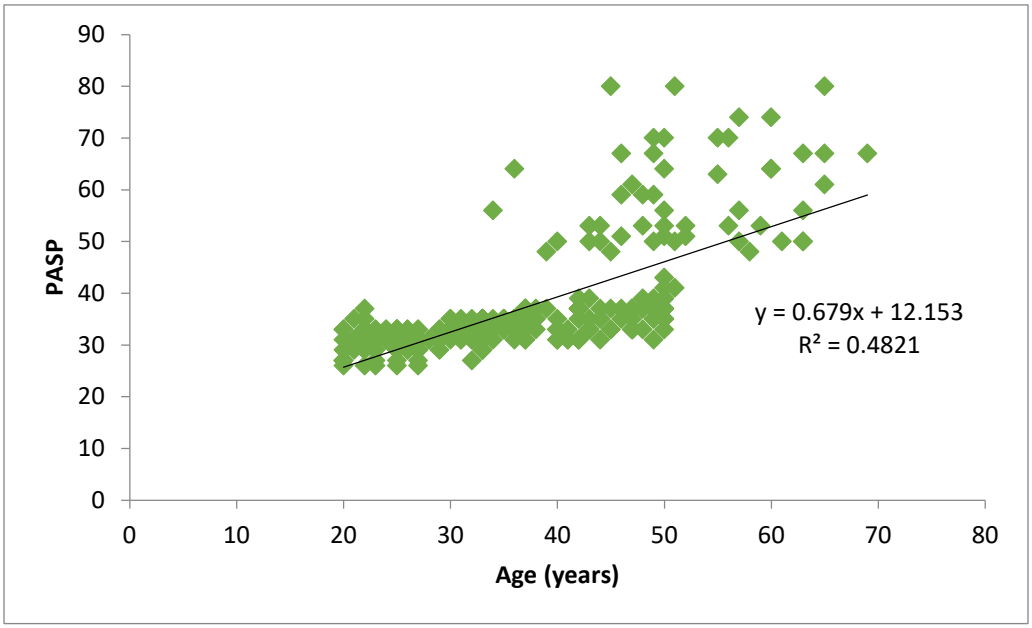

Figure (4-9): Linear regression analysis showed the correlation between Age (years) and PASP

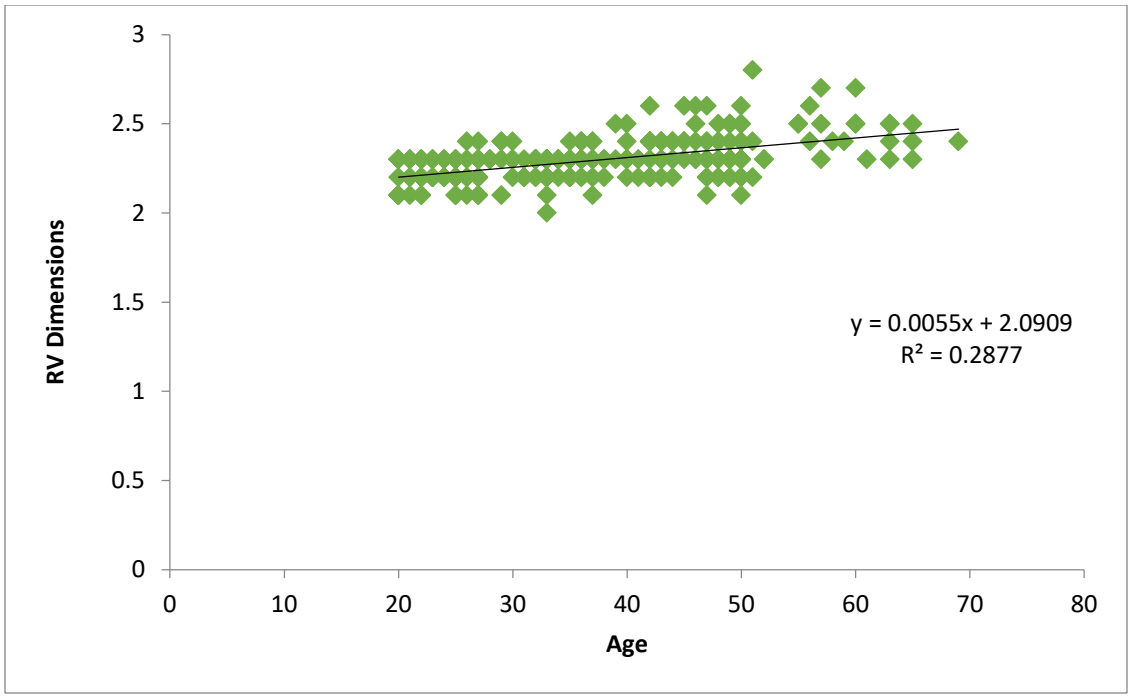

Figure (4-10): Linear regression analysis the correlation between Age (years) and RV Dimensions

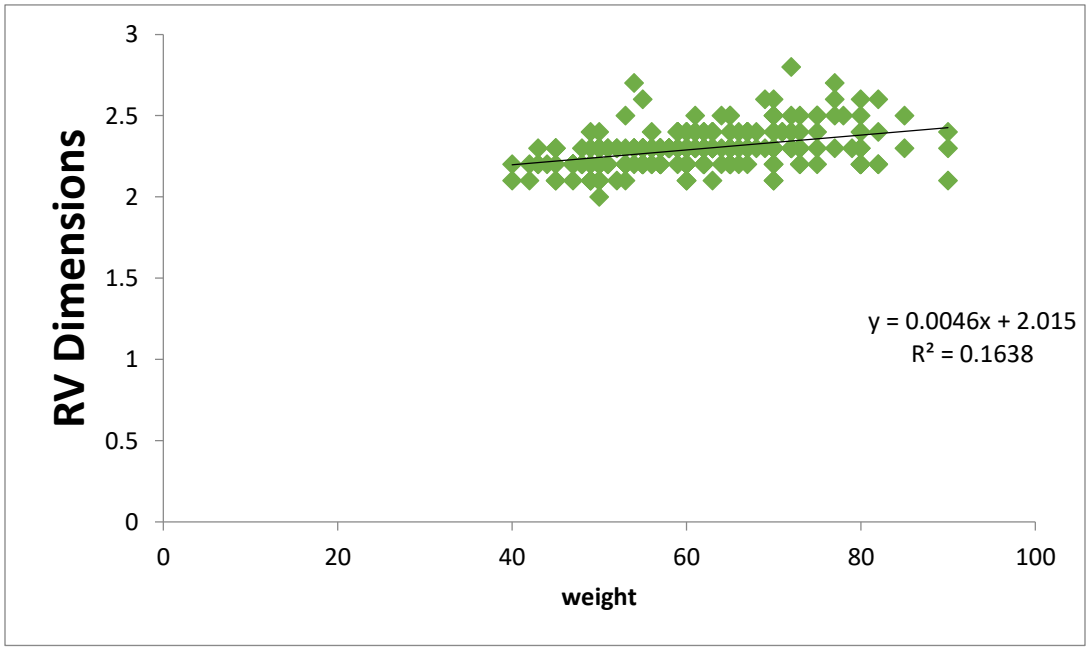

Figure (4-11): Linear regression analysis the correlation between weight and RV Dimensions

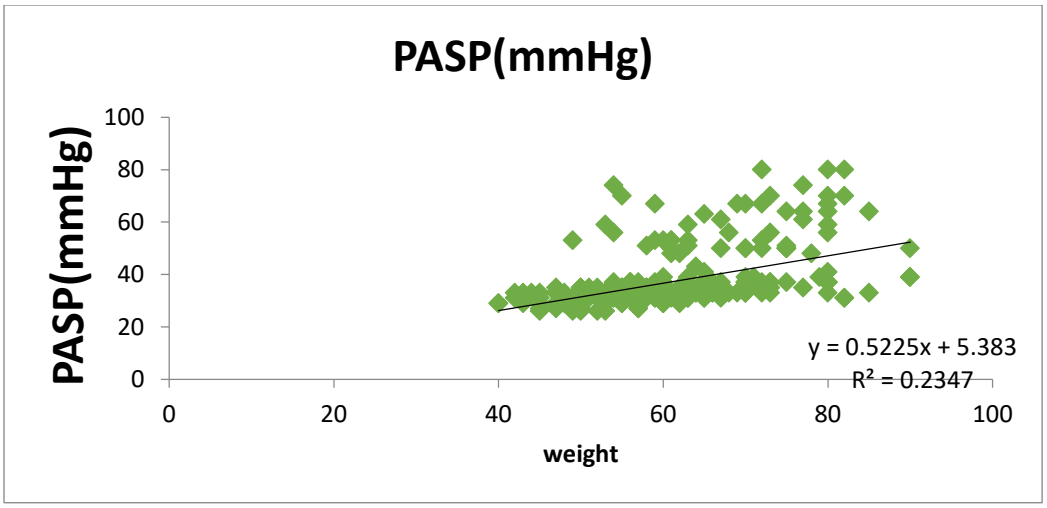

Figure (4-12): Linear regression analysis the correlation between weight and PASP

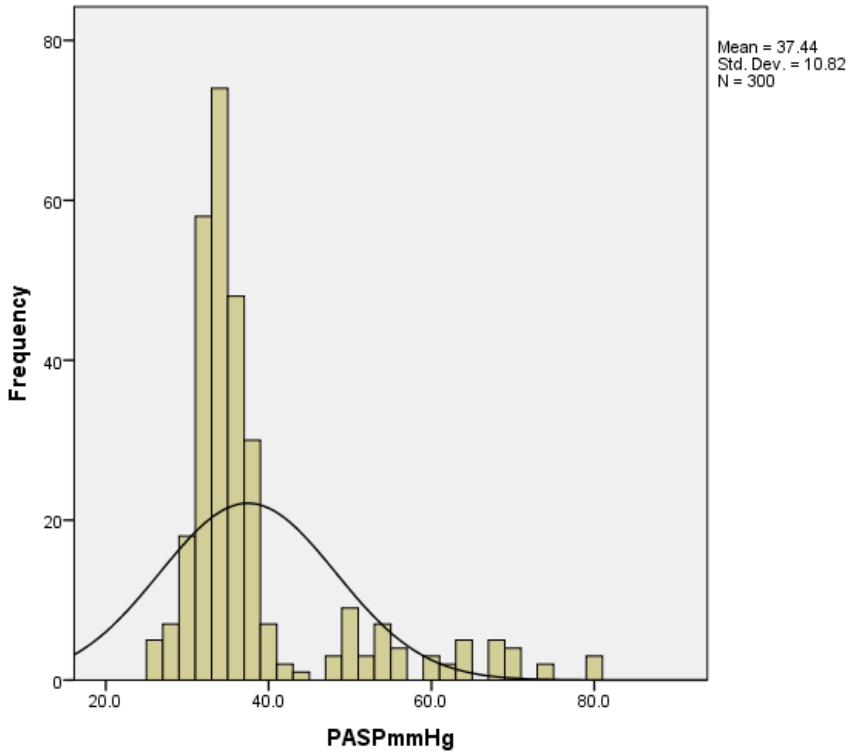

Figure 4.13: The PASP of all subjects

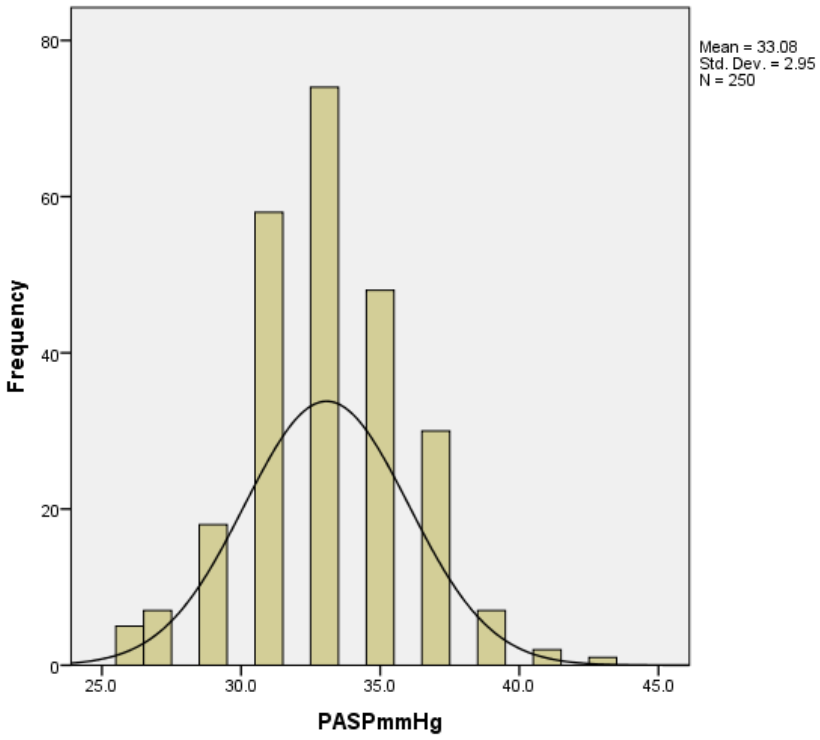

Figure 4.14: The PASP of mild subjects

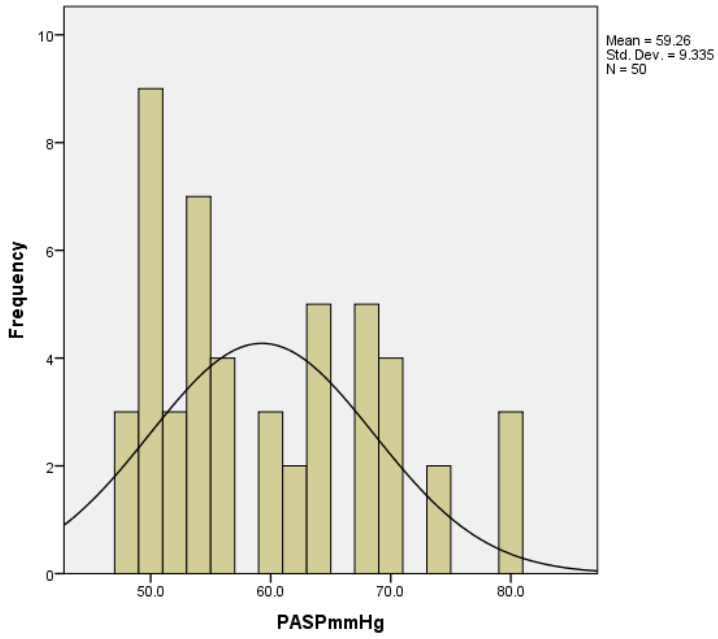

Figure 4.15: The PASP of moderate and severe subjects

Table (4-8): Shows the correlation between the Patient Age and RV dimension

Age * RV dimension		RV dimension							Total
		2.0cm	2.1cm	2.2cm	2.3cm	2.4cm	2.5cm	2.6cm	
age	20-30	1	10	0	0	0	0	0	11
	30-40	33	46	14	3	3	1	1	101
	40-50	55	27	15	6	3	1	0	107
	50-60	30	13	7	5	0	0	0	55
	>60	11	5	6	3	0	1	0	26
P value		0.007							

Table (4-9): The correlation between the Patient Age * TV max

Age * TV max		TVmax																								Total
		2.30m/s	2.35m/s	2.45m/s	2.55m/s	2.65m/s	2.75m/s	2.84m/s	2.95m/s	3.0m/s	3.9m/s	3.17m/s	3.21m/s	3.28m/s	3.30m/s	3.40m/s	3.50m/s	3.58m/s	3.65m/s	3.68m/s	3.78m/s	3.87m/s	3.88m/s	4.00m/s	4.19m/s	
Age	20-30	0	0	2	1	0	0	0	0	0	0	2	0	1	0	1	0	1	0	0	2	0	0	1	0	11
	30-40	0	2	5	18	23	20	10	4	2	1	3	0	1	2	1	1	0	1	2	0	2	1	0	2	101
	40-50	3	1	8	19	31	17	11	2	0	1	3	0	1	1	2	1	0	0	1	1	0	2	1	1	107
	50-60	0	1	1	15	14	11	8	1	1	0	2	0	0	0	0	0	0	0	0	0	0	1	0	0	55
	>60	2	3	2	5	5	1	1	0	0	1	0	2	1	0	0	1	1	0	1	0	0	0	0	0	26
P value		0.000																								

Table (4-10): The correlation between the Patient Gender * Echo finding

	Echo finding																					Total
	with PASP	with PASP	with PASP	with PASP	with PASP	with PASP	with PASP	with PASP	with PASP	with PASP	PASP49mm with		TR with	PASP56mm	PASP54mm TR with	PASP TR with	PASP TR with	PASP TR with	PASP TR with	PASP TR with	with PASP	with PASP	
Gender	M	3	3	14	32	35	27	14	5	2	0	0	5	5	2	1	1	1	3	3	1	0	157
	F	2	5	5	27	37	23	14	3	2	2	1	4	2	2	2	1	2	4	2	2	1	143
Total		5	8	19	59	72	50	28	8	4	2	1	9	7	4	3	2	3	7	5	3	1	300

Table (4-11): The correlation between the Patient Gender * TV max

Gender * TV max		TV max																										Total
		2.30m/s	2.35m/s	2.45m/s	2.55m/s	2.65m/s	2.75m/s	2.84m/s	2.95m/s	3.0m/s	3.9m/s	3.17m/s	3.21m/s	3.28m/s	3.30m/s	3.40m/s	3.50m/s	3.58m/s	3.65m/s	3.68m/s	3.78m/s	3.87m/s	3.88m/s	4.00m/s	4.19m/s		
gender	M	2	3	13	32	35	26	16	4	1	1	6	0	3	2	2	2	0	1	2	1	1	1	2	1		157
	F	3	4	5	26	38	23	14	3	2	2	4	2	1	1	2	1	2	0	2	2	1	3	0	2		143
Total		5	7	18	58	73	49	30	7	3	3	10	2	4	3	4	3	2	1	4	3	2	4	2	3		300
P value		0.860																									

Table (4-12): The correlation between the Patient Gender * PASP

Gender * PASP		PASP																							Total
		26	27	29	31	33	35	37	39	41	43	48	50	51	53	56	59	61	63	64	67	70	74	80	
gender	M	5	4	8	35	35	25	17	4	2	2	1	4	3	3	1	1	1	0	1	1	1	2	1	157
	F	0	3	10	23	38	24	13	3	1	0	1	4	0	4	3	2	1	1	3	4	3	0	2	143
Total		5	7	18	58	73	49	30	7	3	2	2	8	3	7	4	3	2	1	4	5	4	2	3	300
P value		0,460																							

Table (4-13): The correlation between the Patient Weight * Echo finding

Weight * Echo finding		Echo finding																							Total
		PASP 26mmHg with TR with	PASP 27mmHg Mild TR with	PASP 29mmHg Mild TR with	PASP 31mmHg Mild TR with	PASP 33mmHg Mild TR with	PASP 35mmHg Mild TR with	PASP 37mmHg Mild TR with	PASP 39mmHg Mild TR with	PASP 41mmHg Mild TR with	PASP 43mmHg Mild TR with	PASP49mmHg Mild TR with	50mmHg Moderate TR with	PASP56mmHg Moderate TR with	PASP54mmHg Moderate TR with	PASP 52mmHg Moderate TR with	PASP 50mmHg Moderate TR with	PASP 51mmHg moderate TR with	PASP 53mmHg Moderate TR with	PASP 56mmHg Moderate TR with	PASP 61mmHg severe TR with	PASP 74mmHg Severe TR with	
Weight	20-40	2	2	5	18	18	32	21	8	2	1	1	1	0	0	0	0	0	0	0	0	0	0	0	111
	40-60	3	6	13	25	35	16	5	0	1	0	0	3	4	2	2	1	1	5	4	1	0			127
	60-80	0	0	1	16	19	2	2	0	1	1	0	5	2	1	0	1	1	2	1	1	1			57
	80-100	0	0	0	0	0	0	0	0	0	0	0	0	1	1	1	0	1	0	0	1	0			5
Total		5	8	19	59	72	50	28	8	4	2	1	9	7	4	3	2	3	7	5	3	1			300
P value		0.002																							

Table (4-14): The correlation between the Patient Weight * TR max

Weight * TR max		TR max			Total
		Mild TR	Moderate TR	Severe TR	
weight	20-40	97	10	4	111
	40-60	112	9	6	127
	60-80	41	7	9	57
	80-100	0	3	2	5
Total		250	29	21	300
P value		0.000			

Table (4-15): The correlation between the Patient Weight * TR max

Age * TR max		**TR max**			**Total**
		Mild TR	Moderate TR	Severe TR	
Age	20-30	11	0	0	11
	30-40	84	10	7	101
	40-50	90	11	6	107
	50-60	47	6	2	55
	>60	18	2	6	26
Total		250	29	21	300
P value		0.085			

Table (4-16): The correlation between the Patient Gender * TR max

Gender * TR max		TR max			Total
		Mild TR	Moderate TR	Severe TR	
gender	M	136	14	7	157
	F	114	15	14	143
Total		250	29	21	300
P value		0.161			

Table (4-17): The correlation between the Patient Gender * TR max

RVdimension * PASP		PASP																								Total
		26	27	29	31	33	35	37	39	41	43	48	50	51	53	56	59	61	63	64	67	70	74	80		
RVdimension	2.0cm	1	3	2	27	35	30	14	4	2	0	0	4	2	1	3	1	1	0	0	0	0	0	0		130
	2.1cm	4	4	16	27	26	13	9	1	1	0	0	0	0	0	0	0	0	0	0	0	0	0	0		101
	2.2cm	0	0	0	2	12	5	6	1	0	1	1	2	1	5	1	1	0	0	1	2	1	0	0		42
	2.3cm	0	0	0	1	0	1	1	0	0	1	1	2	0	1	0	1	0	1	3	2	1	0	1		17
	2.4cm	0	0	0	0	0	0	0	1	0	0	0	0	0	0	0	0	1	0	0	1	2	0	1		6
	2.5cm	0	0	0	1	0	0	0	0	0	0	0	0	0	0	0	0	0	0	0	0	0	2	0		3
	2.6cm	0	0	0	0	0	0	0	0	0	0	0	0	0	0	0	0	0	0	0	0	0	0	1		1
Total		5	7	18	58	73	49	30	7	3	2	2	8	3	7	4	3	2	1	4	5	4	2	3		300

Table (4-18): The correlation between the Patient Gender * TR max

V dimension * TV max		TV max																							
		2.30m/s	2.35m/s	2.45m/s	2.55m/s	2.65m/s	2.75m/s	2.84m/s	2.95m/s	3.0m/s	3.9m/s	3.17m/s	3.21m/s	3.28m/s	3.30m/s	3.40m/s	3.50m/s	3.58m/s	3.65m/s	3.68m/s	3.78m/s	3.87m/s	3.88m/s	4.00m/s	4.19m/s
RV dimension	2.0cm	3	3	6	26	37	19	16	3	1	1	3	1	1	1	0	2	0	1	1	1	1	2	0	1
	2.1cm	0	1	8	22	32	10	14	1	0	0	3	0	3	1	1	0	1	0	1	2	0	0	1	0
	2.2cm	1	3	2	7	4	10	0	2	1	1	2	0	0	1	2	1	1	0	1	0	1	0	1	1
	2.3cm	0	0	1	3	0	7	0	0	1	1	1	1	0	0	1	0	0	0	0	0	0	1	0	0
	2.4cm	0	0	1	0	0	2	0	1	0	0	1	0	0	0	0	0	0	0	0	0	0	1	0	0
	2.5cm	1	0	0	0	0	1	0	0	0	0	0	0	0	0	0	0	0	0	1	0	0	0	0	0
	2.6cm	0	0	0	0	0	0	0	0	0	0	0	0	0	0	0	0	0	0	0	0	0	0	0	1
P value		0.00																							

Table (4-19): The correlation between the Patient Gender * TR max

		PASP																						
	TVmax * PASP	26	27	29	31	33	35	37	39	41	43	48	50	51	53	56	59	61	63	64	67	70	74
TVmax	2.30m/s	0	0	0	2	1	1	1	0	0	0	0	0	0	0	0	0	0	0	0	0	0	0
	2.35m/s	0	0	0	2	3	1	1	0	0	0	0	0	0	0	0	0	0	0	0	0	0	0
	2.45m/s	0	0	1	3	5	4	2	2	1	0	0	0	0	0	0	0	0	0	0	0	0	0
	2.55m/s	0	0	2	14	15	15	8	2	1	1	0	0	0	0	0	0	0	0	0	0	0	0
	2.65m/s	2	2	6	17	25	14	6	1	0	0	0	0	0	0	0	0	0	0	0	0	0	0
	2.75m/s	1	1	3	6	8	5	4	0	0	0	0	5	3	3	1	1	0	0	1	2	2	1

	2.84m/s	1	3	4	7	7	3	4	1	0	0	0	0	0	0	0	0	0	0	0	0	0	0
	2.95m/s	0	0	0	1	1	2	1	1	0	0	0	0	0	0	0	0	1	0	0	0	0	0
	3.0m/s	0	0	0	1	1	0	0	0	0	0	1	0	0	0	0	0	0	0	0	0	0	0
	3.9m/s	0	0	0	0	1	0	1	0	0	0	0	0	0	0	0	0	0	0	1	0	0	0
	3.17m/s	0	0	0	3	2	1	0	0	0	0	0	1	0	1	0	0	0	0	0	1	1	0
	3.21m/s	0	0	0	0	0	0	0	0	1	0	0	0	0	0	0	0	0	1	0	0	0	0
	3.28m/s	0	0	1	1	1	0	0	0	0	0	0	0	0	0	0	0	1	0	0	0	0	0
	3.30m/s	0	0	0	0	0	1	0	0	0	0	1	0	0	0	0	1	0	0	0	0	0	0
	3.40m/s	0	0	1	0	0	0	0	0	0	0	0	0	0	1	0	0	0	0	2	0	0	0
	3.50m/s	0	0	0	0	0	1	0	0	0	1	0	1	0	0	0	0	0	0	0	0	0	0
	3.58m/s	0	0	0	0	1	0	0	0	0	0	0	0	0	0	0	0	0	0	0	1	0	0
	3.65m/s	0	0	0	0	0	0	1	0	0	0	0	0	0	0	0	0	0	0	0	0	0	0
	3.68m/s	0	0	0	0	0	1	0	0	0	0	0	0	0	1	1	0	0	0	0	0	0	1
	3.78m/s	0	1	0	0	1	0	0	0	0	0	0	0	0	0	1	0	0	0	0	0	0	0
	3.87m/s	0	0	0	0	0	0	0	0	0	0	0	1	0	0	0	1	0	0	0	0	0	0

	3.88m/s	0	0	0	1	0	0	0	0	0	0	0	0	0	1	0	0	0	0	0	1	1	0
	4.00m/s	1	0	0	0	0	0	1	0	0	0	0	0	0	0	0	0	0	0	0	0	0	0
	4.19m/s	0	0	0	0	1	0	0	0	0	0	0	0	0	0	1	0	0	0	0	0	0	0
Total		5	7	18	58	73	49	30	7	3	2	2	8	3	7	4	3	2	1	4	5	4	2

Chapter Five

This part intended to provide details of discussion, conclusion, recommendation and future work.

5.1 Discussion:

Pulmonary hypertension (PH) is a devastating, progressive disease with increasingly debilitating symptoms and usually shortened overall life expectancy due to a narrowing of the pulmonary vasculature and consecutive right heart failure (RHF) (Simonneau et al 2013).. The epidemiology of PH in Africa and the distribution of its multitude of aetiologies have not yet been described, but limited reports suggest that the incidence of PH in Africa is higher than that reported from developed countries, owing to the pattern of diseases prevalent in the region(Thienemann et al,2013), (Sliwa et al 2012).. In this research, we aim to Study of Pulmonary Artery Pressure and Resistance in Sudanese Using Echocardiography.

This is descriptive analyses of a prospectively collected data. A total of 300 consecutive participants arriving at the echocardiography department of the Military hospital in Omdurman- Khartoum-Sudan The sample consisted of 157males and 143 females. Their ages ranged from 20 to 69 (mean: 37.2, SD: 11.0646) years.

Baseline clinical and demographic characteristics were obtained from the subjects. These included: Date of birth, age, gender and indication for echocardiography, and weight.

Two-dimensional guided M-mode echocardiography with the use of commercially available echo-machine Easote my lab 50 ultrasound machine ,Italy, Manufacture 2005 Modules; Doppler. CFM. Phased array. linear and HF. Convex probe echocardiography ,Frequency 5 MHZ was performed on each subject in the partial decubitus position. Echocardiographic examination was performed in the

parasternal long axis, short axis, two chambers, apical four chambers, five chambers and occasionally in the subcostal and suprasternal views.

Measurements and echocardiographic diagnoses were based on standard criteria. Data management and analysis were performed with SPSS software version 21. (SPSS, Inc. Chicago Illinois).

Continuous variables were expressed as mean ± standard deviation while categorical variables are expressed as proportions.

A precise evaluation of pulmonary pressure is of fundamental importance in the diagnosis and management of patients with pulmonary hypertension (PH). Doppler echocardiography is a low-cost, non-invasive method that is widely used for anatomical and functional assessment of the right cardiac chambers and estimation of pulmonary pressure, and the hemodynamic data obtained correlates well with that obtained through cardiac catheterization. Although the most appropriate and common technique for determining pulmonary pressure is the measurement of the gradient between the right ventricle and right atrium through tricuspid regurgitation, it can also be determined by analysis of pulmonary regurgitation or systolic pulmonary flow(Chatterjee et al 2002)..

The most frequency of ages distribute as (40-50 years old (36%), 30-40 years (33%), 50-60 years (18%), more than 60 years (9%)and few percentages in aged group 20-30 years(Table (4-4) and Fig (4-2)) , there is good correlation of age with Systolic pulmonary artery pressure (SPAP) p-value 0.00(Fig (4-9), this agree with finding of Lam et al ,2009. Recently, Argiento et al.,50 in a series of 113 healthy volunteers (mean age, 37 613 years; range, 19–63 years; 57 women [50%]) reported exercise flow-corrected upper limits of normal for MPAP of 34 mm Hg at a cardiac output (CO) of <10 L/min, 45 mm Hg at a CO of <20 L/min, and 52 mm Hg at a CO of <30 L/min(Argiento et al ,2012).

Participant's weight were as (40-60 Kg, in127 participants, 20-40Kg in 111 participants, 60-80 Kgs in 57 participants, and the less one their weight range between 80-100 Kg. Fig (4-3).

In current study, Right ventricles (RV) dimensions as(2.3 cm in 133 (44.3%), 2.2cm RV in 79 (26.3%), and 2.1 cm in 19(6.3%) and 2.8 Cm in one participant 0.3%, Fig (4-4), there is good relationship between RV and age fig (4-10).

In figure (4-6) the result of this study showed that, the PASP measurements were 33 mmHg in 73 of participants, 31mmHg in 58 of the total, 37mmHg in 37.

These results are significant and deal with Sheikhzadeh et al (Sheikhzadeh et al,2014)..

There was a significant correlation between TV max and RV dimension P-value 0.000. Table (4-18)

The most accurate and reliable noninvasive method of echocardiographic PAP assessment is based on tricuspid regurgitation. It reflects the difference between RV and RA pressure and can be calculated by the Bernoulli equation(Sbano et al 2004).. When estimated RA pressure is added to that gradient, systolic RV pressure is obtained. Results from this method, which is simple and easily applied, have correlated well with those from invasive PAP measures in hemodynamics laboratory tests, with a correlation coefficient (r) between 0.89 and 0.94. Although this method is only valid in cases of tricuspid valve insufficiency, this is rarely regarded as a limitation, since approximately 90% of patients with PH present with this condition. The accurate estimation of RA pressure makes for a more precise calculation of systolic pressure in the pulmonary artery, and several noninvasive approaches have been proposed for that assessment. The RA pressure can be determined by the respiratory variation in inferior vena cava diameter observed through the subcostal window). It is important to point out that, due to alterations in intrathoracic pressures, the estimation of the diameter and inspiratory collapse of

the inferior vena cava is not useful in patients under ventilation with positive pressure(Jatene et al ,2000)..

Other approaches to assessing RA pressure include clinical examination of the distention of the jugular (secondary to retrograde circulatory arrest) and the determination of values of 10 mmHg or 14 mmHg for the estimation of the RA pressure. Systolic RV pressure estimated using the techniques for calculating RA pressure also correlates well with values obtained in the hemodynamics laboratory(Rich, 2001).

In this study, we demonstrate descriptive statistics for The mean + Std.Deviation of age, weight, RV, TVMAX and PASP were 37.2 ±11.06 , 61.3 ± 10.03 ,2.29 ± 0.11, 2.8± 0.36 , and 37.4 ± 10.8 respectively. Table (4-1)

These results are significant and deal with Sheikhzadeh et al (Sheikhzadeh et al, 2014).

83% of the patients with mild TR max, 10% moderate and 7% were severe TR max measurements. Severe TR max with PASP with 61mmHg and 74 mmHg in 4 patients(Table (4-10),this agree with finding of Argiento et al (Argiento et al ,2012).

The PASP measurement range from 50 mmHg -74 mmHg common with 40-80 Kg weight with p-value 0.002 considered the significant correlation between them and most common weight-related to moderate TR with PASP were13 of patients their weighted 60-80Kg and severe TR with PASP were 2 of patients and their weighted were 80-100Kg are 4 moderates TR with PASP and one patient were severe TR with PASP with significant relation between weight and echo finding. Table (4-13)

Few patients RV dimension measure 2.4cm to 2.6 cm with high TR max range between 3.68 m/s -4.19m/s respectively which considered high suggested PH. Table(4-18)

In figures (4.13, 4.14, 4.15) shows PASP mean and std. deviation and frequency ofall subjects, Mild TR, Moderate and Severe TR respectively were (37.44±10.82), (33.08±2.95), (59.26±9.36) mmHg PASP.Weak and clinically irrelevant correlations were found between mean PAP and indices of pulmonary artery flow. A statistically significant and clinically relevant correlation was found between systolic PAP and regurgitation tricuspid flow. In 3 patients (14%), pulmonary artery pressure could not be assessed echocardiographically. The current study results was deal with Bouhemad et al (Bouhemad et al ,2008).

Figure (4-8) shows Linear regression analysis showed the correlation between Age (years) and TV max the correlation could be fitted in the following equation: $y = 0.0239x + 1.9043$, $R^2 = 0.5173$.

Figure (4-9) shows Linear regression analysis showed the correlation between Age (years) and PASP the correlation could be fitted in the following equation: $y = 0.0055x + 2.0909$, $R^2 = 0.2877$.

Figure (4-10) shows Linear regression analysis showed the correlation between Age (years) and TV max the correlation could be fitted in the following equation: $y = 0.0239x + 1.9043$ $R^2 = 0.5173$.

Figure (4-11) shows Linear regression analysis showed the correlation between weight and RV Dimensions the correlation could be fitted in the following equation: $y = 0.0046x + 2.015$, $R^2 = 0.1638$.

Figure (4-12) shows Linear regression analysis showed the correlation between weight and PASP the correlation could be fitted in the following equation: $y = 0.5225x + 5.383$,$R^2 = 0.2347$.

PH is presently defined as an increase in mean pulmonary arterial pressure to ≥25 mmHg at rest as assessed by right heart catheterisation (Galie et al2015).. The clinical significance of a mean pulmonary arterial pressure between 21 mmHg and 24 mmHg is unclear. It can complicate many cardiovascular, respiratory and

connective tissue diseases. Untreated, morbidity and mortality levels are high (Hoeper et al 2017),Oudiz,2013).

5.2 Conclusion:

From the results shown above, it can be concluded that:

Detailed echocardiographic assessment of patients with PH allows useful diagnostic information to be collected. It can also be used to assess the severity of right ventricular dysfunction, providing prognostic information and a non-invasive means of following disease progression or response to therapy.

Echocardiography can be used to accurately quantify PAPs, showing their impact on the right heart chambers and systemic veins. It is also useful as an analytical tool in the evaluation of therapeutic responses and prognoses.

Regarding the right ventricle (RV) dimension, 133 participants (44.3%) revealed that their (RV) dimension of 2.3 cm, the maximum and minimum RV dimensions reported were 2.1cm and 2.8cm seen in one participant (0.3%) and one participant (0.3%) respectively. Considering the pulmonary artery systolic pressure (PASP), 33 mmHg was the most frequent value noted in 73 participants, the low and the high value represented 26mmHg and 80 mmHg seen in 5 participants and 30 participants respectively.

The standard value of the pulmonary artery pressure in Sudanese population is markedly greater than the universal reported in the public literature, larger populations may be needed to corroborate our normative thresholds.

This study attempts to simulate the basic clinical or experimental echocardiography M-mode protocol in Sudanese population. echocardiography itself could be used for heart disease screening in clinical patients Precise echocardiographic measurements in a study employing experimental rats could result in a precise description of models with zero-pain and good clinical relevance. We have established reliable regression equations for the calculation of basic echocardiographic parameters Despite its technical limitations.

Conventional echocardiography, alongside newer, richer techniques, provides invaluable information about the extent of heart damage related to PHT and cardiovascular risk, thus helping us to achieve better management and apply better treatment.

This study is small study consisting of randomized populations of people in Khartoum state and the study population cannot be the representation of whole Sudanese population. Relatively the sample size was also small.

5.3 Recommendation:

Based on the outcome of this study, the following recommendations are proposed:

Large population-based prospective studies in Sudan to determine the prevalence and patterns of cardiovascular complications in the general population.

Since echocardiography is not currently endorsed as a routine investigation for Sudanese patients, despite its being a non-invasive and non-expensive method of revealing cardiac functional and morphological changes, we recommend its use in follow up and monitoring of patients in the Sudan.

Echocardiographic machines must be made available in emergency hospitals/departments together with well trained staff.

As technological advances allow more detailed examination of these structures, our knowledge of normal anatomy and pathologic conditions will allow for more accurate and detailed examinations.

Further study needed to show the relation of Echo and other imaging modalities and cardiac function.

One imaging modality is unable to reliably distinguish various cardiac diseases.

Ultrasound investigation should be used as routine for any patient complaining of heart disorders.

All the Echocardiographic reference parameters that we use to compare during Echocardiographic studies are derived from those defined in the western world. We till now do not have a proper reference range based on studies conducted in Sudan or Africa itself. It is a well-known fact that the population in Sudan has a very much different genetic and physical make up as compared to the population in the west. The difference in the body size in itself brings into question the reference range that we quote as normal values derived from studies conducted in the west. We have thus made an effort to study a

hypertensive population in Sudan, for recording changes of echocardiographic parameters.

Our study suggests that adequate control of should remain a clinical priority. Also centers should pursue competence in full utilization of echocardiography, including stress echocardiography as well as to purchase machines that have full options. Subsequent studies should also indicate percentage of patients who are in heart failure.

Limitations

This study was hospital-based; hence it may not necessarily reflect the pattern of echocardiographic features as well.

The echocardiography machine used to conduct this study did not have the tissue Doppler imaging function which would have been more helpful in further categorizing diastolic function in the subjects.

Right heart catheterization is the gold standard for diagnosing pulmonary hypertension, hence, the reliance on echocardiography evaluation may not be too accurate.

Some of our limitations include the non-availability of transesophageal echocardiography,and as such posterior cardiac structures cannot be more precisely studied. The lack of contrast echocardiography studies also implies we could not reliably exclude such conditions as the presence of intracardiac shunts.

We also do not perform stress echocardiography which helps to exclude ischaemic heart disease.

Moreover, patients often have to pay out of their pocket for diagnostic tests, and therefore accessibility to tests is limited due to the financial means of the patient.

References

Abbas, A. E., Fortuin, F. D., Schiller, N. B., Appleton, C. P., Moreno, C. A., & Lester, S. J. (2003). Echocardiographic determination of mean pulmonary artery pressure. *The American journal of cardiology*, *92*(11), 1373-1376.

Ágoston, G. (2015). Echocardiographic assessment of cardiac and pulmonary manifestations in patients with systemic sclerosis (Doctoral dissertation, szte).

Arcasoy, S. M., Christie, J. D., Ferrari, V. A., Sutton, M. S. J., Zisman, D. A., Blumenthal, N. P., ... & Kotloff, R. M. (2003). Echocardiographic assessment of pulmonary hypertension in patients with advanced lung disease. *American journal of respiratory and critical care medicine*, *167*(5), 735-740.

Argiento, P., Vanderpool, R. R., Mulè, M., Russo, M. G., D'Alto, M., Bossone, E., ... & Naeije, R. (2012). Exercise stress echocardiography of the pulmonary circulation: limits of normal and sex differences. *Chest*, *142*(5), 1158-1165.

Argiento, P., Vanderpool, R. R., Mulè, M., Russo, M. G., D'Alto, M., Bossone, E., ... & Naeije, R. (2012). Exercise stress echocardiography of the pulmonary circulation: limits of normal and sex differences. *Chest*, *142*(5), 1158-1165

Arkles, J. S., Opotowsky, A. R., Ojeda, J., Rogers, F., Liu, T., Prassana, V., ... & Forfia, P. R. (2011). Shape of the right ventricular Doppler envelope predicts hemodynamics and right heart function in pulmonary hypertension. *American journal of respiratory and critical care medicine*, *183*(2), 268-276.

Augustine, D. X., Coates-Bradshaw, L. D., Willis, J., Harkness, A., Ring, L., Grapsa, J., ... & Mathew, T. (2018). Echocardiographic assessment of pulmonary hypertension: a guideline protocol from the British Society of Echocardiography. Echo research and practice, 5(3), G11-G24.

Avdić S, Mujčinović Z, Aščerić M., et al. Left ventricular diastolic dysfunction in essential hypertension. Bosn J Basic Med Sci 2007;7;15-20.

Barst, R. J. (2008). Pulmonary hypertension: past, present and future. *Annals of thoracic medicine*, *3*(1), 1.

basic facts and implementation. Radiographics. 22:651–71. doi: 10.1148/radiographics.22.3.g02ma11651

Borgarelli, M., Abbott, J., Braz-Ruivo, L., Chiavegato, D., Crosara, S., Lamb, K., ... & Haggstrom, J. (2015). Prevalence and prognostic importance of pulmonary hypertension in dogs with myxomatous mitral valve disease. *Journal of veterinary internal medicine*, *29*(2), 569-574.

Bossone, E., D'Andrea, A., D'Alto, M., Citro, R., Argiento, P., Ferrara, F., ... & Naeije, R. (2013). Echocardiography in pulmonary arterial hypertension: from diagnosis to prognosis. Journal of the American Society of Echocardiography, 26(1), 1-14.

Bouhemad, B., Ferrari, F., Leleu, K., Arbelot, C., Lu, Q., & Rouby, J. J. (2008). Echocardiographic Doppler estimation of pulmonary artery pressure in critically ill patients with severe hypoxemia. The Journal of the American Society of Anesthesiologists, 108(1), 55-62.

Bouhemad, B., Ferrari, F., Leleu, K., Arbelot, C., Lu, Q., & Rouby, J. J. (2008). Echocardiographic Doppler estimation of pulmonary artery pressure in critically ill patients with severe hypoxemia. *The Journal of the American Society of Anesthesiologists*, *108*(1), 55-62.

Brecker, S. J., Gibbs, J. S., Fox, K. M., Yacoub, M. H., & Gibson, D. G. (1994). Comparison of Doppler derived haemodynamic variables and simultaneous high fidelity pressure measurements in severe pulmonary hypertension. *Heart*, *72*(4), 384-389.

Brierre, G., Blot-Souletie, N., Degano, B., Têtu, L., Bongard, V., & Carrie, D. (2010). New echocardiographic prognostic factors for mortality in pulmonary arterial hypertension. *European Journal of Echocardiography*, *11*(6), 516-522.

Buba, F., Okeahialam, B.N. and Anjorin, C.O., 2008. The Value of Chest Radiogram and Electrocardiogram in the Assessment of Left Ventricular Hypertrophy among Adult Hypertensives. J. Med. Sci, 8(3), pp.298-301.

Chatterjee, K., De Marco, T., & Alpert, J. S. (2002). Pulmonary hypertension: hemodynamic diagnosis and management. *Archives of internal medicine*, *162*(17), 1925-1933.

Chatterjee, K., De Marco, T., & Alpert, J. S. (2002). Pulmonary hypertension: hemodynamic diagnosis and management. *Archives of internal medicine*, *162*(17), 1925-1933.

Cloez, J. L., Schmidt, K. G., Birk, E., & Silverman, N. H. (1988). Determination of pulmonary to systemic blood flow ratio in children by a simplified Doppler echocardiographic method. *Journal of the American College of Cardiology*, *11*(4), 825-830.

Costa AF, Andrade GN. HAP e cor pulmonale. In: Bethlem N, editor. Pneumologia. 4a ed. São Paulo: Atheneu; 1995. p.817-30.

Crawley SF, Johnson MK, Dargie HJ, Peacock AJ. LA volume by CMR distinguishes idiopathic from pulmonary hypertension due to HFpEF. JACC Cardiovasc Imaging. 2013;6:1120–1121. DOI: 10.1016/j. jcmg.2013.05.014.

Currie, P. J., Seward, J. B., Chan, K. L., Fyfe, D. A., Hagler, D. J., Mair, D. D., ... & Tajik, A. J. (1985). Continuous wave Doppler determination of right ventricular pressure: a simultaneous Doppler-catheterization study in 127 patients. *Journal of the American College of Cardiology*, *6*(4), 750-756.

Devereux, R. B., Roman, M. J., Palmieri, V., Okin, P. M., Boman, K., Gerdts, E., ... & Dahlöf, B. (2000). Left ventricular wall stresses and wall stress–mass–heart rate products in hypertensive patients with electrocardiographic left ventricular hypertrophy: the LIFE study. *Journal of hypertension*, *18*(8), 1129-1138.

Dorr, M., Wolff, B., Robinson, D. M., John, U., Ludemann, J., Meng, W., ... & Volzke, H. (2005). The association of thyroid function with cardiac mass and left ventricular hypertrophy. *The Journal of Clinical Endocrinology & Metabolism*, *90*(2), 673-677..

Farrag, A., El-Aroussy, W., Zaghloul, S., El-Guindy, M., & Yacoub, M. (2012). Prevalence and severity of pulmonary hypertension in asymptomatic rural residents with schistosomal infection in the Nile Delta. Tropical Medicine & International Health, 17(1), 112-118.

flow measurement with phase-contrast MR imaging:

Forfia, P. R., Fisher, M. R., Mathai, S. C., Housten-Harris, T., Hemnes, A. R., Borlaug, B. A., ... & Hassoun, P. M. (2006). Tricuspid annular displacement predicts survival in pulmonary hypertension. *American journal of respiratory and critical care medicine*, *174*(9), 1034-1041.

Frost, A., Badesch, D., Gibbs, J. S. R., Gopalan, D., Khanna, D., Manes, A., ... & Torbicki, A. (2019). Diagnosis of pulmonary hypertension. *European Respiratory Journal*, *53*(1).

GALIE, N., HUMBERT, M., VACHIERY, J. L., GIBBS, S., LANG, I., TORBICKI, A., ... & HOEPER, M. (2015). 2015 ESC/ERS Guidelines for the diagnosis and treatment of pulmonary hypertension: web addenda. *European Respiratory Journal*.

GALIE, N., HUMBERT, M., VACHIERY, J. L., GIBBS, S., LANG, I., TORBICKI, A., ... & HOEPER, M. (2015). 2015 ESC/ERS Guidelines for the diagnosis and treatment of pulmonary hypertension: web addenda. *European Respiratory Journal*.

Galiè, N., Humbert, M., Vachiery, J. L., Gibbs, S., Lang, I., Torbicki, A., ... & Hoeper, M. (2016). 2015 ESC/ERS guidelines for the diagnosis and treatment of pulmonary hypertension: the joint task force for the diagnosis and treatment of pulmonary hypertension of the European Society of Cardiology (ESC) and the European Respiratory Society (ERS): endorsed by: Association for European Paediatric and Congenital Cardiology (AEPC), International Society for Heart and Lung Transplantation (ISHLT). *European heart journal*, *37*(1), 67-119.

Ganong, W.F. , 2003,, review of medical physiology 21st Ed, (appelton&lange California) , Section VI 509 - 521

Giaid, A. (1998). Nitric oxide and endothelin-1 in pulmonary hypertension. *Chest*, *114*(3), 208S-212S.

Grapsa, J., Dawson, D., & Nihoyannopoulos, P. (2011). Assessment of right ventricular structure and function in pulmonary hypertension. *Journal of cardiovascular ultrasound*, *19*(3), 115-125.

Guyton, A.C.. 2006.Text book of medical physiology ,Eleventh edition (igaku-shon/saunders) , ,p 150-163

Haider, A. W., Larson, M. G., Benjamin, E. J., & Levy, D. (1998). Increased left ventricular mass and hypertrophy are associated with increased risk for sudden death. *Journal of the American College of Cardiology*, *32*(5), 1454-1459.

Hoeper, M. M., Kramer, T., Pan, Z., Eichstaedt, C. A., Spiesshoefer, J., Benjamin, N., ... & Grünig, E. (2017). Mortality in pulmonary arterial hypertension: prediction by the 2015 European pulmonary hypertension guidelines risk stratification model. *European Respiratory Journal*, *50*(2).

Howard LS, Grapsa J, Dawson D, Bellamy M, Chambers JB, Masani ND, Nihoyannopoulos P, Simon R Gibbs J. Echocardiographic assessment of pulmonary hypertension: standard operating procedure. Eur Respir Rev. 2012 Sep 1;21(125):239-48. doi: 10.1183/09059180.00003912. Erratum in: Eur Respir Rev. 2012 Dec 1;21(126):370. PMID: 22941889.

Howard, L. S., Grapsa, J., Dawson, D., Bellamy, M., Chambers, J. B., Masani, N. D., ... & Gibbs, J. S. R. (2012). Echocardiographic assessment of pulmonary hypertension: standard operating procedure. *European Respiratory Review*, *21*(125), 239-248.

Jatene, F. B., Bernardo, W. M., Monteiro, R., Hueb, A. C., Terra-Filho, M., & Oliveira, S. A. (2000). Tratamento cirúrgico da hipertensão pulmonar tromboembólica. *Rev Soc Cardiol Estado de São Paulo*, *5*, 640-51.

Johnson, L., Boon, J., & Orton, E. C. (1999). Clinical characteristics of 53 dogs with Doppler-derived evidence of pulmonary hypertension: 1992–1996. *Journal of Veterinary Internal Medicine*, *13*(5), 440-447.

Kannel, W. B., & Cobb, J. (1992). Left ventricular hypertrophy and mortality–results from the Framingham Study. *Cardiology*, *81*(4-5), 291-298.

Kanwar, M. K., Tedford, R. J., Thenappan, T., De Marco, T., Park, M., & McLaughlin, V. (2021). Elevated Pulmonary Pressure Noted on Echocardiogram: A Simplified Approach to Next Steps. Journal of the American Heart Association, 10(7), e017684.

Kaul, S., Tei, C., Hopkins, J. M., & Shah, P. M. (1984). Assessment of right ventricular function using two-dimensional echocardiography. *American heart journal*, *107*(3), 526-531.

Kellihan, H. B., & Stepien, R. L. (2012). Pulmonary hypertension in canine degenerative mitral valve disease. *Journal of Veterinary Cardiology*, *14*(1), 149-164.

Kim D, Lee KM, Freiman MR, Powell WR, Klings ES, Rinne ST, Miller DR, Rose AJ, Wiener RS. Phosphodiesterase-5 inhibitor therapy for pulmonary hypertension in the United States. Actual versus recommended use. Ann Am Thorac Soc. 2018;15:693–701. DOI: 10.1513/ AnnalsATS.201710-762OC.

Lam, C. S., Borlaug, B. A., Kane, G. C., Enders, F. T., Rodeheffer, R. J., & Redfield, M. M. (2009). Age-associated increases in pulmonary artery systolic pressure in the general population. *Circulation*, *119*(20), 2663-2670.

Lee, V. S., Spritzer, C. E., Carroll, B. A., Pool, L. G., Bernstein, M. A., Heinle, S. K., & MacFall, J. R. (1997). Flow quantification using fast cine phase-contrast MR imaging, conventional cine phase-contrast MR imaging, and Doppler sonography: in vitro and in vivo validation. *AJR. American journal of roentgenology*, *169*(4), 1125-1131.

Lewis, G. D., Bossone, E., Naeije, R., Grünig, E., Saggar, R., Lancellotti, P., ... & Rubenfire, M. (2013). Pulmonary vascular hemodynamic response to exercise in cardiopulmonary diseases. *Circulation*, *128*(13), 1470-1479.

Lima, M. S. M., Villarraga, H. R., Abduch, M. C. D., Lima, M. F., Cruz, C. B. B. V., Bittencourt, M. S., ... & Tsutsui, J. M. (2015). Comprehensive left ventricular mechanics analysis by speckle tracking echocardiography in Chagas disease. Cardiovascular ultrasound, 14(1), 1-11.

Lin, S. C., Chen, R. J. C., & Lee, J. H. (2009). The correlation between right descending pulmonary artery diameter and echocardiographyestimated systolic pulmonary artery pressure. Acta Cardiol Sin, 25, 213-7.

Lopes, A. A., Barst, R. J., Haworth, S. G., Rabinovitch, M., Dabbagh, M. A., Cerro, M. J. D., ... & Adatia, I. (2014). Repair of congenital heart disease with associated pulmonary hypertension in children: what are the minimal investigative procedures? Consensus statement from the Congenital Heart Disease and Pediatric Task Forces, Pulmonary Vascular Research Institute (PVRI). *Pulmonary circulation*, *4*(2), 330-341.

Lotz J, Meier C, Leppert A, Galanski M. (2002) Cardiovascular

Loyd, J. E., Primm, R. K., & Newman, J. H. (1984). Familial primary pulmonary hypertension: clinical patterns. *American Review of Respiratory Disease*, *129*(1), 194-197.

Mansencal, N., Martin, F., Farcot, J. C., Digne, F., Joseph, T., Pilliére, R., ... & Dubourg, O. (2005). Echocardiographic automated cardiac output measurement of pulmonary output and quantification of intracardiac shunt. *International journal of cardiology*, *104*(1), 25-31.

Masuyama, T., Kodama, K. A. Z. U. H. I. S. A., Kitabatake, A. K. I. R. A., Sato, H. I. R. O. S. H. I., Nanto, S. H. I. N. S. U. K. E., & Inoue, M. I. C. H. I. T. O. S. H. I. (1986). Continuous-wave Doppler echocardiographic detection of pulmonary regurgitation and its application to noninvasive estimation of pulmonary artery pressure. *Circulation*, *74*(3), 484-492.

McDonnell CHIII, Herfkens RJ, Norbash AM, Rubin GD.Magnetic resonance imaging and measurement of blood flow.West J Med. (1994) 160:237–42.

McLaughlin, V. V., Archer, S. L., Badesch, D. B., Barst, R. J., Farber, H. W., Lindner, J. R., ... & Varga, J. (2009). ACCF/AHA 2009 expert consensus document on pulmonary hypertension: a report of the American College of Cardiology Foundation Task Force on expert consensus documents and the American Heart Association developed in collaboration with the American College of Chest Physicians; American Thoracic Society, Inc.; and the Pulmonary Hypertension Association. *Journal of the American college of cardiology*, *53*(17), 1573-1619.

McLaughlin, V. V., Archer, S. L., Badesch, D. B., Barst, R. J., Farber, H. W., Lindner, J. R., ... & Varga, J. (2009). A report of the american college of cardiology foundation task force on expert consensus documents and the american heart association. *Circulation*, *119*(16), 2250-2294.

Modena, M. G., Muia Jr, N., Aveta, P., Molinari, R., & Rossi, R. (1999). Effects of transdermal 17β-estradiol on left ventricular anatomy and performance in hypertensive women. *Hypertension*, *34*(5), 1041-1046.

Moore, K.L. and Dalley, A.F., 2006,Clinically Oriented Anatomy ,fifth edition , Lippincott Williams & Wilkins ,p 141 -165

Mousseaux, E., Tasu, J. P., Jolivet, O., Simonneau, G., Bittoun, J., & Gaux, J. C. (1999). Pulmonary arterial resistance: noninvasive measurement with indexes of pulmonary flow estimated at velocity-encoded MR imaging—preliminary experience. *Radiology*, *212*(3), 896-902.

Opotowsky, A. R., Ojeda, J., Rogers, F., Prasanna, V., Clair, M., Moko, L., ... & Forfia, P. R. (2012). A simple echocardiographic prediction rule for hemodynamics in pulmonary hypertension. *Circulation: Cardiovascular Imaging*, *5*(6), 765-775.

Oudiz, R. J. (2013). Death in pulmonary arterial hypertension., *American Journal of Respiratory and Critical Care Medicine* 2013 **188** 269–270. (https://doi.org/10.1164/rccm.201305-0898ED)

Pleister, A., Kahwash, R., Haas, G., Ghio, S., Cittadini, A., & Baliga, R. R. (2015). Echocardiography and heart failure: a glimpse of the right heart. Echocardiography, 32, S95-S107.

Rhinehart, J. D. (2016). Clinical Evaluation of Echocardiographic Variability in Estimating Pulmonary Artery Pressure and Pulmonary Vascular Resistance in Dogs (Doctoral dissertation, The Ohio State University).

Rich, S. (2001). Pulmonary hypertension. In *Cardiology for the primary care Physician* (pp. 313-318). Current Medicine Group.

Rich, S. E. (1998). Primary Pulmonary Hypertension: Exective Summary from the World Symposium-Primary Pulmonary Hypertension. *http://www. who. int/ncd/cvd/pph. html*.

Rich, S., & Rabinovitch, M. (2008). Diagnosis and treatment of secondary (non–category 1) pulmonary hypertension. *Circulation*, *118*(21), 2190-2199.

Rosenzweig, E. B., Abman, S. H., Adatia, I., Beghetti, M., Bonnet, D., Haworth, S., ... & Berger, R. M. (2019). Paediatric pulmonary arterial hypertension: updates on definition, classification, diagnostics and management. *European Respiratory Journal*, *53*(1).

Rudski, L. G., Lai, W. W., Afilalo, J., Hua, L., Handschumacher, M. D., Chandrasekaran, K., … & Schiller, N. B. (2010). Guidelines for the echocardiographic assessment of the right heart in adults: a report from the American Society of Echocardiography: endorsed by the European Association of Echocardiography, a registered branch of the European Society of Cardiology, and the Canadian Society of Echocardiography. *Journal of the American society of echocardiography*, *23*(7), 685-713.

Sbano, J. C. N., Tsutsui, J. M., Terra-Filho, M., & Mathias Junior, W. (2004). Evaluation of pulmonary hypertension with dopper echodopplercardiography. *Jornal Brasileiro de Pneumologia*, *30*, 78-86

Schulman, L. L., Grossman, B. A., & Owen, J. (1993). Platelet activation and fibrinopeptide formation in pulmonary hypertension. *Chest*, *104*(6), 1690-1693.

Shahgaldi, K., Gudmundsson, P., Manouras, A., Brodin, L. Å., & Winter, R. (2009). Visually estimated ejection fraction by two dimensional and triplane echocardiography is closely correlated with quantitative ejection fraction by real-time three dimensional echocardiography. *Cardiovascular ultrasound*, *7*(1), 1-7.

Sheikhzadeh, S., De Backer, J., Gorgan, N. R., Rybczynski, M., Hillebrand, M., Schüler, H., ... & von Kodolitsch, Y. (2014). The main pulmonary artery in adults: a controlled multicenter study with assessment of echocardiographic reference values, and the frequency of dilatation and aneurysm in Marfan syndrome. Orphanet journal of rare diseases, 9(1), 1-10.

Sheikhzadeh, S., De Backer, J., Gorgan, N. R., Rybczynski, M., Hillebrand, M., Schüler, H., ... & von Kodolitsch, Y. (2014). The main pulmonary artery in adults: a controlled multicenter study with assessment of echocardiographic reference values, and the frequency of dilatation and aneurysm in Marfan syndrome. *Orphanet journal of rare diseases*, *9*(1), 1-10.

Sheikhzadeh, S., De Backer, J., Gorgan, N. R., Rybczynski, M., Hillebrand, M., Schüler, H., ... & von Kodolitsch, Y. (2014). The main pulmonary artery in adults: a controlled multicenter study with assessment of echocardiographic reference values, and the frequency of dilatation and aneurysm in Marfan syndrome. *Orphanet journal of rare diseases*, *9*(1), 1-10.

Simonneau, G., Gatzoulis, M. A., Adatia, I., Celermajer, D., Denton, C., Ghofrani, A., ... & Souza, R. (2013). Updated clinical classification of pulmonary hypertension. *Journal of the American College of Cardiology*, *62*(25S), D34-D41.

Sliwa, K., Carrington, M. J., Becker, A., Thienemann, F., Ntsekhe, M., & Stewart, S. (2012). Contribution of the human immunodeficiency virus/acquired immunodeficiency syndrome epidemic to de novo presentations of heart disease in the Heart of Soweto Study cohort. *European heart journal*, *33*(7), 866-874.

Sliwa, K., Wilkinson, D., Hansen, C., Ntyintyane, L., Tibazarwa, K., Becker, A., & Stewart, S. (2008). Spectrum of heart disease and risk factors in a black urban population in South Africa (the Heart of Soweto Study): a cohort study. *The Lancet*, *371*(9616), 915-922.

Snell, R.S.,, ,2000, clinical anatomy for medical students , six edition , Lippincott Williams &wilkins ,chapter 3 p95-105

Stepien, R. L. (2009). Pulmonary arterial hypertension secondary to chronic left-sided cardiac dysfunction in dogs. *Journal of Small Animal Practice*, *50*, 34-43.

Stewart, S., Mocumbi, A. O., Carrington, M. J., Pretorius, S., Burton, R., & Sliwa, K. (2011). A not-so-rare form of heart failure in urban black Africans: pathways to right heart failure in the Heart of Soweto Study cohort. *European journal of heart failure*, *13*(10), 1070-1077..

Takahama, H., McCully, R. B., Frantz, R. P., & Kane, G. C. (2017). Unraveling the RV ejection Doppler envelope: insight into pulmonary artery hemodynamics and disease severity. *JACC: Cardiovascular Imaging*, *10*(10 Part B), 1268-1277.

Tei, C., Dujardin, K. S., Hodge, D. O., Bailey, K. R., McGoon, M. D., Tajik, A. J., & Seward, J. B. (1996). Doppler echocardiographic index for assessment of global right ventricular function. *Journal of the American Society of Echocardiography*, *9*(6), 838-847.

Thenappan, T., Prins, K. W., Pritzker, M. R., Scandurra, J., Volmers, K., & Weir, E. K. (2016). The critical role of pulmonary arterial compliance in pulmonary hypertension. *Annals of the American Thoracic Society*, *13*(2), 276-284.

Thenappan, T., Shah, S. J., Rich, S., & Gomberg-Maitland, M. (2007). A USA-based registry for pulmonary arterial hypertension: 1982–2006. *European Respiratory Journal*, *30*(6), 1103-1110.

Thienemann, F., Dzudie, A., Mocumbi, A. O., Blauwet, L., Sani, M. U., Karaye, K. M., ... & Sliwa, K. (2014). Rationale and design of the Pan African Pulmonary hypertension Cohort (PAPUCO) study: implementing a contemporary registry on pulmonary hypertension in Africa. BMJ open, 4(10), e005950.

Thienemann, F., Sliwa, K., & Rockstroh, J. K. (2013). HIV and the heart: the impact of antiretroviral therapy: a global perspective. *European heart journal*, *34*(46), 3538-3546.

Uehara, Y. (1993). An attempt to estimate the pulmonary artery pressure in dogs by means of pulsed Doppler echocardiography. *Journal of Veterinary Medical Science*, *55*(2), 307-312.

Van Dissel, A. C., Mulder, B. J., & Bouma, B. J. (2017). The changing landscape of pulmonary arterial hypertension in the adult with congenital heart disease. Journal of Clinical Medicine, 6(4), 40.

Verdecchia, P., Schillaci, G., Guerrieri, M., Gatteschi, C., Benemio, G., Boldrini, F., & Porcellati, C. (1990). Circadian blood pressure changes and left ventricular hypertrophy in essential hypertension. *Circulation*, *81*(2), 528-536.

Yock, P. G., & Popp, R. L. (1984). Noninvasive estimation of right ventricular systolic pressure by Doppler ultrasound in patients with tricuspid regurgitation. *Circulation*, *70*(4), 657-662.

Yuan, J. X. J., Aldinger, A. M., Juhaszova, M., Wang, J., Conte Jr, J. V., Gaine, S. P., ... & Rubin, L. J. (1998). Dysfunctional voltage-gated K+ channels in pulmonary artery smooth muscle cells of patients with primary pulmonary hypertension. *Circulation*, *98*(14), 1400-1406.

APPENDICES

Appendix (1)

Data Collecting Form

1-No ☐ **2-Age** ☐ **3-Hender** ☐ **4-Weight** ☐

5-PMH

NONE ☐

Heart diseases ☐

Lung diseases ☐

6-RV dimensions ☐

7-Doppler Flow

TR ☐

TV max ☐

PASP ☐

$PASP=4(V)^2+RAP$

RAP = 5 -10 mm Hg

PASP= 25mm Hg (normal)

Appendix (2)

Cases

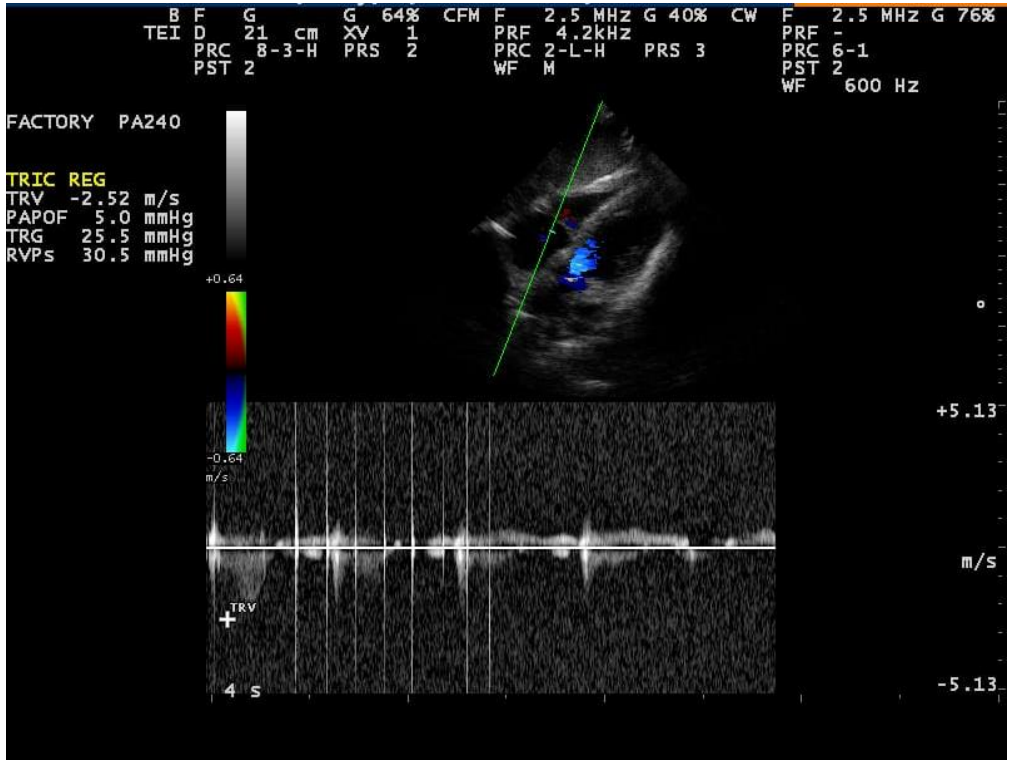

Case (1) 70 yrs. M with mild tricuspid regurgitant jet TV max (2.52 m/s) PAP 5 mmHg the PASP 30.5 mmHg (Bernoulli equation) 4 $(TV\ max)^2$ + PAP,

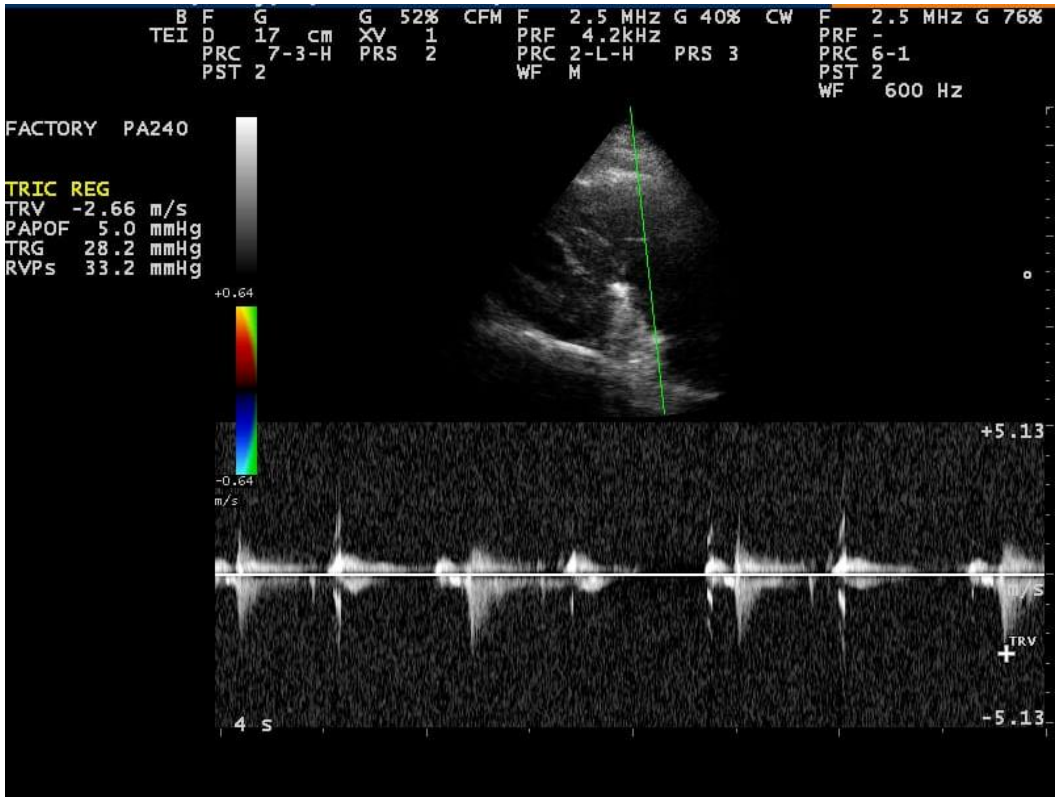

Case (2) 66 yrs. F with mild tricuspid regurgitant jet TV max (2. 66 m/s) PAP 5 mmHg the PASP 33.2 mmHg (Bernoulli equation) 4 (TV max)2 + PAP,

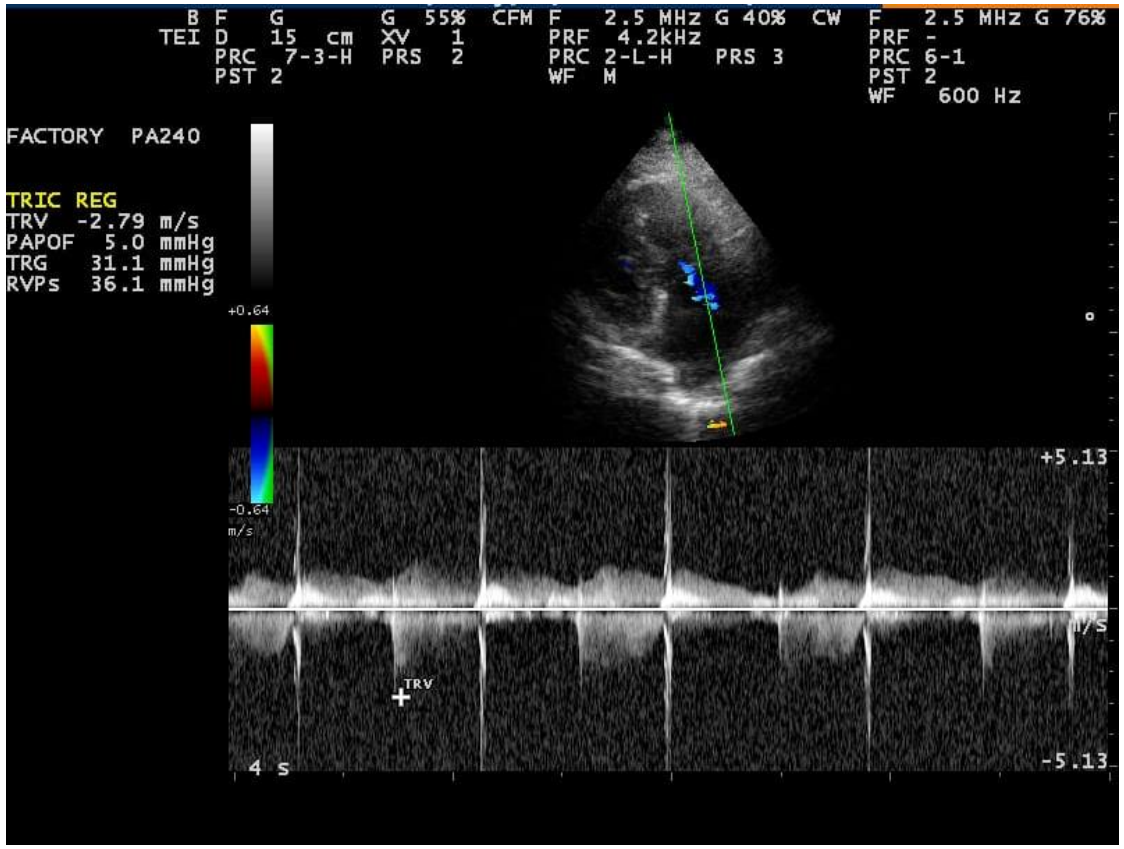

Case (3) 42 yrs. F with mild tricuspid regurgitant jet TV max (2. 79 m/s) PAP 5 mmHg the PASP 36.1 mmHg (Bernoulli equation) 4 (TV max)2 + PAP,

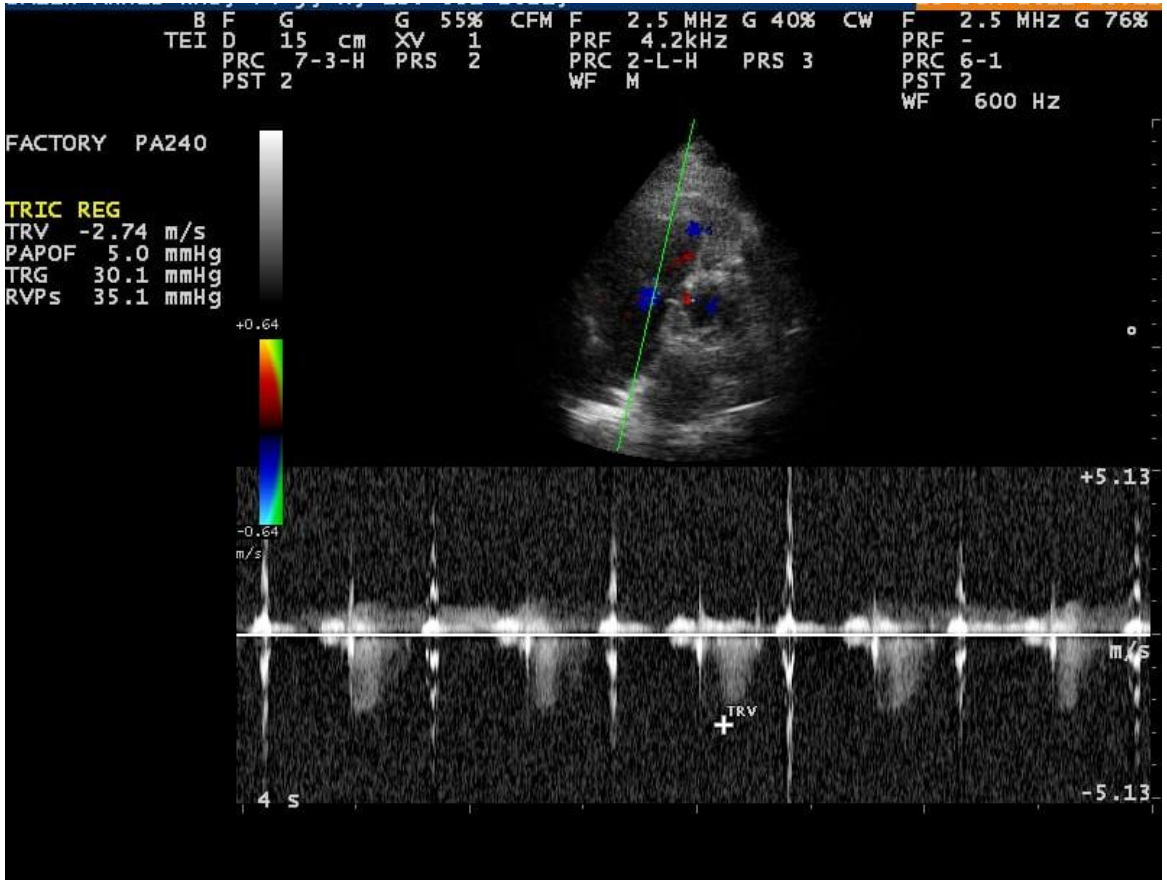

Case (4) 74 yrs. M with mild tricuspid regurgitant jet TV max (2. 74 m/s) PAP 5 mmHg the PASP 35.1 mmHg (Bernoulli equation) 4 (TV max)2 + PAP.

Case (5) 54 yrs. F with mild tricuspid regurgitant jet TV max (2. 70 m/s) PAP 5 mmHg the PASP 34.1 mmHg (Bernoulli equation) 4 (TV max)2 + PAP.

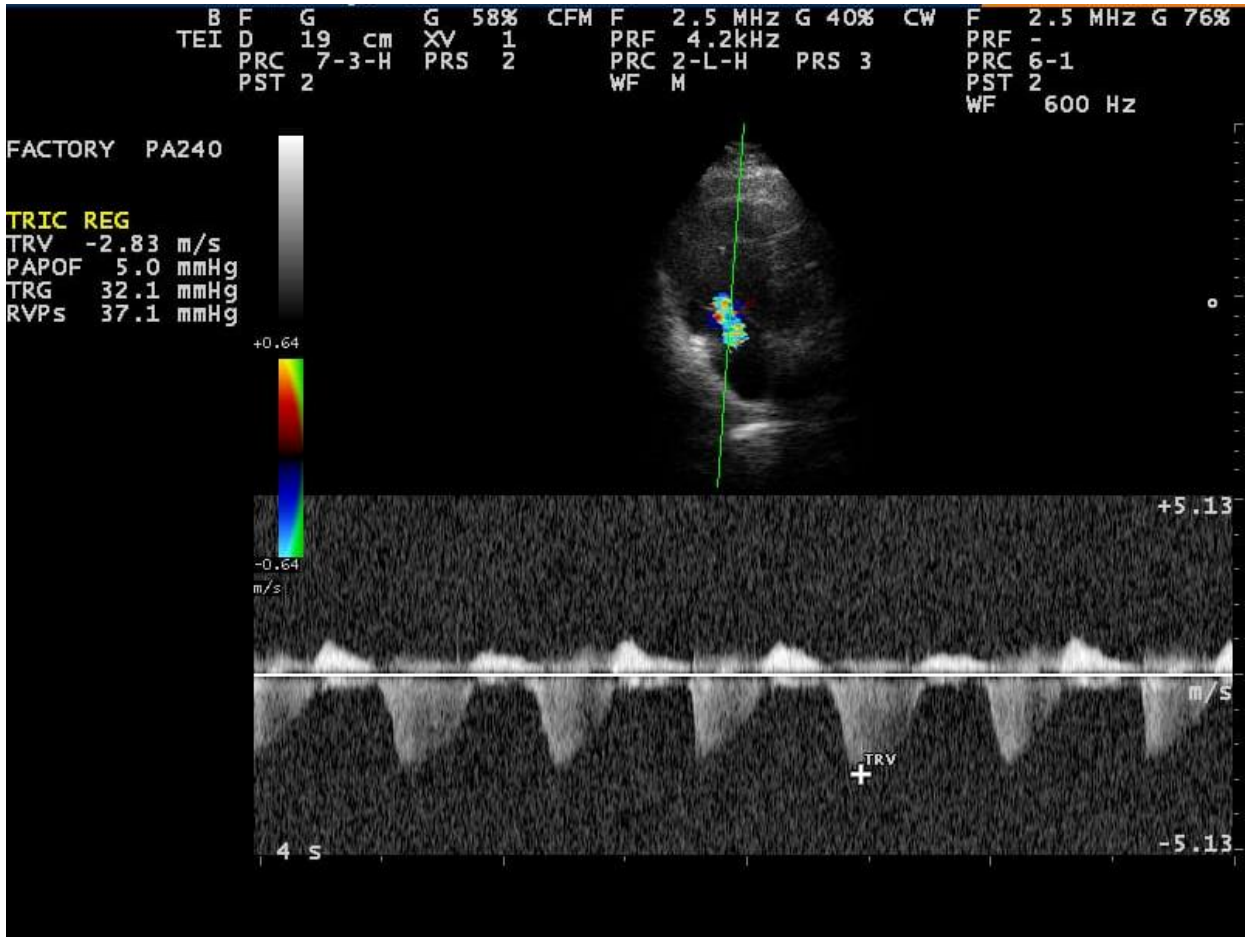

Case (6) 41 yrs. M with mild tricuspid regurgitant jet TV max (2. ٨٣ m/s) PAP 5 mmHg the PASP ٣٧.1 mmHg (Bernoulli equation) 4 (TV max)2 + PAP,

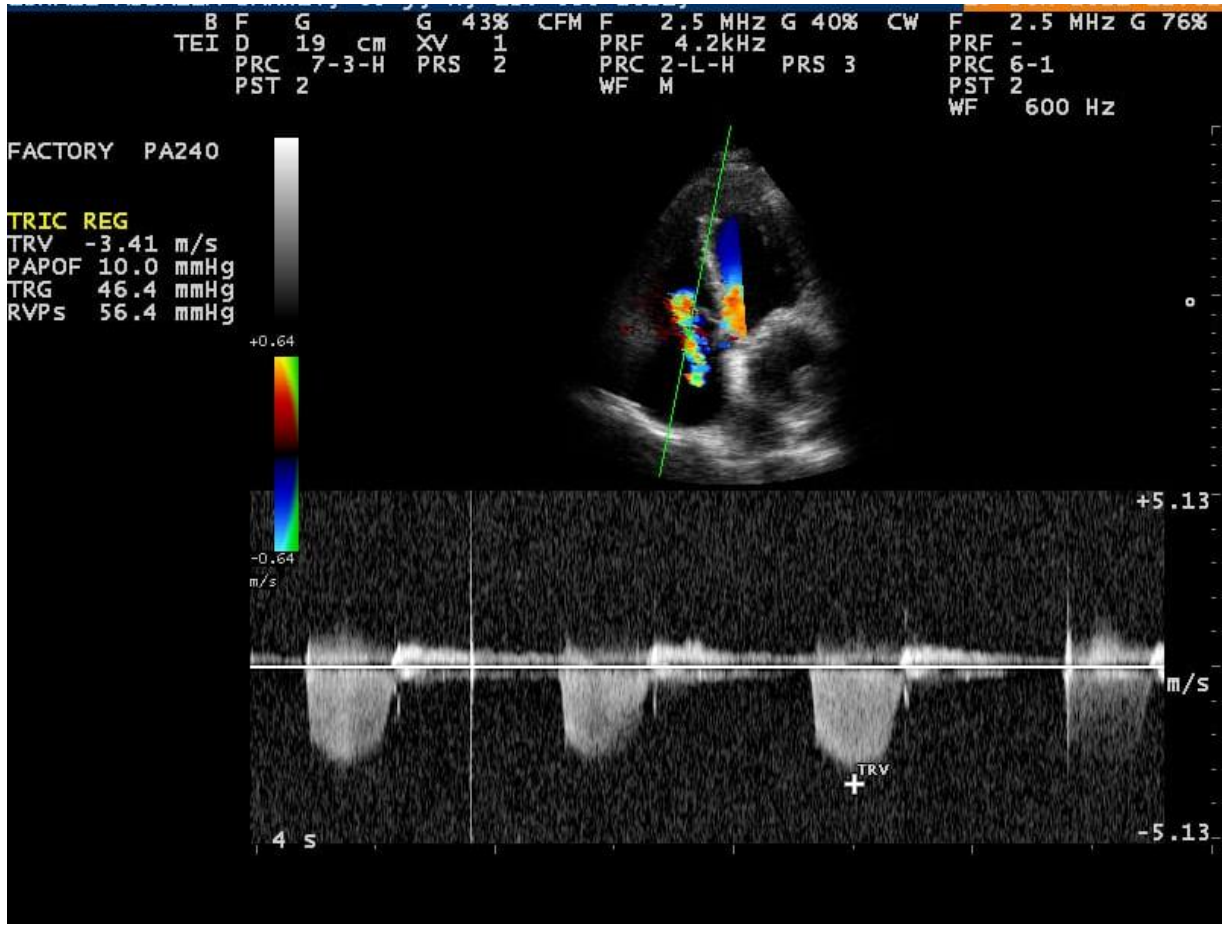

Case (7) 42 yrs. M with moderate Tricuspid regurgitant jet TV max (3. 23 m/s) PAP elvated by 10 mmHg with PASP 51.7 mmHg (Bernoulli equation) 4 $(\text{TV max})^2$ + PAP,

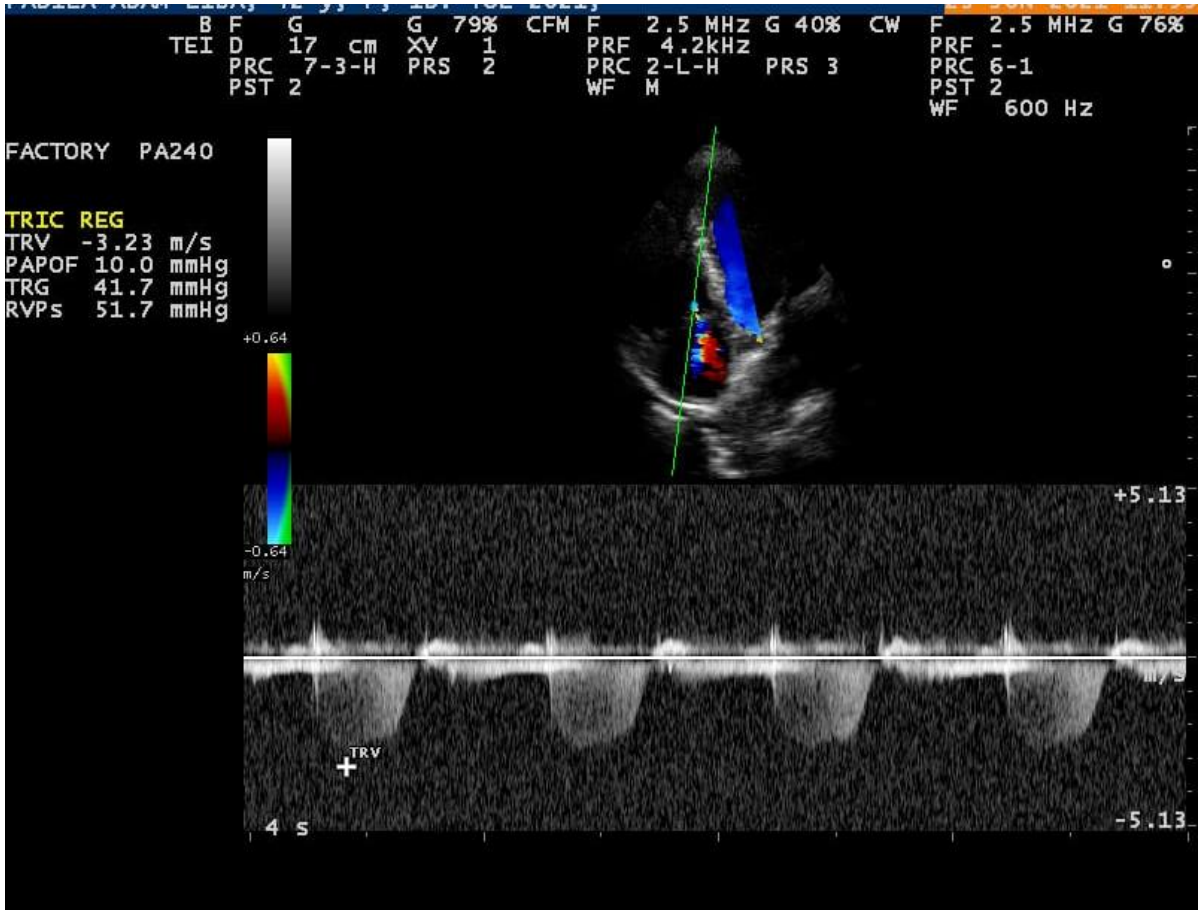

Case (8) 65 yrs. M with moderate Tricuspid regurgitant jet TV max (3. 41 m/s) PAP elvated by 10 mmHg with PASP 56.4 mmHg (Bernoulli equation) 4 $(\text{TV max})^2$ + PAP.

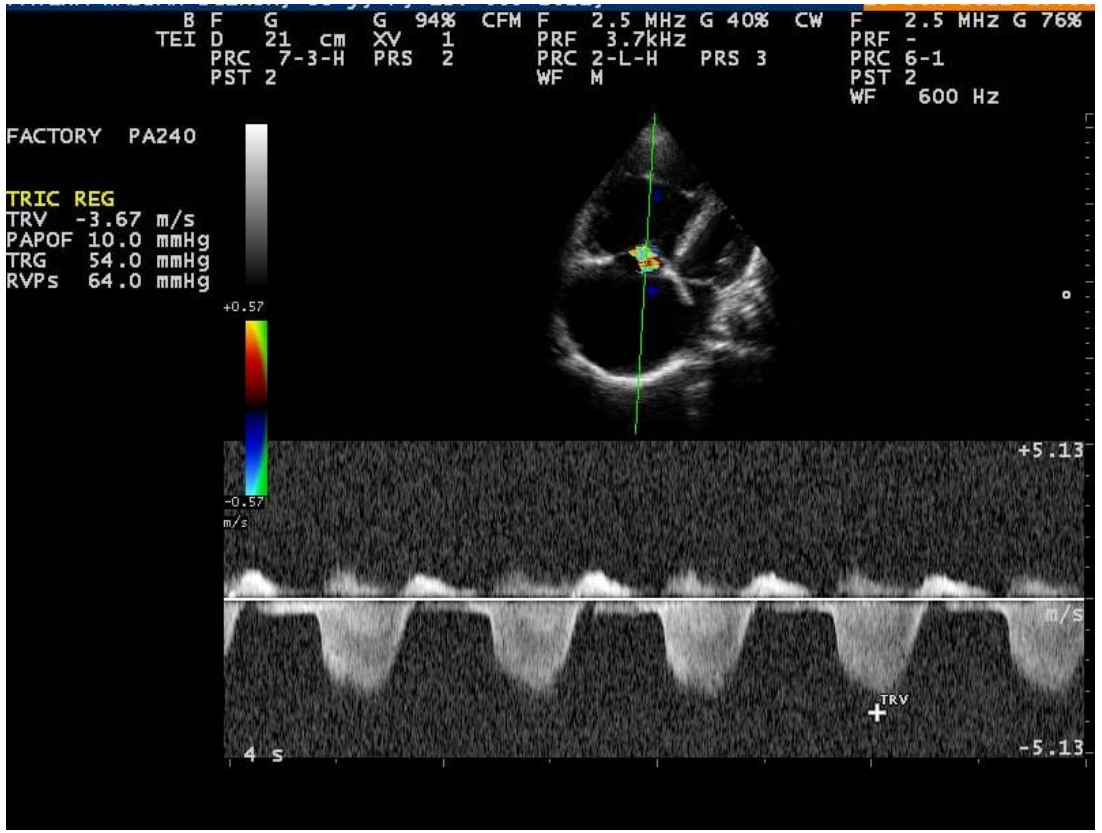

Case (9) 38 yrs. F with sever Tricuspid regurgitant jet TV max (3. 67 m/s) PAP elvated by 10 mmHg with PASP 64 mmHg (Bernoulli equation) 4 (TV max)^2 + PAP.

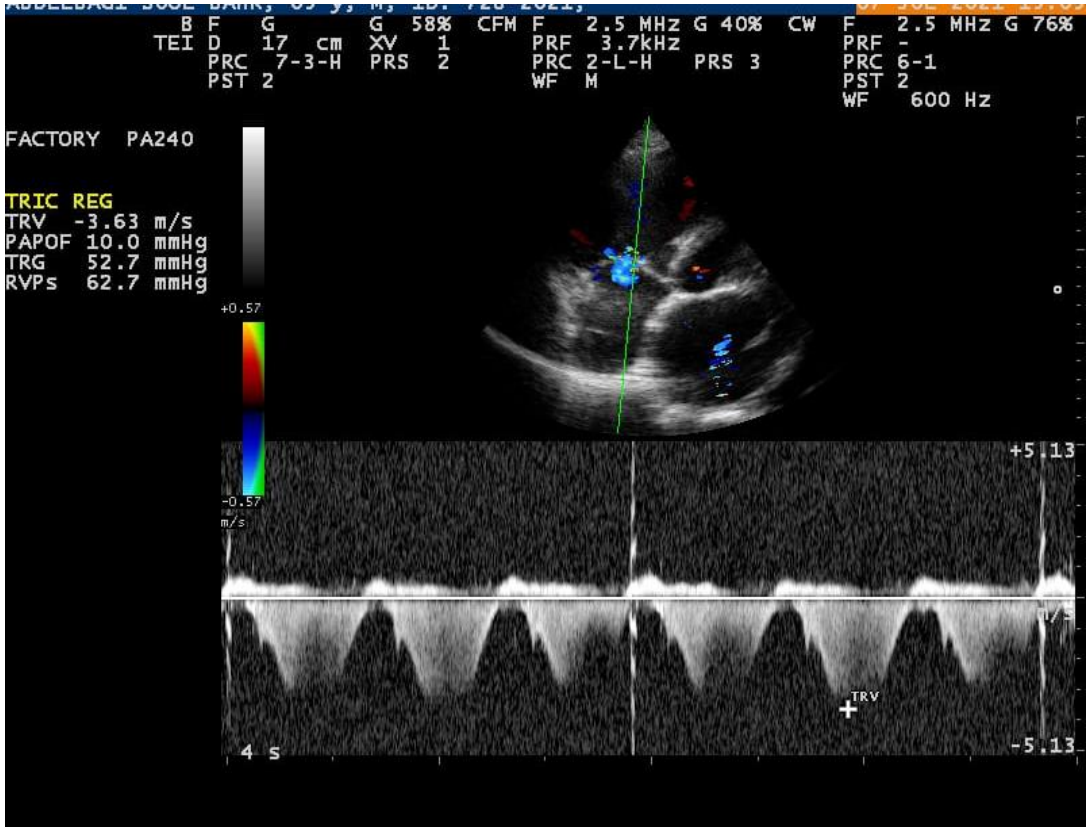

Case (10) 65 yrs. M with sever Tricuspid regurgitant jet TV max (3. 63 m/s) PAP elvated by 10 mmHg with PASP 62 mmHg (Bernoulli equation) 4 (TV max)^2 + PAP.

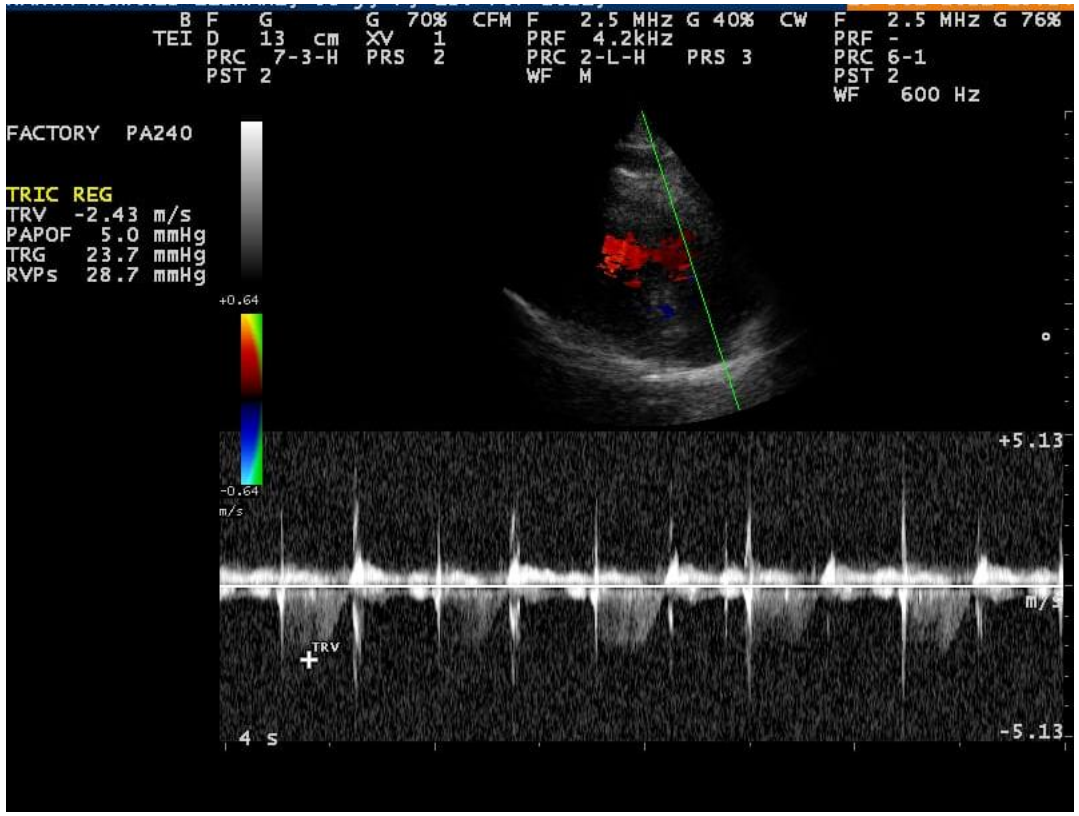

Case (11) 51 yrs. M with mild Tricuspid regurgitant jet TV max (2. 43 m/s) PAP elevated by 5 mmHg with PASP 28.7 mmHg (Bernoulli equation) 4 (TV max)^2 + PAP.

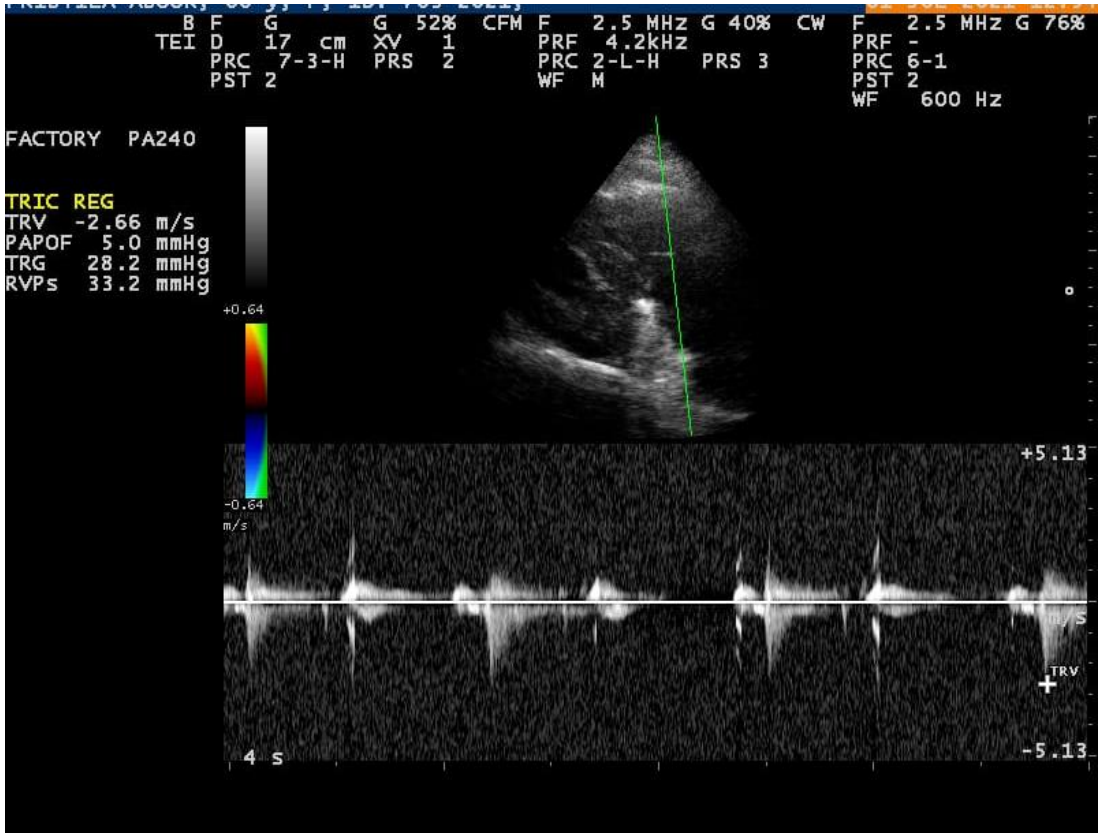

Case (12) 66 yrs. f with mild Tricuspid regurgitant jet TV max (2. 66 m/s) PAP elevated by 5 mmHg with PASP 33.2 mmHg (Bernoulli equation) 4 (TV max)2 + PAP.

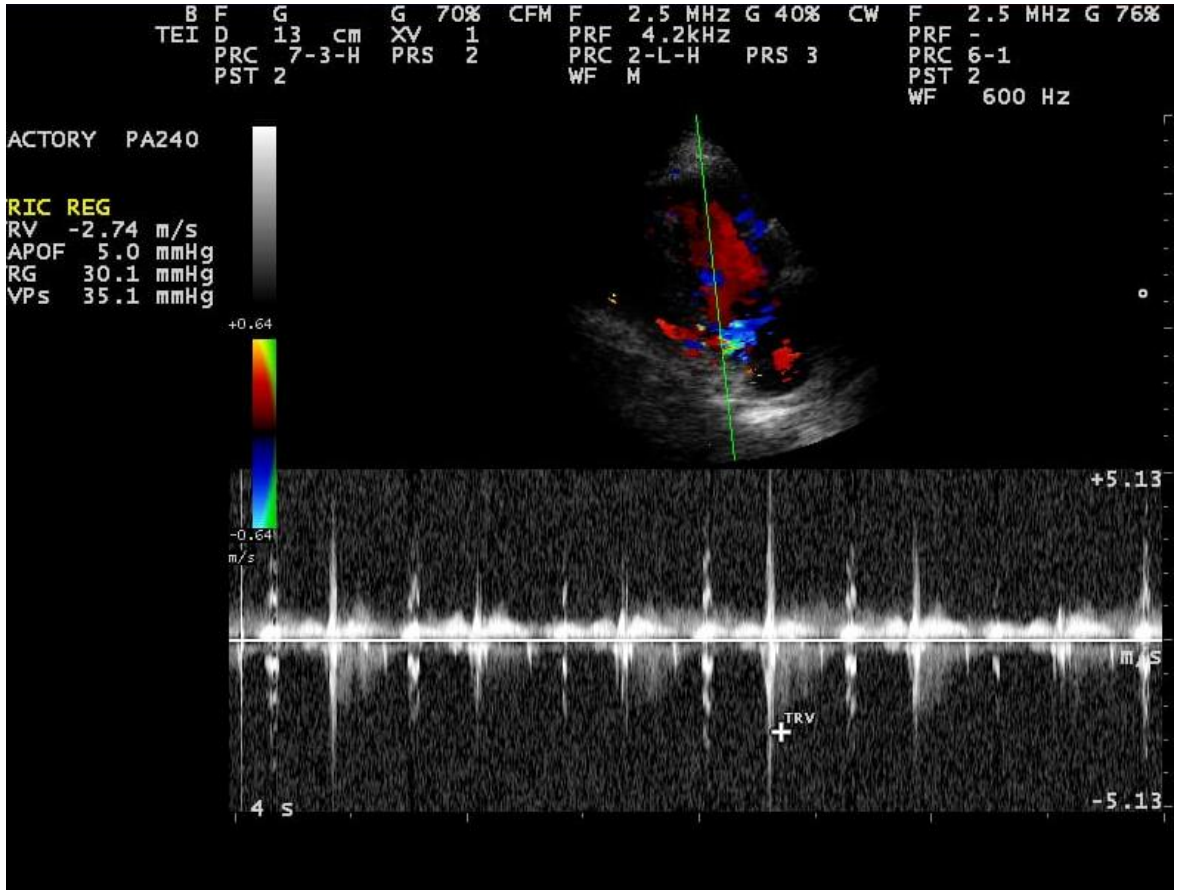

Case (13) 65 yrs. m with mild Tricuspid regurgitant jet TV max (2. 74 m/s) PAP elevated by 5 mmHg with PASP 35.1 mmHg (Bernoulli equation) 4 (TV max)^2 + PAP.

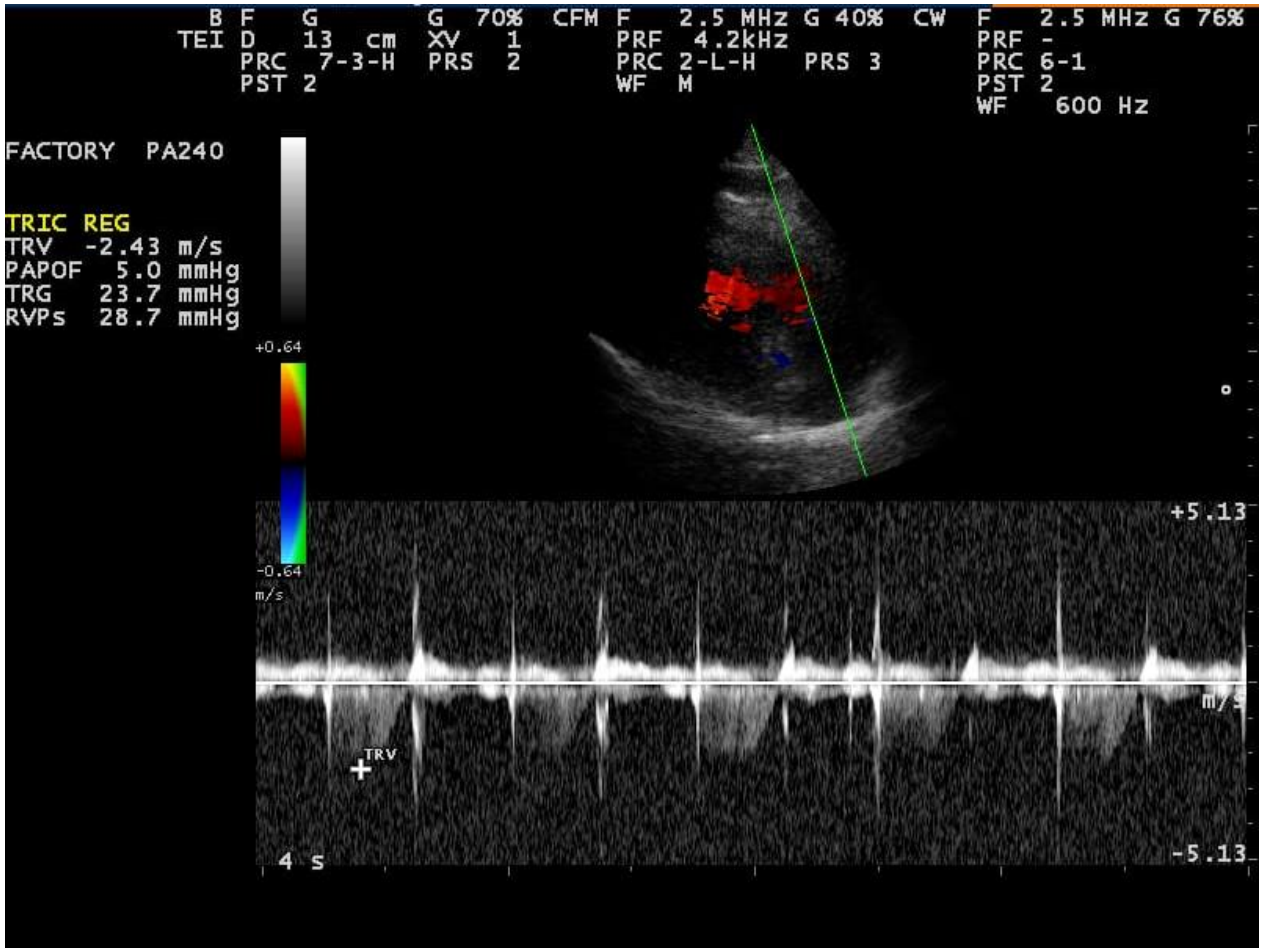

Case (14) 53 yrs. f with mild Tricuspid regurgitant jet TV max (2. 43 m/s) PAP elevated by 5 mmHg with PASP 28.7 mmHg (Bernoulli equation) 4 (TV max)^2 + PAP

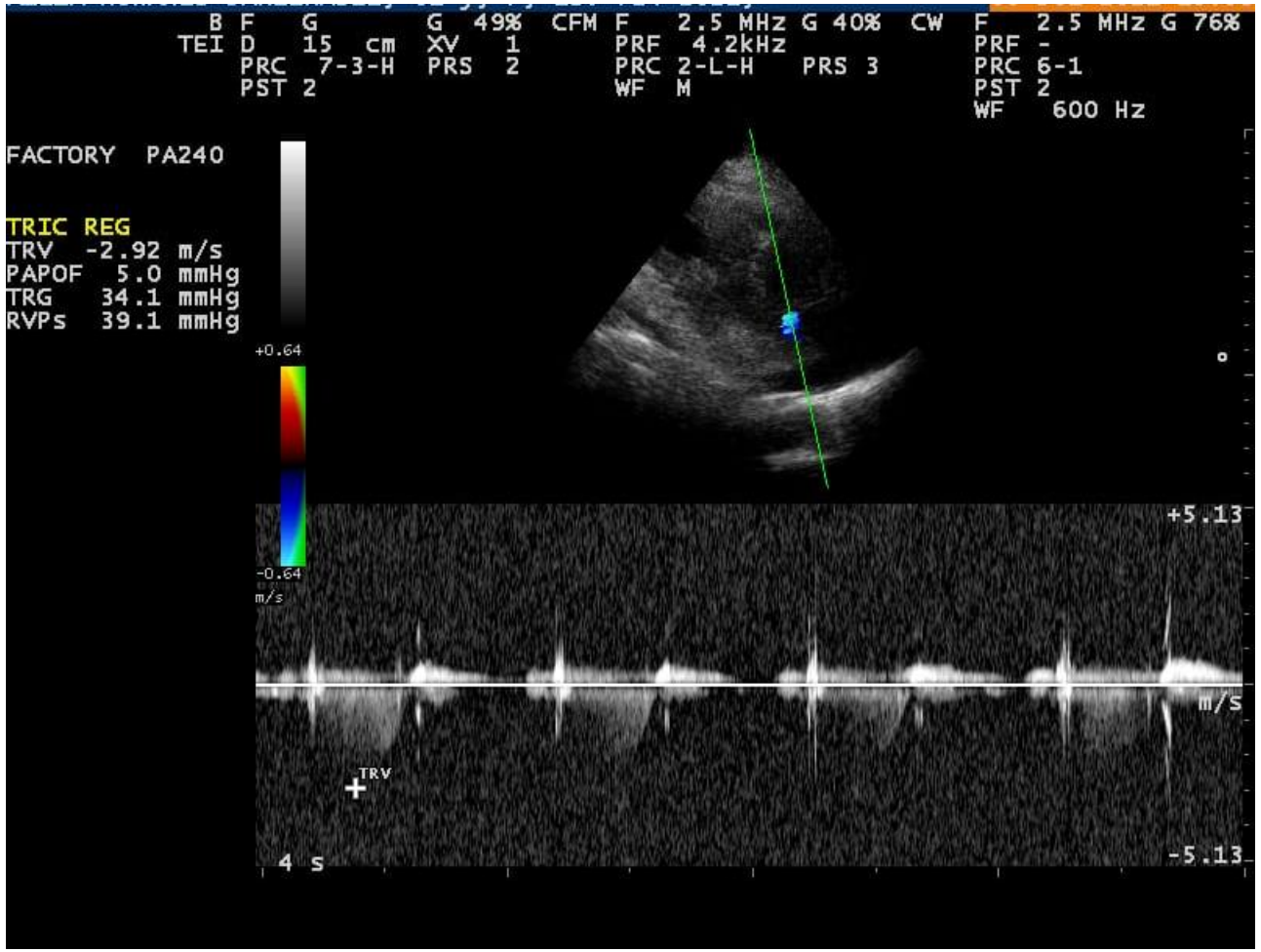

Case (15) 61 yrs. f with mild Tricuspid regurgitant jet TV max (2. 92 m/s) PAP elevated by 5 mmHg with PASP 39.1. mmHg (Bernoulli equation) 4 (TV max)^2 + PAP.

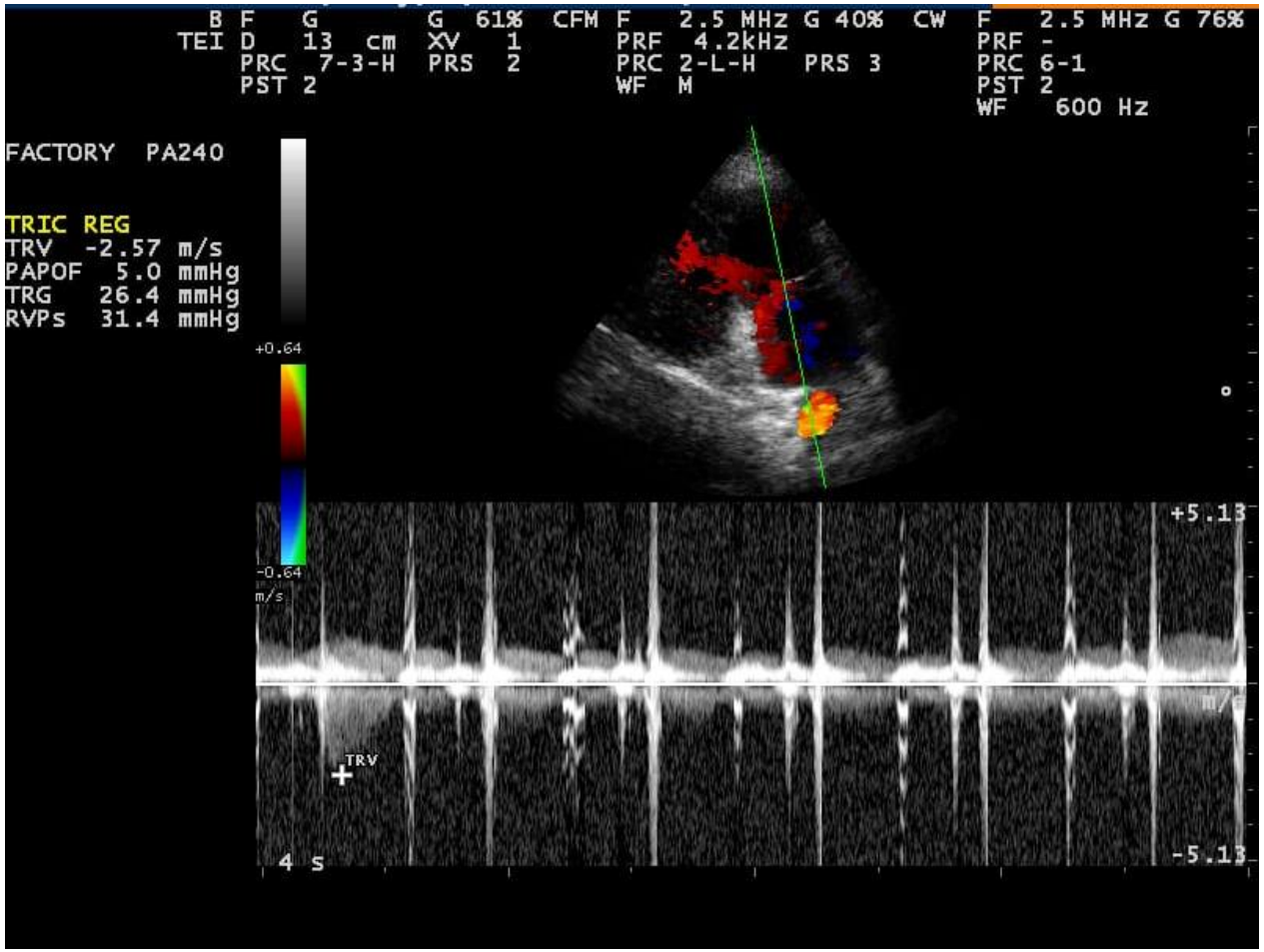

Case (16) 76 yrs. f with mild Tricuspid regurgitant jet TV max (2. 57 m/s) PAP elevated by 5 mmHg with PASP 31.4. mmHg (Bernoulli equation) 4 (TV max)2 + PAP.

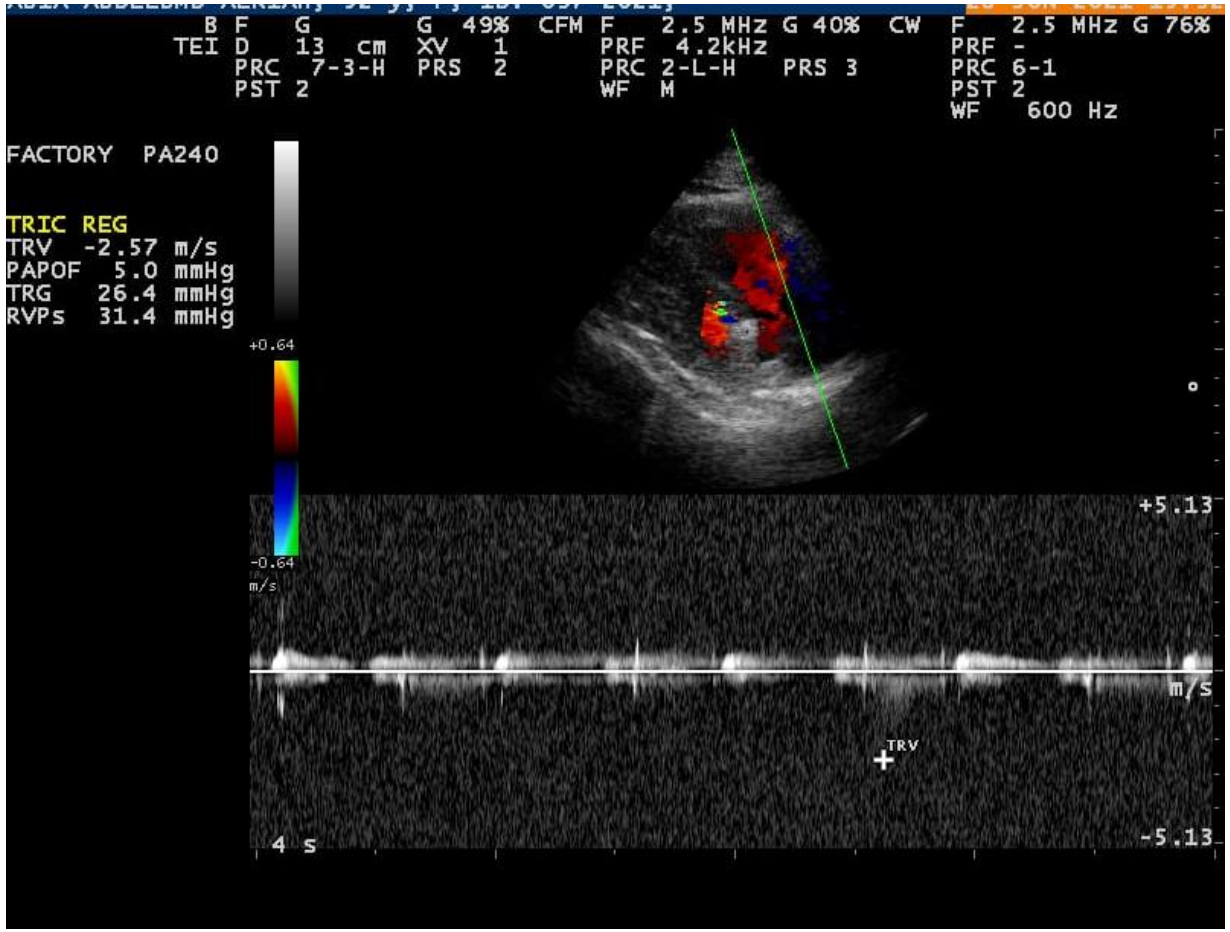

Case (17) 52 yrs. f with mild Tricuspid regurgitant jet TV max (2. 57 m/s) PAP elevated by 5 mmHg with PASP 31.4. mmHg (Bernoulli equation) 4 (TV max)^2 + PAP.

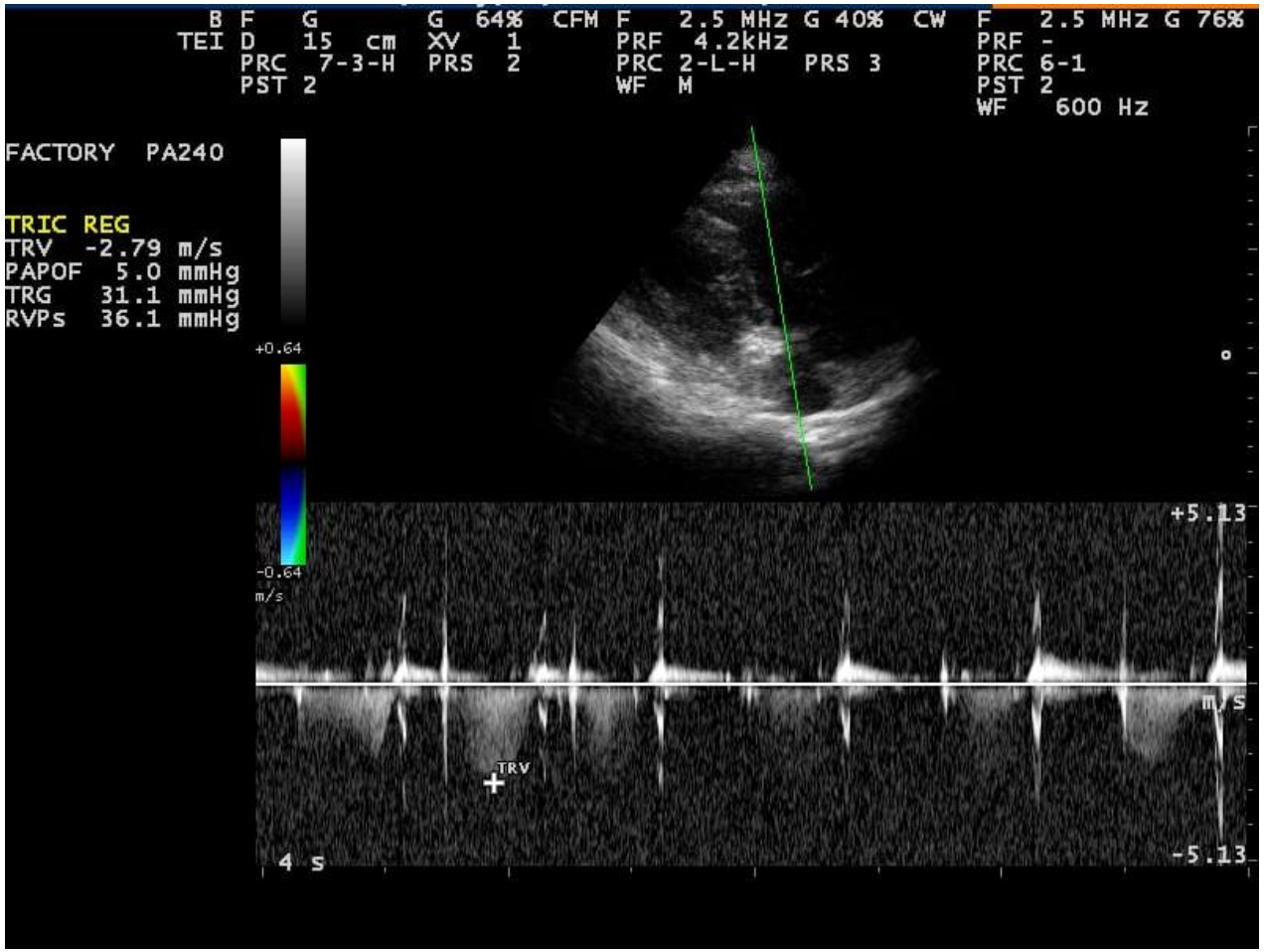

Case (18) 70 yrs. f with mild Tricuspid regurgitant jet TV max (2. 79 m/s) PAP elevated by 5 mmHg with PASP 36.1. mmHg (Bernoulli equation) 4 (TV max)^2 + PAP.

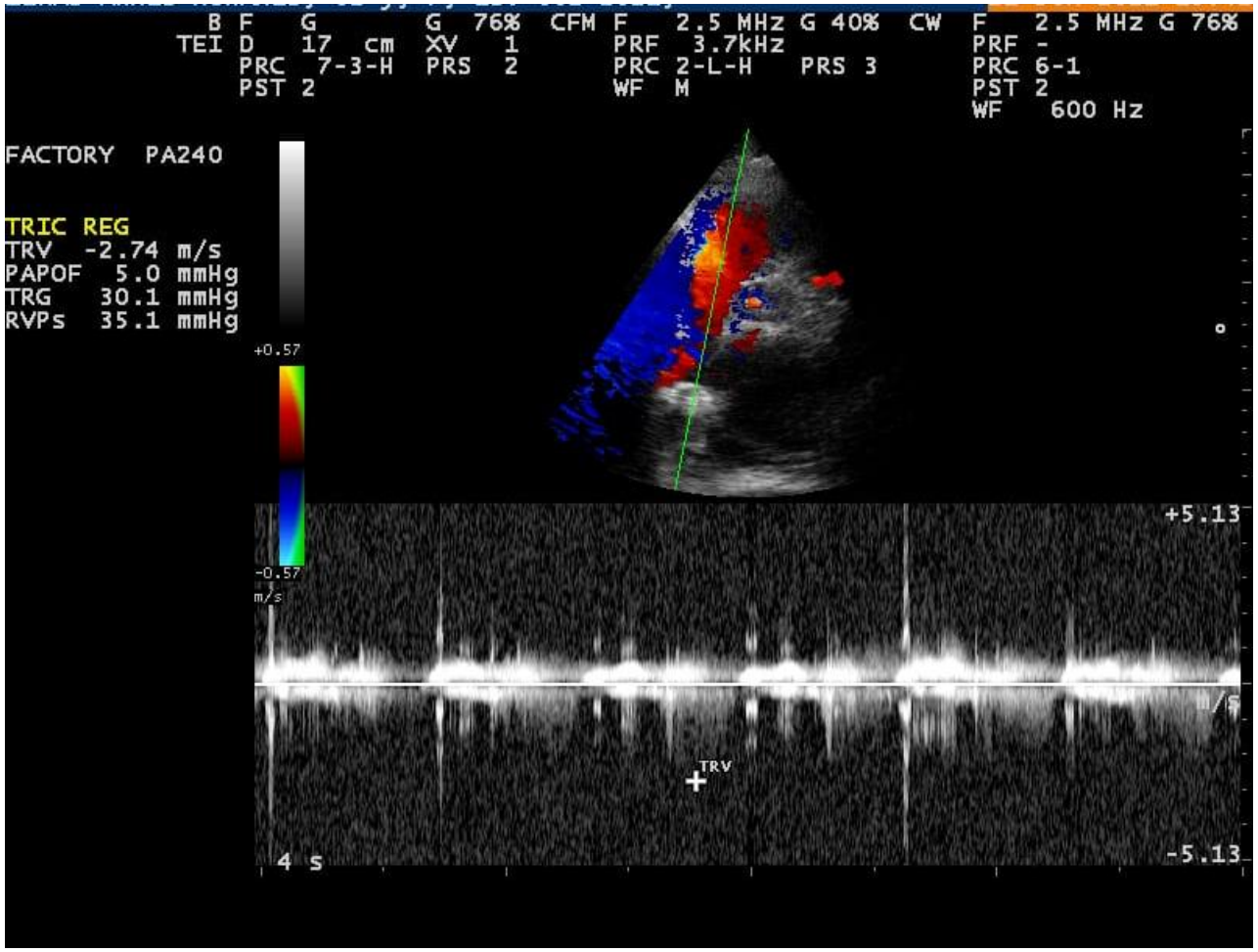

Case (19) 62 yrs. f with mild Tricuspid regurgitant jet TV max (2. 74 m/s) PAP elevated by 5 mmHg with PASP 35.1. mmHg (Bernoulli equation) 4 (TV max)^2 + PAP.

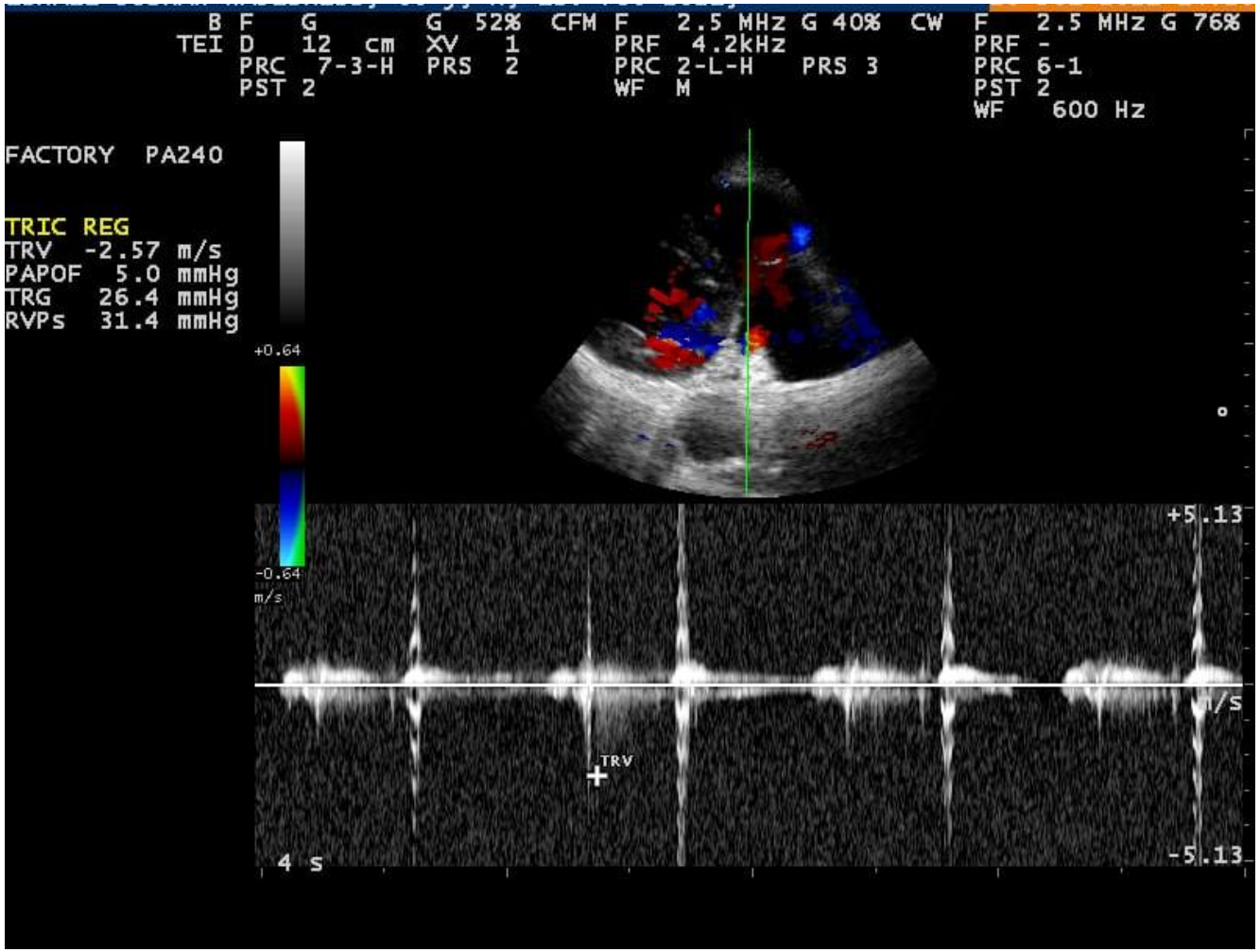

Case (20) 60 yrs. M with mild Tricuspid regurgitant jet TV max (2.57 m/s) PAP elevated by 5 mmHg with PASP 31.4. mmHg (Bernoulli equation) 4 (TV max)^2 + PAP.

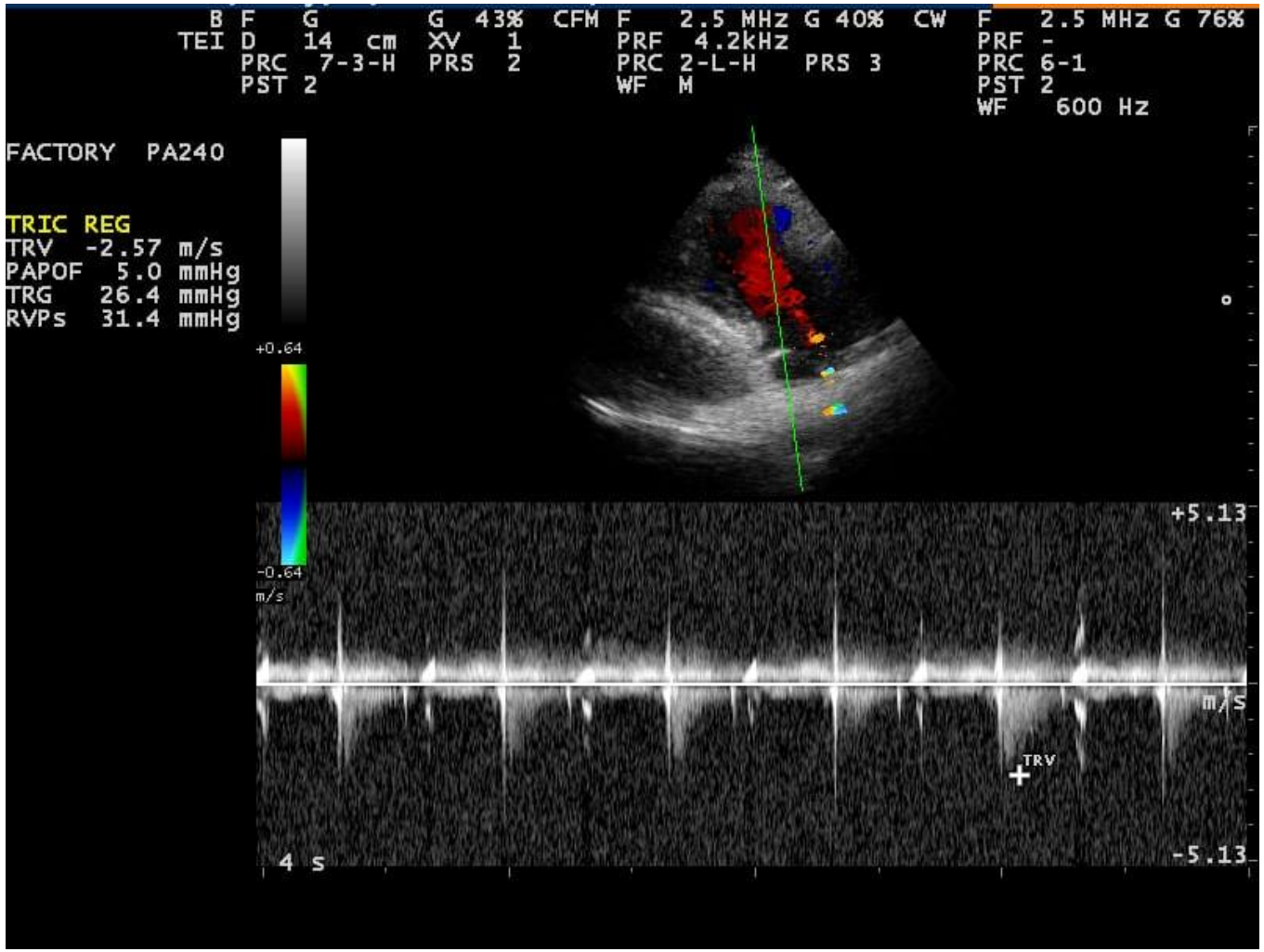

Case (21) 30 yrs. f with mild Tricuspid regurgitant jet TV max (2.57 m/s) PAP elevated by 5 mmHg with PASP 31.4. mmHg (Bernoulli equation) 4 (TV max)^2 + PAP.

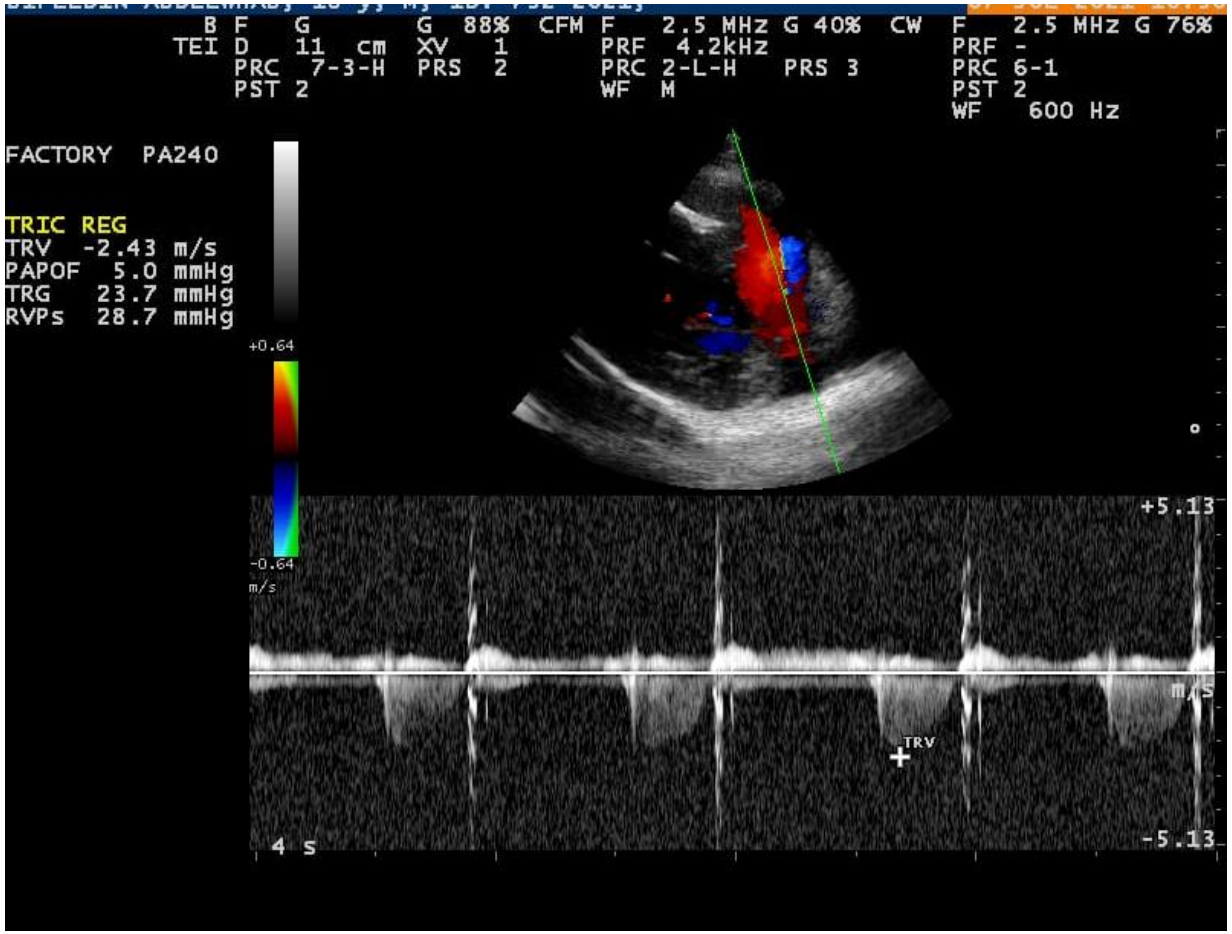

Case (22) 18 yrs. f with mild Tricuspid regurgitant jet TV max (2.43 m/s) PAP elevated by 5 mmHg with PASP 28.7. mmHg (Bernoulli equation) 4 (TV max)^2 + PAP.

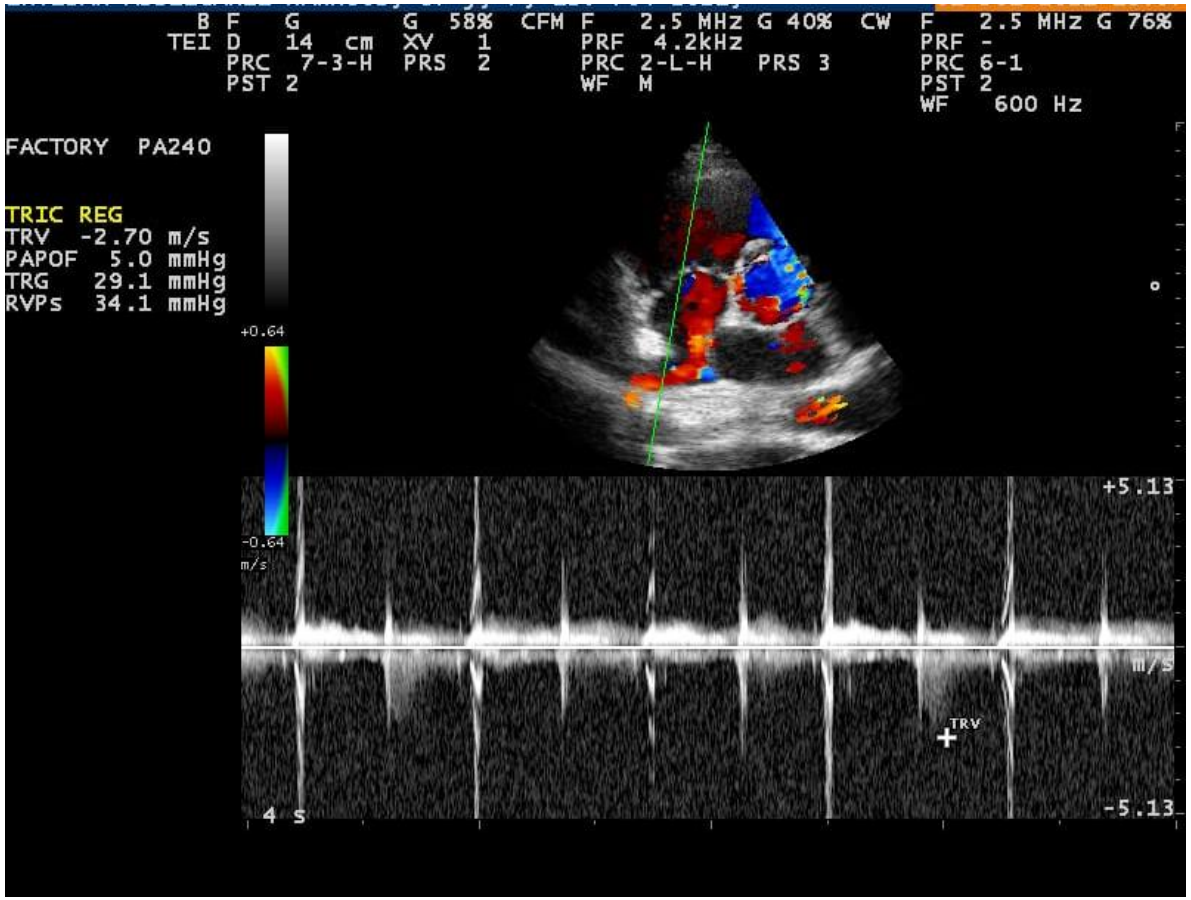

Case (23) 37 yrs. f with mild Tricuspid regurgitant jet TV max (2.70 m/s) PAP elevated by 5 mmHg with PASP 34.1. mmHg (Bernoulli equation) 4 (TV max)^2 + PAP.

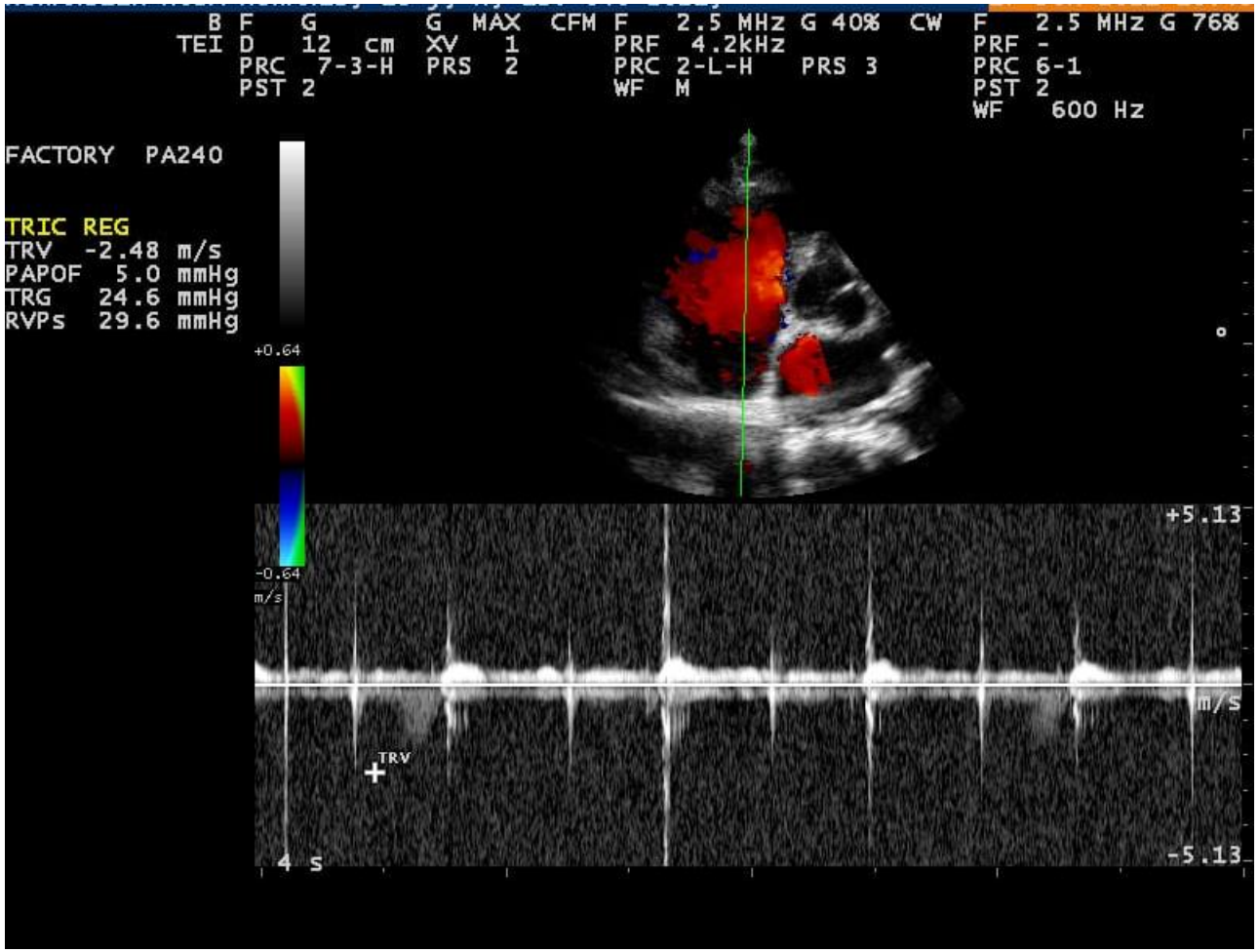

Case (24) 19 yrs. M with mild Tricuspid regurgitant jet TV max (2.48 m/s) PAP elevated by 5 mmHg with PASP 29.6 mmHg (Bernoulli equation) 4 (TV max)^2 + PAP.

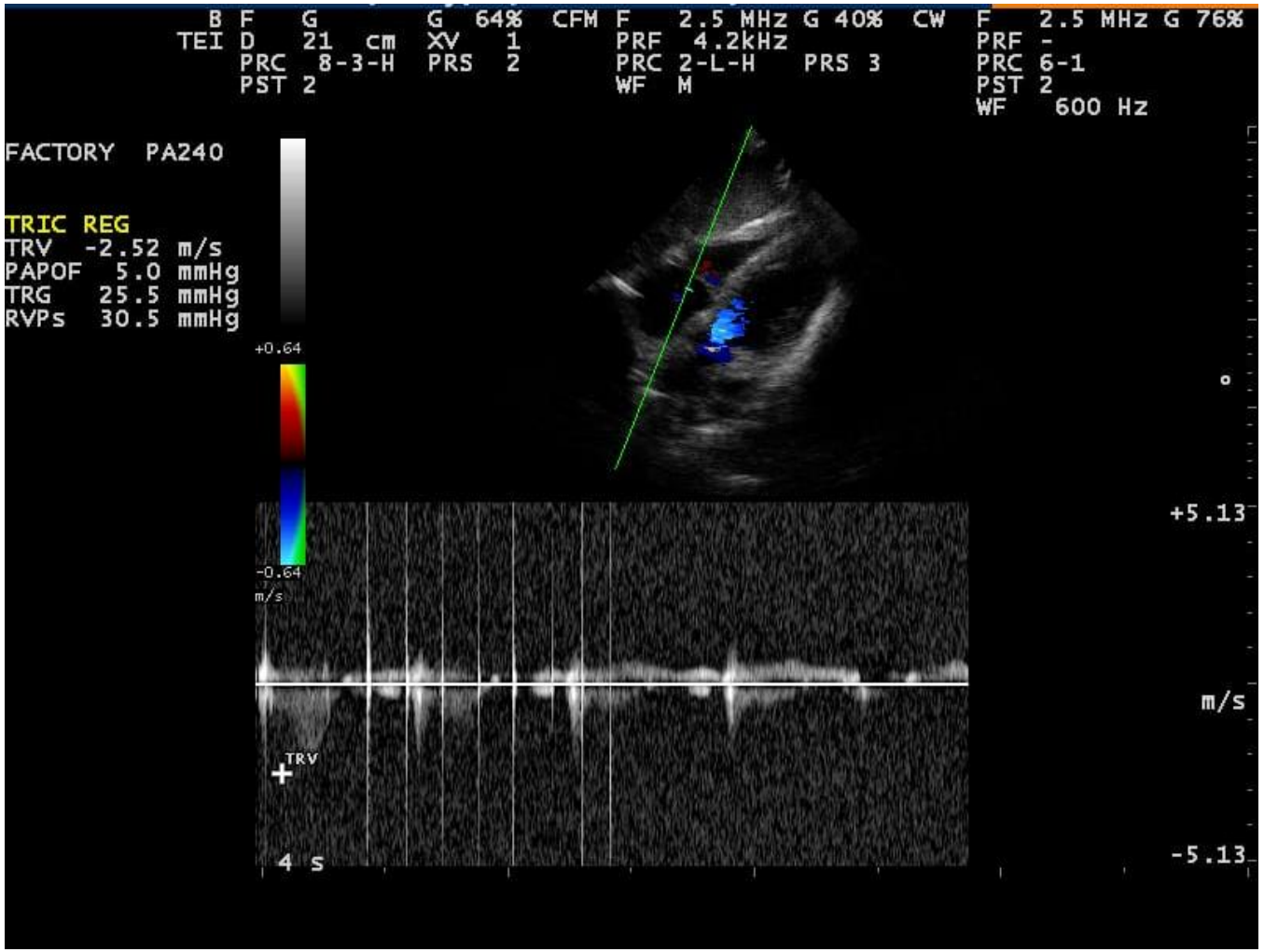

Case (25) 70 yrs. M with mild Tricuspid regurgitant jet TV max (2.52 m/s) PAP elevated by 5 mmHg with PASP 30.5 mmHg (Bernoulli equation) 4 (TV max)^2 + PAP.

Case (26) 54 yrs. F with mild Tricuspid regurgitant jet TV max (2.70 m/s) PAP elevated by 5 mmHg with PASP 34.1 mmHg (Bernoulli equation) 4 (TV max)^2 + PAP.

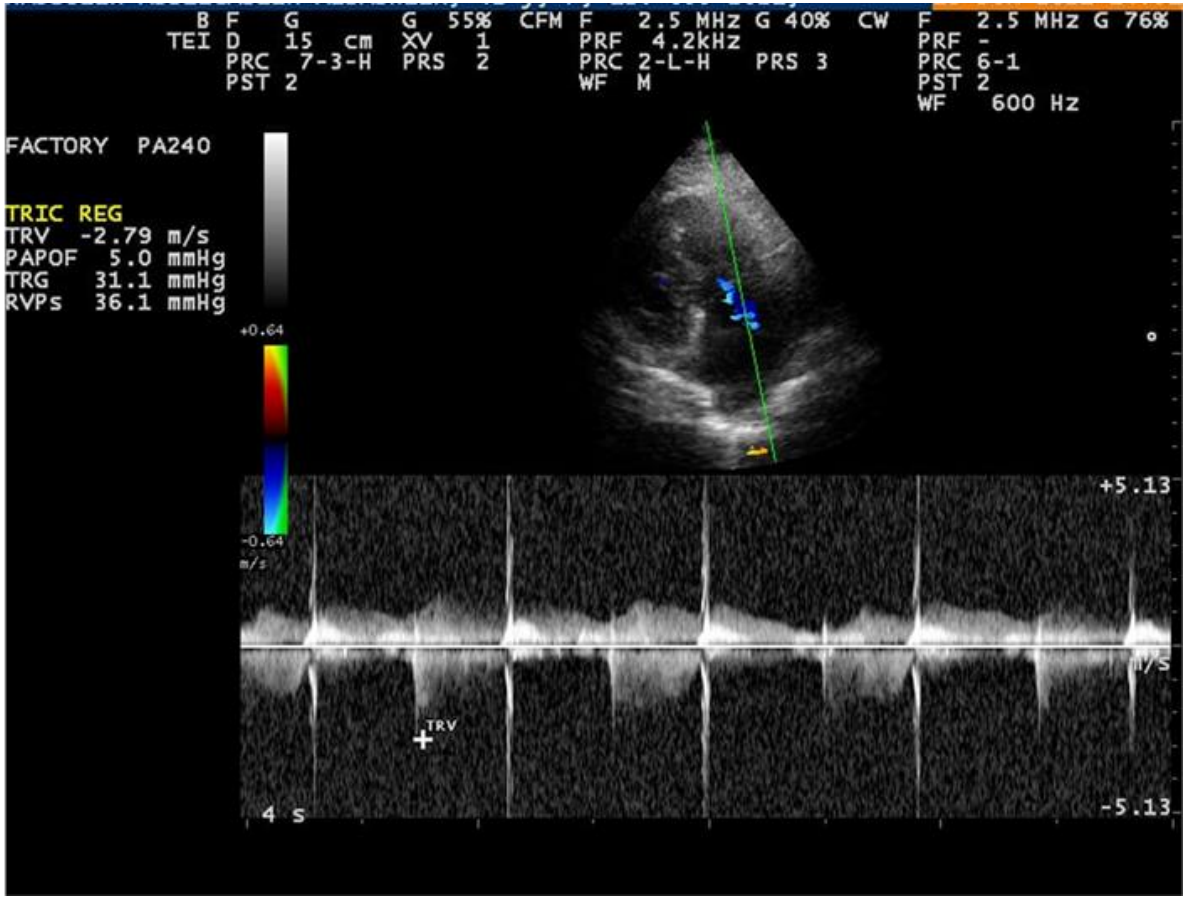

Case (27) 42 yrs. F with mild Tricuspid regurgitant jet TV max (2.79 m/s) PAP elevated by 5 mmHg with PASP 36.1 mmHg (Bernoulli equation) 4 $(\text{TV max})^2$ + PAP.

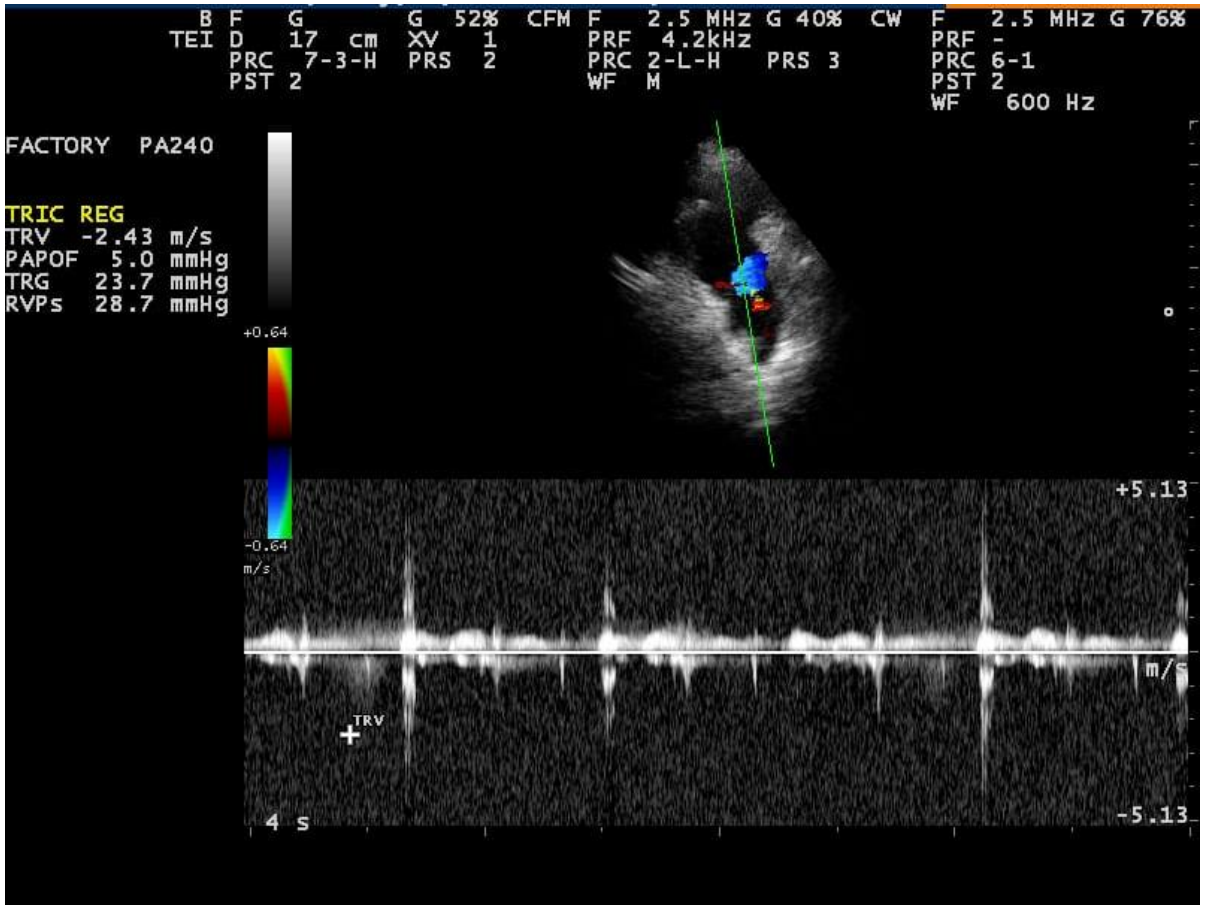

Case (28) 64 yrs. m with mild Tricuspid regurgitant jet TV max (2.43 m/s) PAP elevated by 5 mmHg with PASP 28.7 mmHg (Bernoulli equation) 4 (TV max)^2 + PAP.

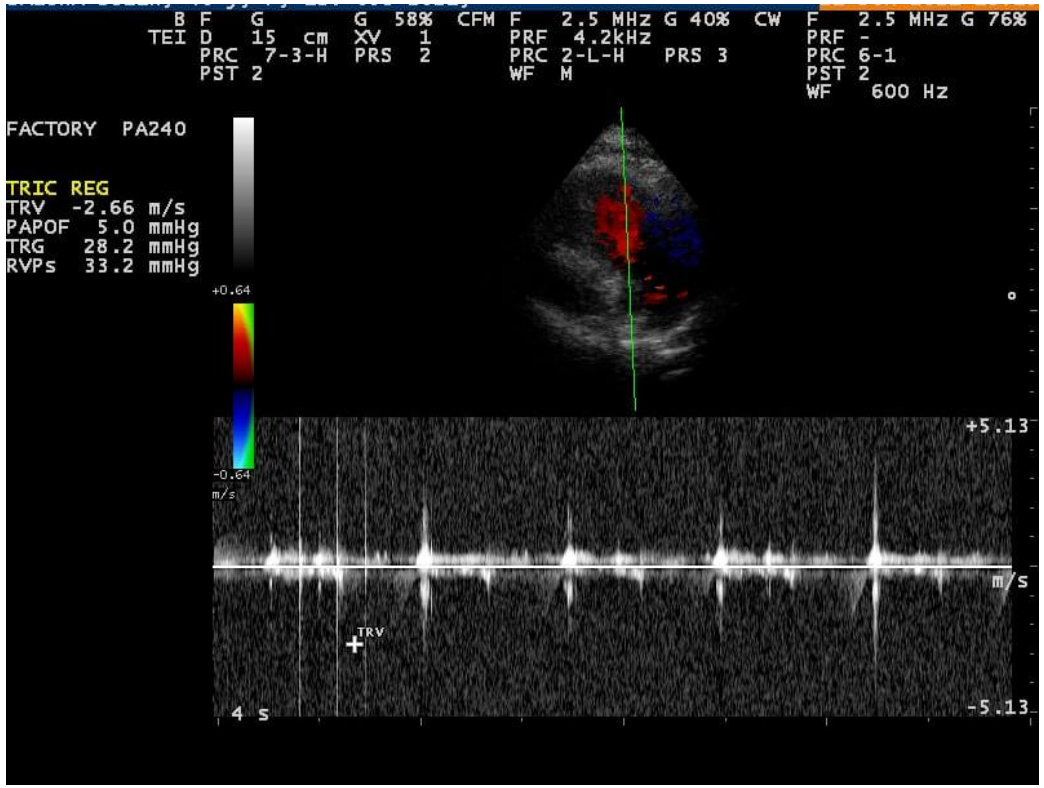

Case (29) 46 F yrs. m with mild Tricuspid regurgitant jet TV max (2.66 m/s) PAP elevated by 5 mmHg with PASP 33.2 mmHg (Bernoulli equation) $4\ (\text{TV max})^2 + \text{PAP}$.

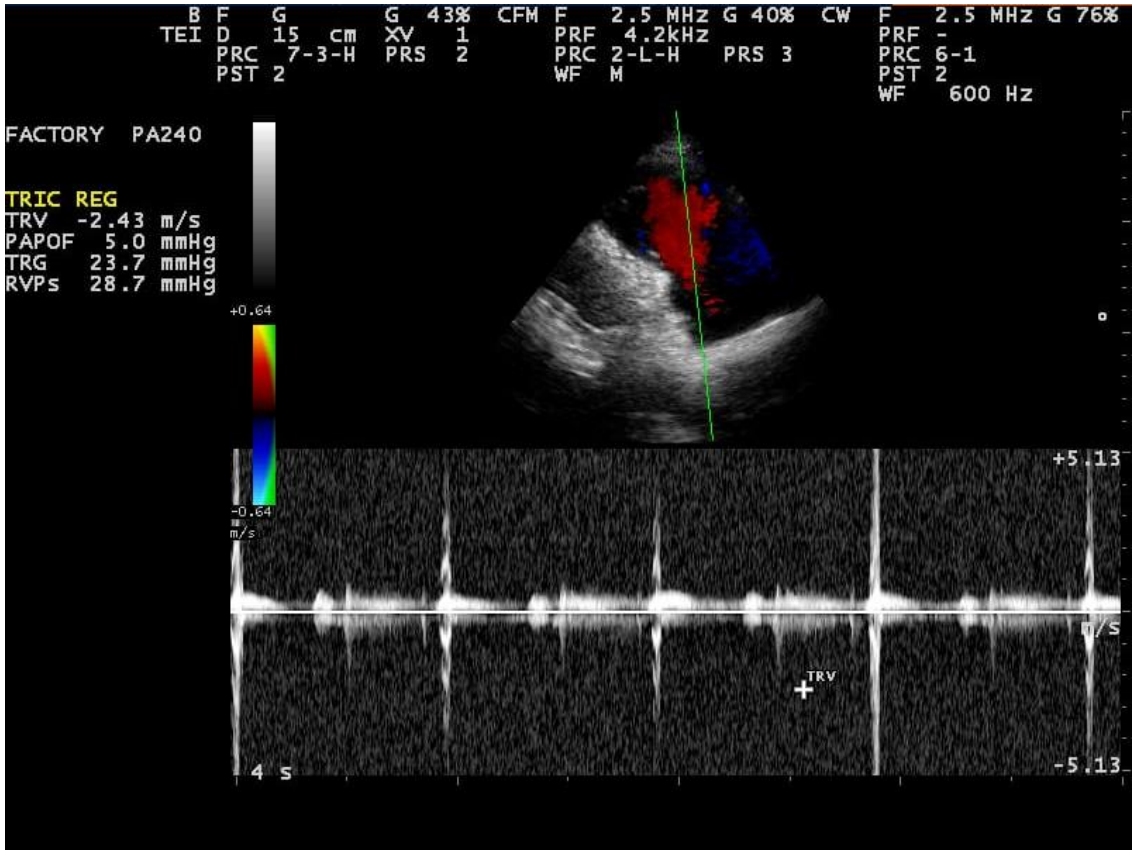

Case (30) 42 yrs. M with mild Tricuspid regurgitant jet TV max (2.43 m/s) PAP elevated by 5 mmHg with PASP 28.7 mmHg (Bernoulli equation) 4 (TV max)^2 + PAP.

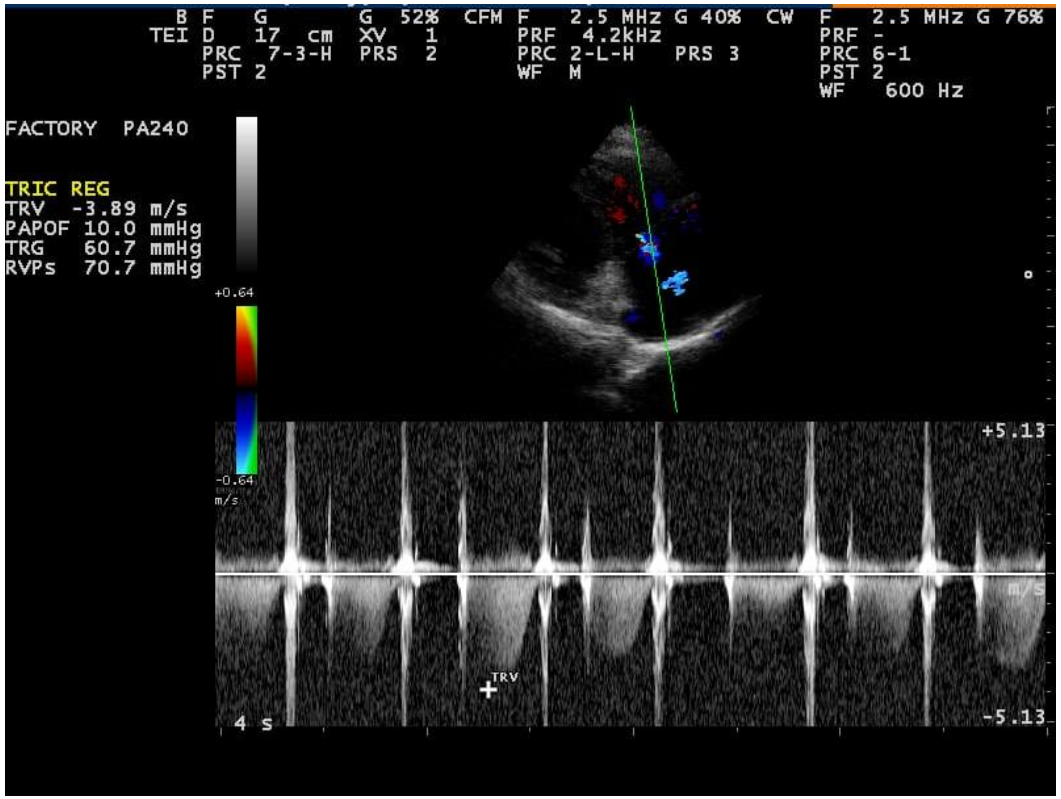

Case (31) 55 yrs. M with severe Tricuspid regurgitant jet TV max (2.79 m/s) PAP elevated by 10 mmHg with PASP 70.7 mmHg (Bernoulli equation) $4\ (\text{TV max})^2 + \text{PAP}$.

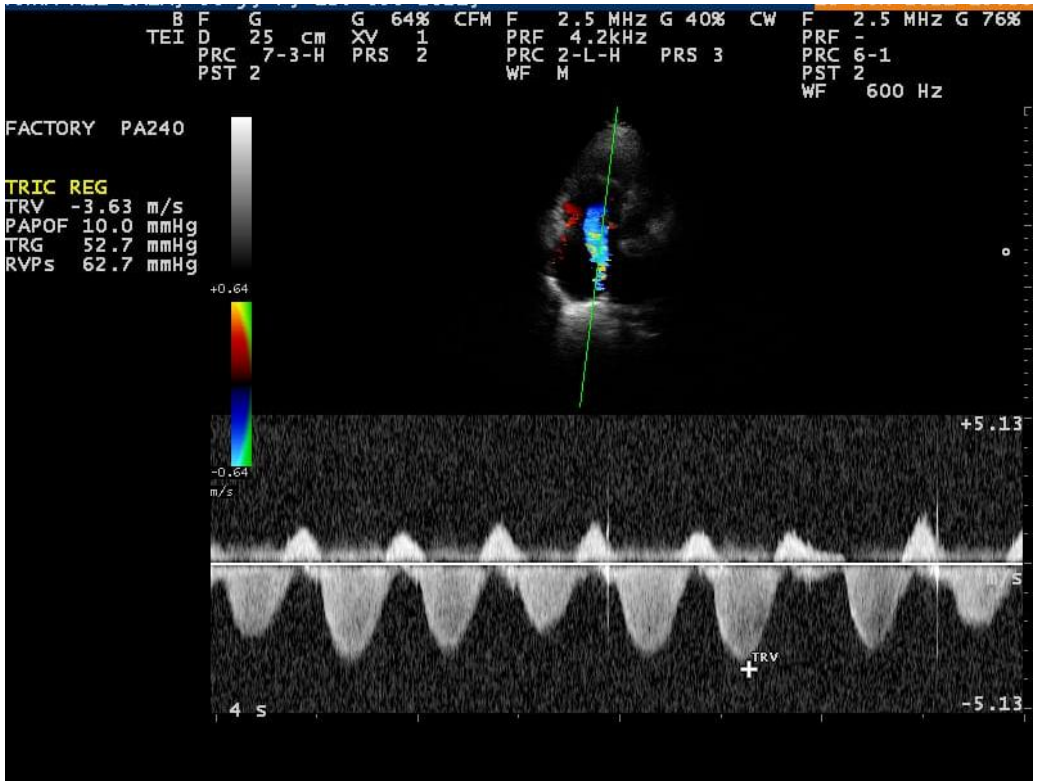

Case (32) 50 yrs. F with severe Tricuspid regurgitant jet TV max (2.79 m/s) PAP elevated by 10 mmHg with PASP 62.7 mmHg (Bernoulli equation) 4 $(TV\ max)^2$ + PAP.

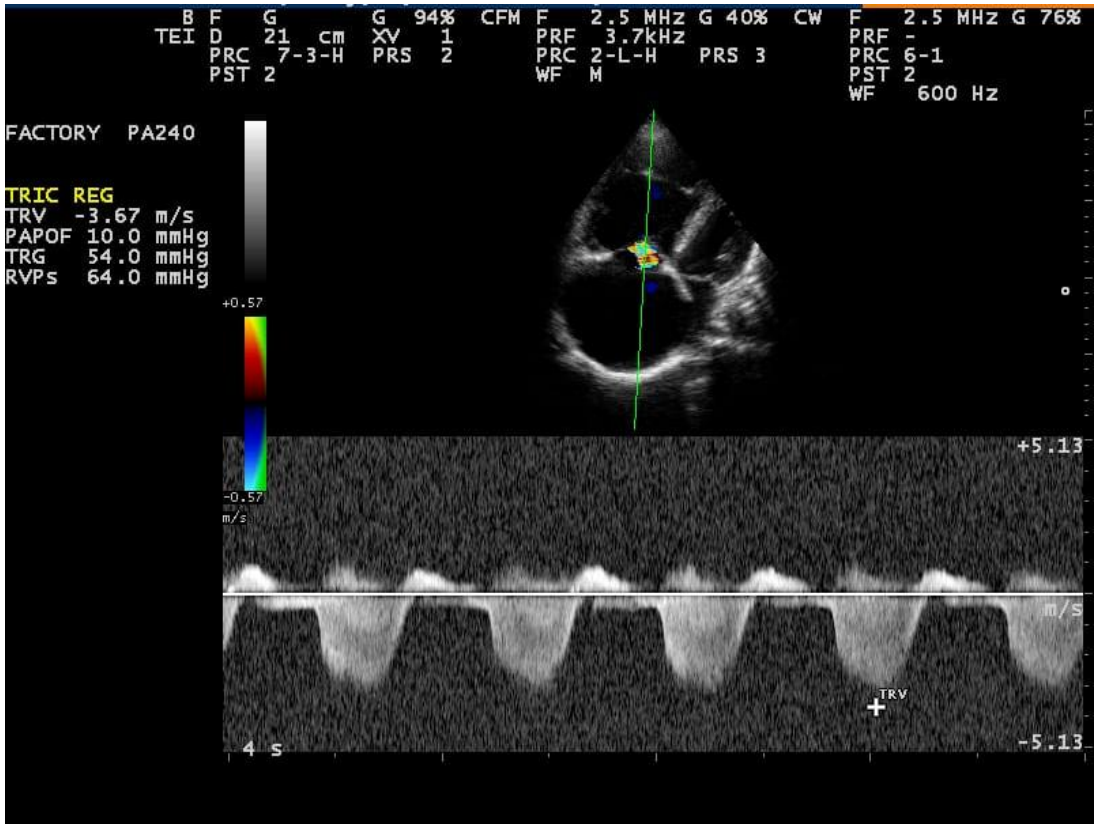

Case (33) 38 yrs. F with severe Tricuspid regurgitant jet TV max (2.67 m/s) PAP elevated by 10 mmHg with PASP 64.0 mmHg (Bernoulli equation) $4\ (\text{TV max})^2 + \text{PAP}$.

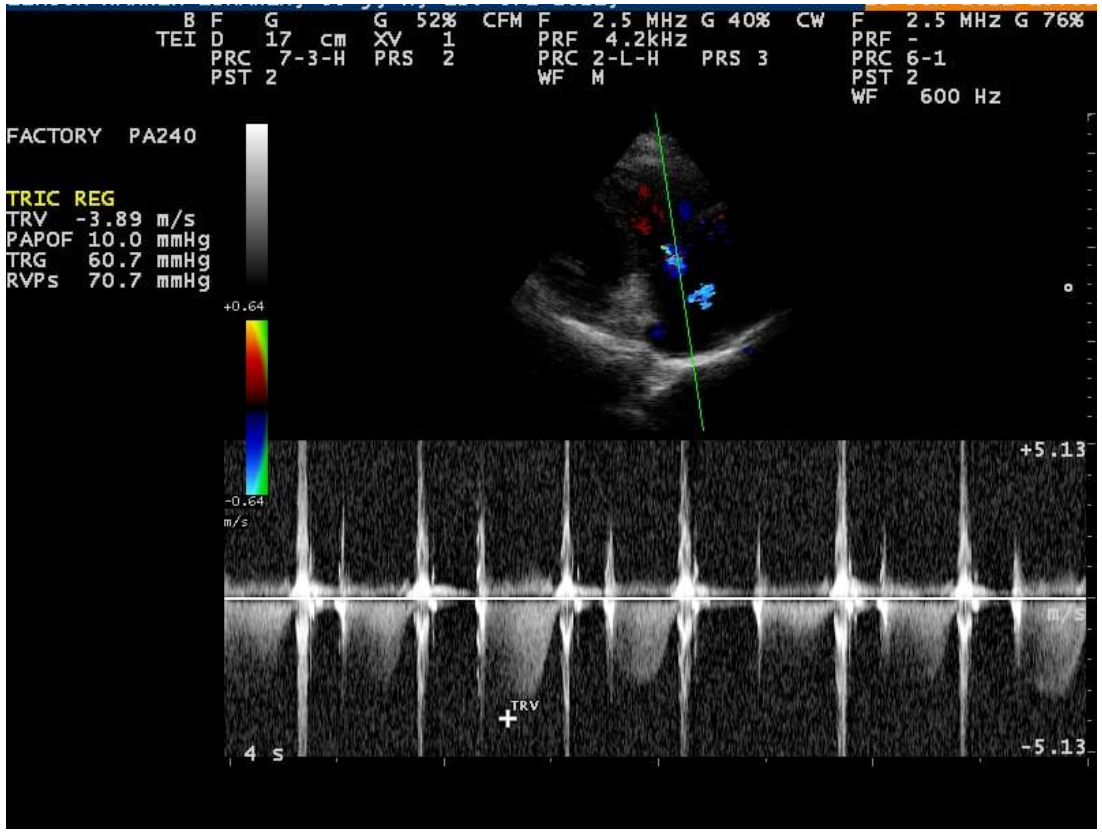

Case (34) 55 yrs. M with severe Tricuspid regurgitant jet TV max (2.89 m/s) PAP elevated by 10 mmHg with PASP 70.7 mmHg (Bernoulli equation) $4\ (\text{TV max})^2 + \text{PAP}$.

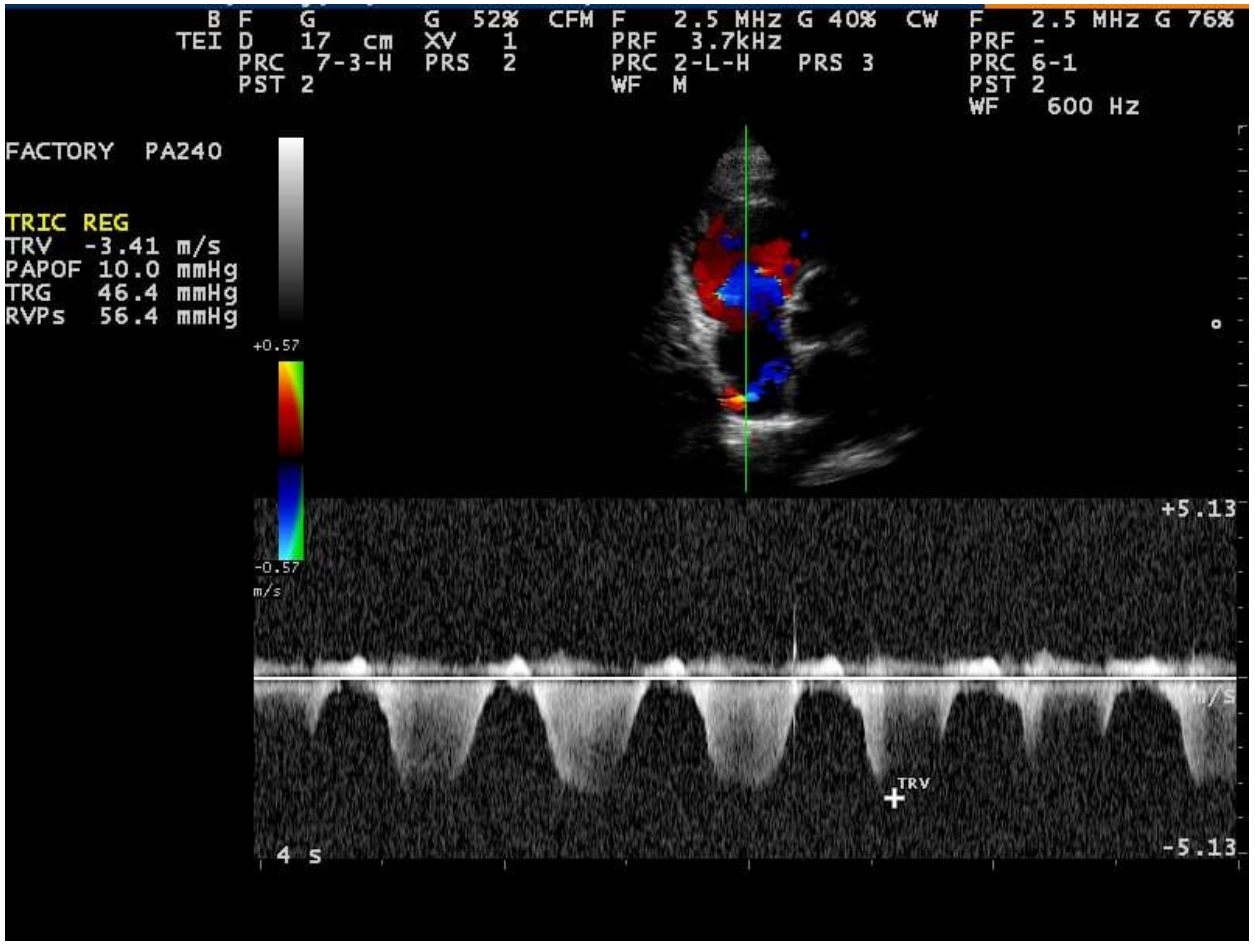

Case (35) 58 yrs. M with moderate Tricuspid regurgitant jet TV max (3.41 m/s) PAP elevated by 10 mmHg with PASP 56.4 mmHg (Bernoulli equation) 4 $(TV\ max)^2$ + PAP.

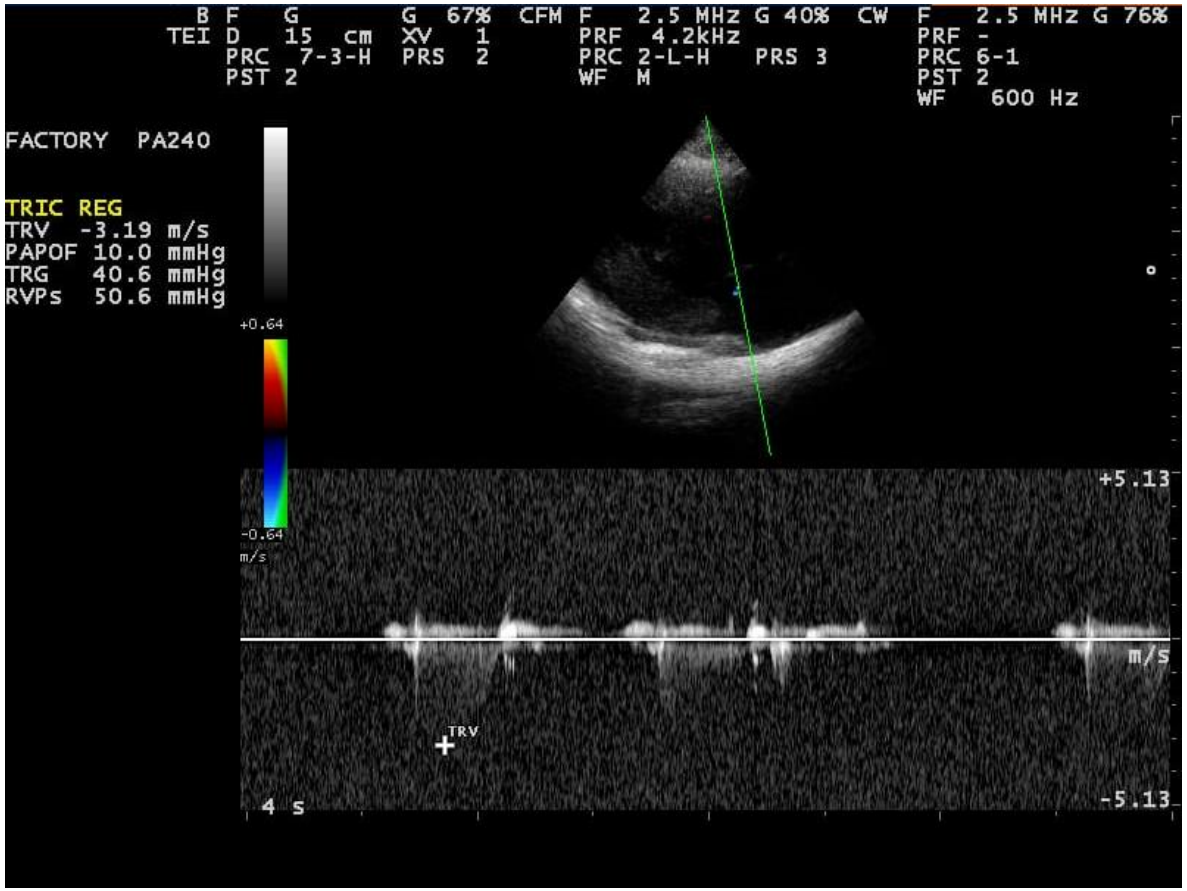

Case (36) 40 yrs. M with moderate Tricuspid regurgitant jet TV max (3.19 m/s) PAP elevated by 10 mmHg with PASP 50.6 mmHg (Bernoulli equation) $4\ (\text{TV max})^2 + \text{PAP}$.

Case (37) 42 yrs. F with moderate Tricuspid regurgitant jet TV max (3.23 m/s) PAP elevated by 10 mmHg with PASP 51.7 mmHg (Bernoulli equation) $4\ (\text{TV max})^2 + \text{PAP}$.

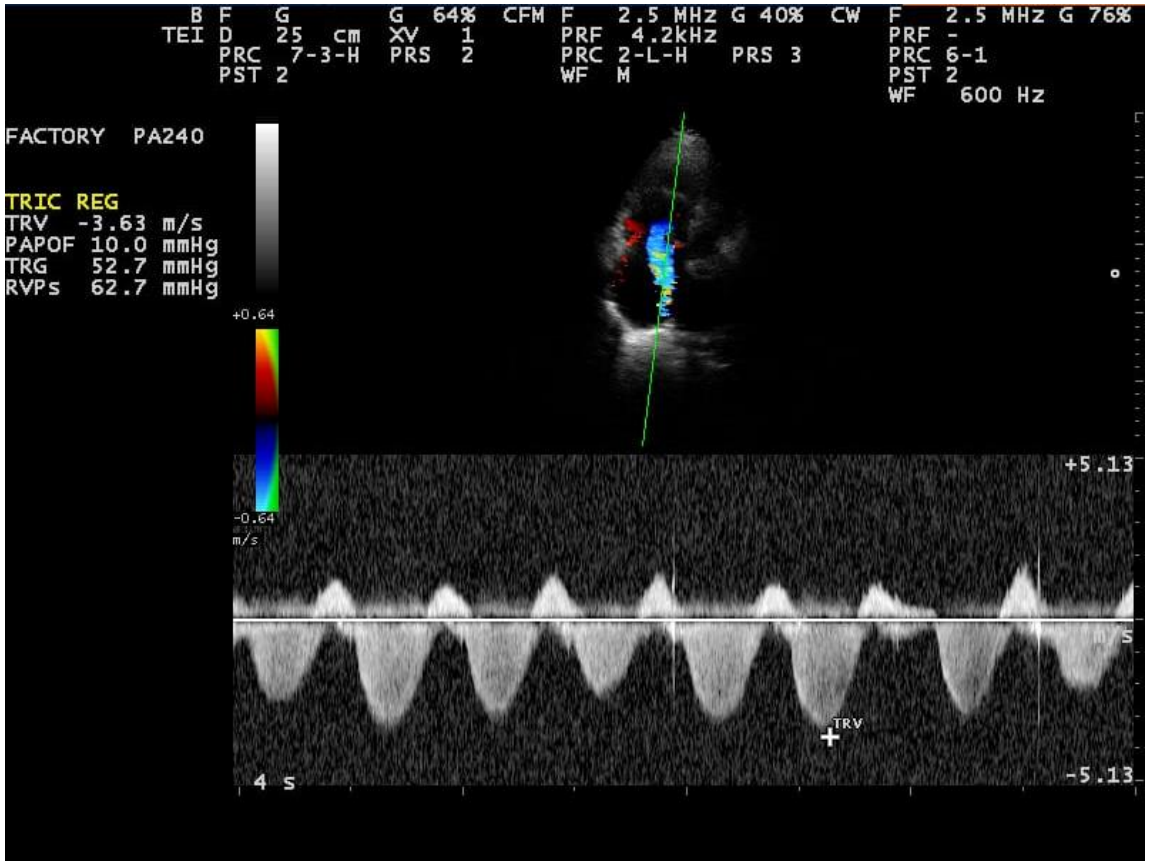

Case (38) 50 yrs. F with severe Tricuspid regurgitant jet TV max (3.63 m/s) PAP elevated by 10 mmHg with PASP 62.7 mmHg (Bernoulli equation) $4\ (\text{TV max})^2 + \text{PAP}$.

Case (39) 52 yrs. M with moderate Tricuspid regurgitant jet TV max (3.27 m/s) PAP elevated by 10 mmHg with PASP 52.9 mmHg (Bernoulli equation) 4 $(\text{TV max})^2$ + PAP.

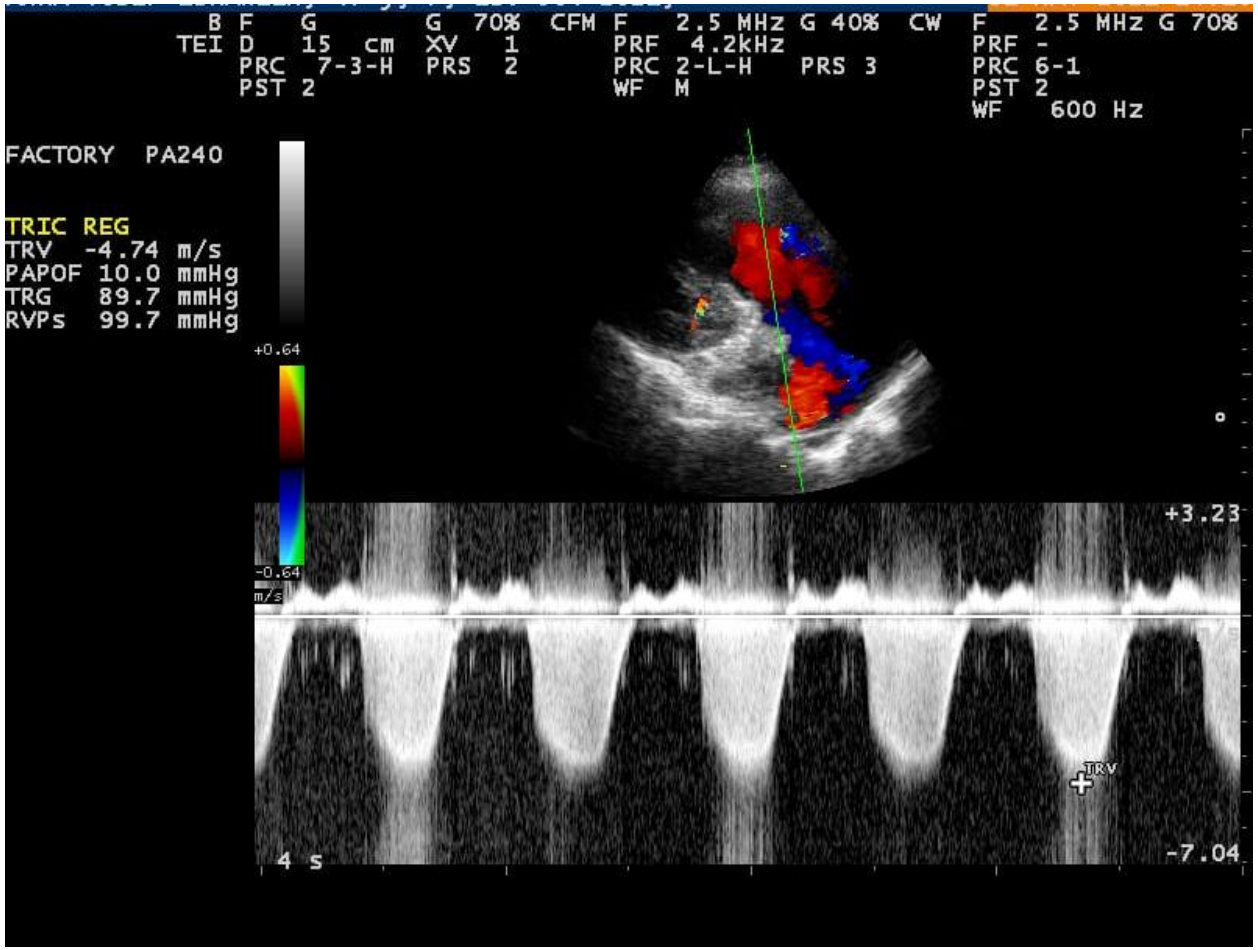

Case (40) 47 yrs. F with severe Tricuspid regurgitant jet TV max (4.74 m/s) PAP elevated by 10 mmHg with PASP 99.7 mmHg (Bernoulli equation) 4 $(TV\ max)^2$ + PAP.